Thermodynamics of Incompressible and Compressible Fluid Flow

AIR1168/1

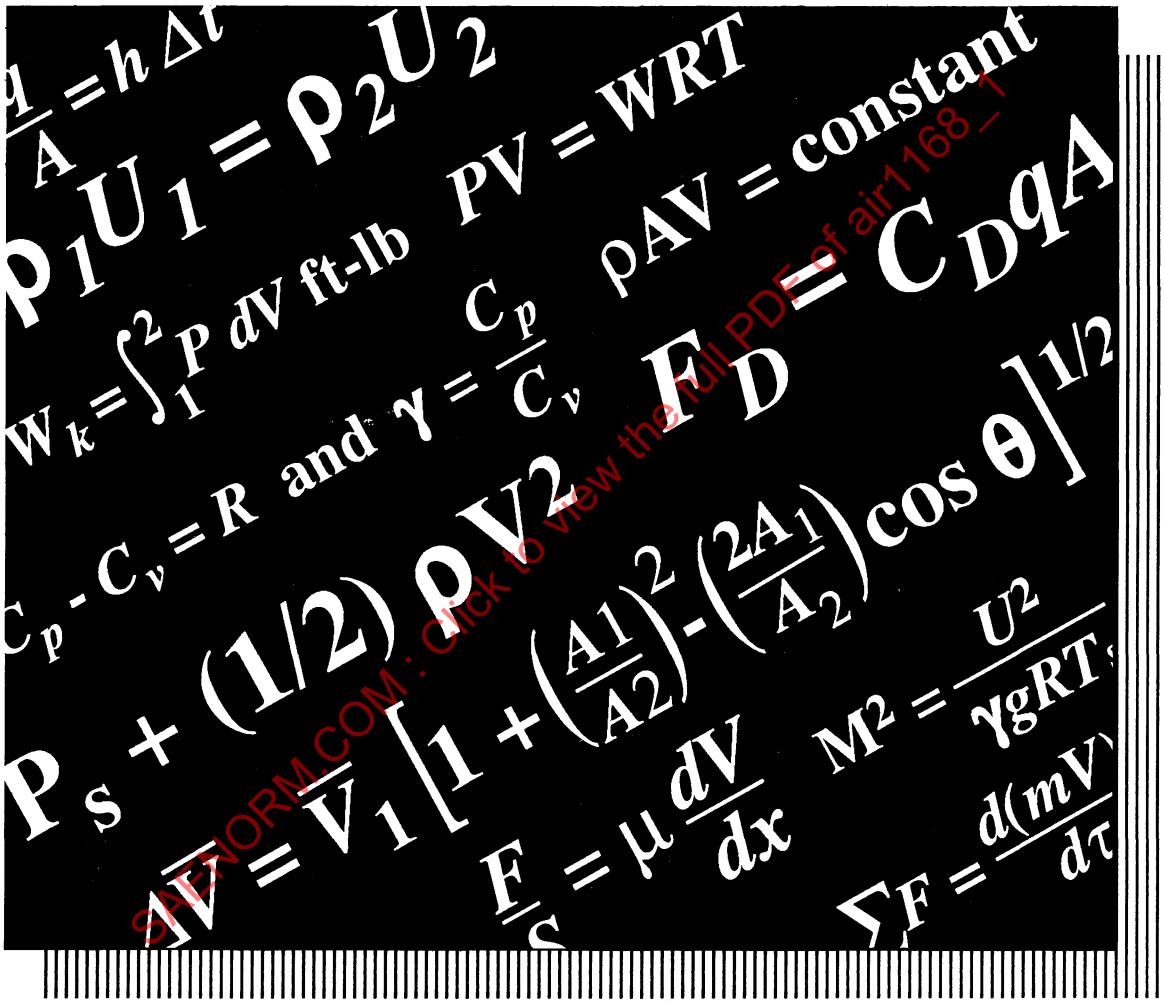

SAE Aerospace Applied Thermodynamics Manual

SAE The Engineering Society For Advancing Mobility Land Sea Air and Space®
INTERNATIONAL

SAE Aerospace
An SAE International Group

AEROSPACE INFORMATION REPORT

SAE AIR1168/1

Issued 1990-03
Reaffirmed 2011-06

Thermodynamics of Incompressible and Compressible Fluid Flow

PREFACE

This document is one of 14 Aerospace Information Reports (AIR) of the Third Edition of the SAE Aerospace Applied Thermodynamics Manual. The manual provides a reference source for thermodynamics, aerodynamics, fluid dynamics, heat transfer, and properties of materials for the aerospace industry. Procedures and equations commonly used for aerospace applications of these technologies are included.

In the Third Edition, no attempt was made to update material from the Second Edition nor were SI units added. However, all identified errata were corrected and incorporated and original figure numbering was retained, insofar as possible.

The SAE AC-9B Subcommittee originally created the SAE Aerospace Applied Thermodynamics Manual and, for the Third Edition, used a new format consisting of AIR1168/1 through AIR1168/10. AIR1168/11 through AIR1168/14 were created by the SAE SC-9 Committee.

The AIRs comprising the Third Edition are shown below. Applicable sections of the Second Edition are shown parenthetically in the third column.

AIR1168/1	Thermodynamics of Incompressible and Compressible Fluid Flow	(1A,1B)
AIR1168/2	Heat and Mass Transfer and Air-Water Mixtures	(1C,1D,1E)
AIR1168/3	Aerothermodynamic Systems Engineering and Design	(3A,3B,3C,3D)
AIR1168/4	Ice, Rain, Fog, and Frost Protection	(3F)

TO PLACE A DOCUMENT ORDER: Tel: 877-606-7323 (inside USA and Canada)
Tel: 724-776-4970 (outside USA)
Fax: 724-776-0790
Email: CustomerService@sae.org
SAE WEB ADDRESS: http://www.sae.org

AIR1168/5	Aerothermodynamic Test Instrumentation and Measurement	(3G)
AIR1168/6	Characteristics of Equipment Components, Equipment Cooling System Design, and Temperature Control System Design	(3H,3J,3K)
AIR1168/7	Aerospace Pressurization System Design	(3E)
AIR1168/8	Aircraft Fuel Weight Penalty Due to Air Conditioning	(3I)
AIR1168/9	Thermophysical Properties of the Natural Environment, Gases, Liquids, and Solids	(2A,2B,2C,2D)
AIR1168/10	Thermophysical Characteristics of Working Fluids and Heat Transfer Fluids	(2E,2F)
AIR1168/11	Spacecraft Boost and Entry Heat Transfer	(4A,4B)
AIR1168/12	Spacecraft Thermal Balance	(4C)
AIR1168/13	Spacecraft Equipment Environmental Control	(4D)
AIR1168/14	Spacecraft Life Support Systems	(4E)

F.R. Weiner, formerly of Rockwell International and past chairman of the SAE AC-9B Subcommittee, is commended for his dedication and effort in preparing the errata lists that were used in creating the Third Edition.

Table of Contents

List of Figures

List of Tables

COMMON ABBREVIATIONS

abs	— Absolute
AFTR	— Air Force Technical Report
AIR	— Aerospace Information Report
ASTIA	— Armed Services Technical Information Agency
atm	— Atmosphere
av	— Average
Btu	— British Thermal Unit
cal	— Calorie
comp	— Compressible
cr	— Critical
d	— Differential notation
deg	— Degree (angle)
Dept.	— Department
dia	— Diameter
Eng	— Engineering
Eq./Eqs.	— Equation/Equations
°F	— Degrees Fahrenheit
Fig./Figs.	— Figure/Figures
fpm	— Feet per minute
fps	— Feet per second
ft	— Feet
ft/min	— Feet per minute
ft/sec	— Feet per second
Hg	— Mercury
hp	— Horsepower
hr	— Hour
in.	— Inch
$in.^2$	— Square inches
in. Hg	— Inches of mercury
in. Hg abs	— Inches of mercury absolute
in. H_2O	— Inches of water
in. H_2O abs	— Inches of water absolute
incomp	— Incompressible
isen	— Isentropic
K	— Degrees Kelvin
lb	— Pound
$lb/in.^2$	— Pounds per square inch
$lb/in.^2$ abs	— Pounds per square inch absolute
lb/ft^2	— Pounds per square foot

lb/ft^2 abs	— Pounds per square foot absolute
lb/min	— Pounds per minute
lb/hr	— Pounds per hour
lb/sec	— Pounds per second
ln	— Natural logarithm to the base *e*
max	— Maximum
min	— Minimum
NACA	— National Advisory Committee for Aeronautics
no.	— Number
%	— Percent
Par./Pars.	— Paragraph/Paragraphs
p.	— Page
pp.	— Pages
psf	— Pounds per square foot
psfa	— Pounds per square foot absolute
psi	— Pounds per square inch
psia	— Pounds per square inch absolute
psig	— Pounds per square inch gage
PTC	— Power Test Code
°R	— Degrees Rankine
R.A.E.	— Royal Aircraft Establishment (now Royal Aerospace Establishment)
Ref./Refs.	— Reference/References
RM	— Research Memorandum
rpm	— Revolutions per minute
SAE	— Society of Automotive Engineers
Sat	— Saturated
S.L.	— Sea level
sta.	— Station
sec	— Second
TN	— Technical Note
TR	— Technical Report
tr	— Triple
Trans. ASME	— Transactions of the American Society of Mechanical Engineers
W	— Watts
WADC	— Wright Air Development Center (now, Wright Research and Development Center)
Δ	— Increment
Σ	— Summation

SECTION 1A - INCOMPRESSIBLE FLUID FLOW

1. INTRODUCTION

1.1 Scope

The fluid flow treated in this section is isothermal, subsonic, and incompressible. The effects of heat addition, work on the fluid, variation in sonic velocity, and changes in elevation are neglected. An incompressible fluid is one in which a change in pressure causes no resulting change in fluid density. The assumption that liquids are incompressible introduces no appreciable error in calculations, but the assumption that a gas is incompressible introduces an error of a magnitude that is dependent on the fluid velocity and on the loss coefficient of the particular duct section or piece of equipment. Fig. 1A-1 shows the error in pressure drop resulting from assuming that air is incompressible.

With reasonably small loss coefficients and the accuracy that is usually required in most calculations, compressible fluids may be treated as incompressible for velocities less than Mach 0.2. At higher velocities and for large loss coefficients (K_t and $4fL/D$), compressible flow analysis should be used.

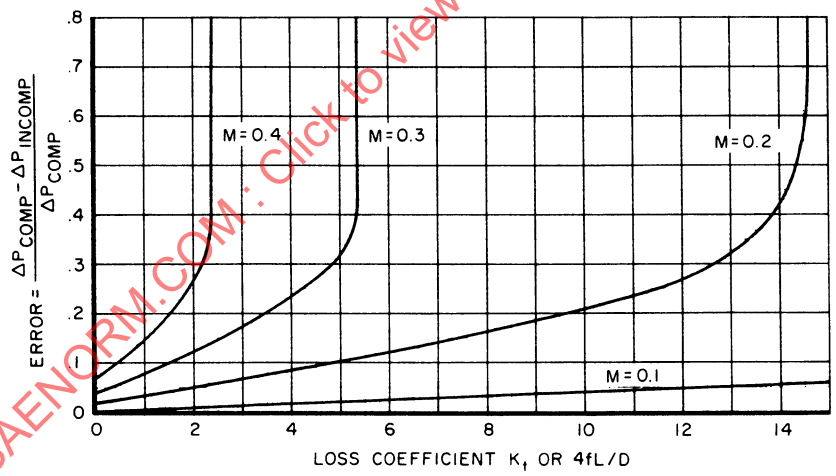

Figure 1A-1 - Incompressible Flow, Pressure Loss Error

1.2 Nomenclature

a	= Dimension of rectangle or ellipse, ft, in.
A	= Area, ft^2, $in.^2$
b	= Dimension of rectangle or ellipse, ft, in.
b	= Width, ft, in.
c or C	= Chord, ft, in.
C	= Correction factor, dimensionless

C = Unit conversion factor (Table 1A-1), dimensionless
C = Expansion factor in Fig. 1A-48, dimensionless
C' = Constant (Table 1A-6), dimensionless
C_C = Contraction coefficient (Eq. 1A-41), dimensionless
C_D = Drag coefficient, dimensionless
D = Diameter, ft, in.
D_e = Equivalent diameter, ft, in.
f = Fanning friction factor, dimensionless
f = Friction coefficient, dimensionless
F = Force, lb
g = Gravitational acceleration, ft/sec^2
G = Weight flow per unit area per unit time, lb/sec-ft^2, lb/min-in.^{2}, lb/hr-ft^2
K or K_t = Pressure loss coefficient, dimensionless
L = Length, ft, in.
m = Mass (W/g), lb-sec^2/ft, lb
n = Number of vanes or elbows
N_{Re} = Reynolds number ($VD\rho g/\mu$, $Vx\rho g/\mu$), dimensionless
P = Pressure, psi, lb/ft^2, in. Hg
P_s = Static pressure, psi, lb/ft^2
P_t = Total pressure, lb/ft^2, in. H_2O
q = Dynamic pressure, $(1/2)\rho V^2$, lb/ft^2, in. Hg, in. H_2O
Q = Volumetric flow rate, ft^3/sec, ft^3/min
r = Radius, ft, in.
R_{fa} = Ratio of free area to total area of exit, dimensionless
s = Curvilinear distance, ft, in.
s or S = Gap between vanes, ft, in.
S = Area, ft^2
t = Temperature, °F
T = Temperature, absolute, °R
V = Velocity, ft/sec, ft/min
w = Mass flow rate, lb/sec, lb/min
x,y = Distance, ft
X,Y = Nomograph coordinates
α = Angle of attack, deg
α = Angle, deg
β = Duct merge angle, deg
δ = Duct merge angle, deg
ε = Surface roughness, average, in.
η = Efficiency, dimensionless
θ = Angle, deg

λ = Function of α, β or δ (See paragraphs 3.4.1 and 3.4.2)
μ = Proportionality factor, dimensionless
μ = Absolute viscosity, lb-sec/ft^2
ρ = Mass density, lb-sec^2/ft^4
ρg = Specific weight (density), lb/ft^3
τ = Time, sec
ϕ = Expansion angle, deg
ϕ = Solidity, dimensionless

Subscripts:

av = Average
c = Compressible
c = Inside chord
COMP = Compressible
D = Drag
ef = Effective
i = Inner
INCOMP = Incompressible
m = Mean
max = Maximum
o = Outer
o = Freestream
o = Outside
p = Pressure
r = Resistance
t = Total
t = Vena contracta
0.5 = Location where velocity is 1/2 of centerline velocity
90 = For 90° bend
1 = Point 1
2 = Point 2

Superscripts:

$\bar{}$ = Mean Value

2. BASIC FLUID MECHANICS

2.1 Continuity Equation

The continuity equation is generally expressed in the form

$$\rho AV = \text{constant} \qquad (1A\text{-}1)$$

and reduces to

$$AV = \text{constant}$$

for ideal incompressible flow.

2.2 Momentum Equation

The form of the momentum equation most commonly used in fluid flow is

$$\sum F = \frac{d(mV)}{d\tau} \tag{1A-2}$$

where the summation of the forces is equal to the pressure, wall, and frictional forces on the fluid.

2.3 Energy Equation

The energy equation for incompressible frictionless flow can be expressed in a form called Bernoulli's equation:

$$P_s + (1/2)\rho V^2 = \text{constant} \tag{1A-3}$$

where the first term is the static pressure and the second term is the dynamic pressure of the fluid. The sum of the two is called the total pressure. To give physical meaning to the above pressures, they can be defined as follows:

(a) Static Pressure: This is the pressure sensed by a probe moving with the same velocity as the fluid stream. Practically, it is measured by a pressure probe located normal to the fluid stream.

(b) Dynamic Pressure: This is the static pressure rise that a fluid experiences when it is reversibly brought to rest, commonly noted as q.

(c) Total Pressure: This is the pressure of a moving fluid if it is reversibly brought to rest. It is equal to the sum of the static and dynamic pressure.

2.4 Viscosity Concepts

In Bernoulli's equation, Eq. 1A-3, fluid frictional forces caused by viscosity have not been considered. In any real fluid these forces are caused by the shearing stresses that exist between the individual streamlines, where they are flowing at different velocities. For conditions of laminar flow, shearing stress is given by Newton's equation

$$\frac{F}{S} = \mu\frac{dV}{dx} \tag{1A-4}$$

where the proportionality factor μ is the property of the fluid called absolute viscosity and dV/dx is the velocity gradient normal to the flow. The shearing stress that exists in a fluid is therefore proportional to the viscosity and the velocity gradient that exists in the fluid normal to the direction of its flow. In most liquids and gases the absolute viscosity depends primarily on the temperature of the fluid. There is only a slight dependency of absolute viscosity on pressure, except when the fluid is near the critical point, or if the gases have dissociated.

2.5 Boundary Layer Flow

When a real fluid is in motion along a wall, the fluid particles adjacent to the wall are retarded by frictional forces. These retarding forces cause a velocity gradient near the wall, thereby defining a zone of flow called the "boundary layer."

The thickness of the boundary layer is usually defined by the two extremes of velocity: zero at the wall and 99% (or 99.5%) of local free stream velocity at the outer edge. Within this layer, the distribution of velocity is dependent on whether the flow is laminar or turbulent, and thereby it determines the velocity gradient at the wall and the shear force or "drag" on the wall. In a constant area duct, this drag force per unit surface area per unit length is balanced and thus is equal to a pressure loss or pressure drop per unit cross-sectional area per unit length.

2.5.1 Laminar-Turbulent

In laminar flow, the streamlines are orderly and undisturbed, and all shear developed is purely by molecular interaction. In turbulent flow, random eddies exist, causing momentum transfer across streamlines due to the irregular movement of finite masses of fluid.

2.5.2 Reynolds Number

In order to predict whether the boundary layer flow will be laminar or turbulent, the ratio of inertia forces to viscous forces must be considered. This ratio is, by definition, the Reynolds number (N_{Re}) and is equal to $Vx\rho g/\mu$ or $VD_e\rho g/\mu$. Flow conditions in a smooth closed channel will usually be laminar if the Reynolds number (based on hydraulic diameter) is less than 2000 and turbulent if above 4000. A "transition" type of flow exists between these values. For the case of a smooth flat plate submerged in an infinite flow field, the transition occurs at approximately N_{Re} = 500,000 to 1,000,000 where the distance along the surface from the leading edge is the characteristic dimension used in the Reynolds number.

The growth in thickness of the boundary layer is illustrated in Fig. 1A-2. Over a flat plate (negligible pressure gradient), the laminar portion increases in thickness as the square root of the distance, and the turbulent region increases as the 0.8 power of the distance. Fig. 1A-2 also indicates the transition from laminar to turbulent flow as well as the limitation (beyond the entry region) of the growth of the boundary layer when the flow is confined to a duct or channel.

2.5.3 Friction Drag and Duct Pressure Loss Concepts

Eq. 1A-4 defined the shear stress that acts on the internal surface of a duct when a known velocity gradient exists at the wall. Downstream of the entrance region of a duct, the velocity gradient is independent of duct length, as indicated in the lower part of Fig. 1A-2. The shear stress causes a force along the wall proportional to the area in contact with the fluid, and this force is referred to as a drag or friction force.

In classical aerodynamic theory, the drag force acting on a surface A is expressed as

$$F_D = C_D q A, \quad \text{where } q = (1/2)\rho V^2$$

For a round duct, the surface area is

$$A = \pi DL$$

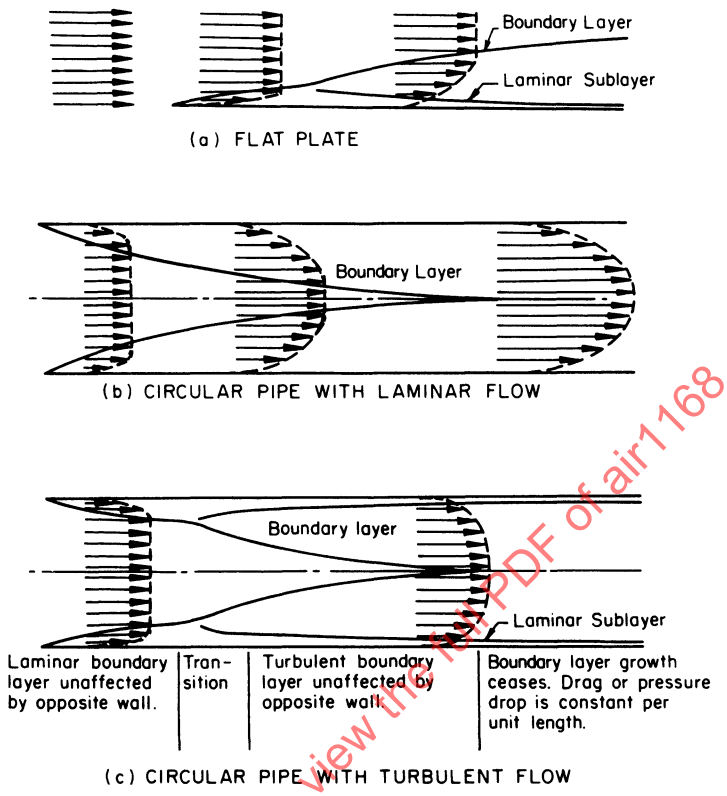

Figure 1A-2 - Boundary Layers and Velocity Distribution

The drag or friction force must be overcome by a pressure force corresponding to the duct pressure drop, so that

$$F_D = (P_{\Omega 1} - P_{\Omega 2})\left(\frac{\pi D^2}{4}\right) = \Delta P_t \left(\frac{\pi D^2}{4}\right) \tag{1A-5}$$

Equating:

$$\Delta P_t = C_D \left(\frac{\pi DL}{\pi D^2/4}\right) q = 4C_D\left(\frac{L}{D}\right) q = \frac{4fL}{D} q \tag{1A-6}$$

In duct flow, C_D is replaced by the symbol of the Fanning friction factor, f. As mentioned above, the shear stress at the wall becomes a constant value for pipe flow in equilibrium, and therefore the friction factor is also a constant. Fig. 1A-3 shows the friction factor and the ratio of average to maximum velocity in pipe flow for these equilibrium conditions.

The roughness of a pipe changes the velocity profile at the wall. It also changes the shear stress and the friction factor. (See Fig. 1A-4.)

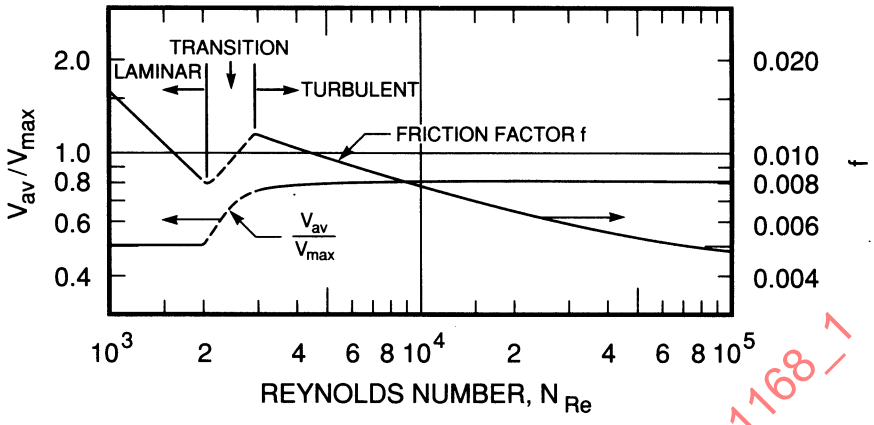

Figure 1A-3 - Pipe Velocity and Friction Factors

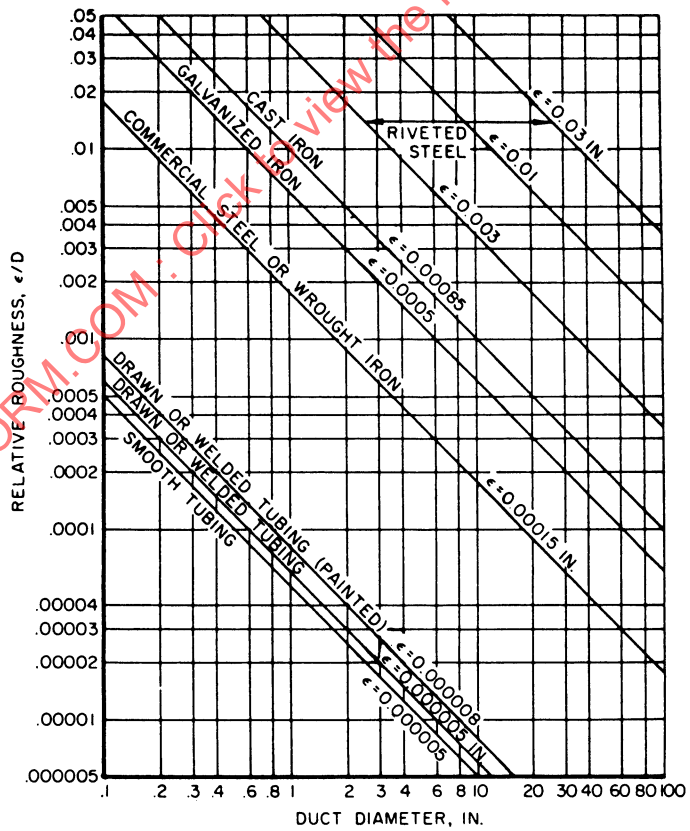

Figure 1A-4 - Relative Roughness, Circular Ducts

2.6 Total Pressure Loss Due to Change of Fluid Velocity Profile

In the discussion above, it was shown how the viscosity caused a velocity gradient at the fluid boundaries, with its associated friction drag and pressure loss. It may be logically reasoned from this that any change in the fluid velocity profile will cause a loss of energy and result in a corresponding pressure loss. Any change in direction, cross-sectional area, or shape will cause a loss in total pressure. In dealing with losses of this type, the following equation is used:

$$\Delta P_t = K_t (1/2)\,\rho V^2 = K_t\, q \qquad \text{(1A-7)}$$

where K_t is the pressure loss coefficient for the change in direction, shape, or other type of loss. It should be emphasized that the loss coefficients are determined for one particular arrangement of ducting leading into and out of the device whose loss coefficient is being measured. Therefore, when combinations of devices are used, the loss coefficient of the system will not necessarily be the sum of the individual loss coefficients, but may be either larger or smaller. By careful selection of the location of bends, diffusers, and contractions to achieve the minimum change in velocity profile, the pressure loss can be reduced to a minimum. Examples of this would be the use of one 180 deg bend instead of two 90 deg bends separated by a straight section of pipe. Do not diffuse around a bend, and avoid large area changes at duct junctions.

In summary, the total losses in a system can be expressed by the equation

$$\Delta P_t = \sum K_t \left(\frac{1}{2}\rho V^2\right) + \sum \frac{4fL}{D}\left(\frac{1}{2}\rho V^2\right) \qquad \text{(1A-8)}$$

where the dynamic or velocity pressure $(1/2)\rho V^2$ is evaluated at the reference area of the loss coefficient and the friction factor f. For convenience, the dynamic pressure $(1/2)\rho V^2$ can be evaluated from Tables 1A-1 and 1A-2 and the equation

$$q = \frac{1}{2}\rho V^2 = \frac{G^2}{\rho g C} \qquad \text{(1A-9)}$$

where C = a unit conversion factor, dimensionless

Table 1A-1 - Table for Unit Conversion Factor C for ρg (lb/ft^3)

Units of q	Units of G				
	lb/hr-ft^2	lb/min-ft^2	lb/sec-ft^2	lb/sec-in.^{2}	lb/min-in.^{2}
lb/ft^2	8.35×10^8	2.32×10^5	64.4	3.11×10^{-3}	11.20
lb/in.^{2}	1.202×10^{11}	3.34×10^7	9.28×10^3	0.447	1.61×10^3
in. H_2O	4.34×10^9	1.205×10^6	3.35×10^2	1.615×10^{-2}	58.14
in. Hg	5.90×10^{10}	1.64×10^7	4.56×10^3	0.2196	7.91×10^2

Table 1A-2 - Table for ρg of Air

	Units of P_s (T = °R)			
	in. Hg abs	psia lb/in.^{2} abs	psfa lb/ft^2 abs	in. H_2O abs
lb/ft^3	$1.326\ \frac{P_s}{T}$	$2.70\ \frac{P_s}{T}$	$1.875 \times 10^{-2}\ \frac{P_s}{T}$	$9.76 \times 10^{-2}\ \frac{P_s}{T}$

A sample usage of Tables 1A-1 and 1A-2 is

$\rho g = 2.70 P_s/T$, lb/ft^3 (from Table 1A-2)

$G = w/A$, lb/min-in.^{2}

$C = 58.14$ (from Table 1A-1)

$$q = \frac{TG^2}{2.70\, P_s(58.14)},\ \text{in. } H_2O$$

where w is in lb/min, P_s in psia, T in °R, and A in in.^{2}.

3. SPECIFIC PRESSURE LOSS DATA:

3.1 Pressure Losses, Straight Ducts

As noted in Par. 2.5.3, the pressure loss in straight ducts can be determined as follows:

$$\Delta P_t = \frac{4fL}{D}\left(\frac{1}{2}\right)\rho V^2 \qquad (1A\text{-}10)$$

For most aircraft ducting, the ducts can be treated as smooth tubes, but to obtain a physical feel for the roughness where actual data are lacking, Fig. 1A-4 is presented for a number of common materials. The relative roughness presented in this figure is the mean roughness projection (ε) and is the arithmetic average surface deviation from the mean line of the surface, in inches. Friction factors are shown in Fig. 1A-5 for long pipe lengths, where entrance effects are small. Nomographs for determining Reynolds numbers are shown in Figs. 1A-6 and 1A-7 together with Tables 1A-3 and 1A-4 for gases and liquids.

In computing the pressure drop from Eq. 1A-10 and the Reynolds number for ducts of noncircular section, an equivalent diameter of the section must be used and is defined as

$$D_e = \frac{4 \times (\text{cross-sectional area})}{\text{wetted perimeter}}. \qquad (1A\text{-}11)$$

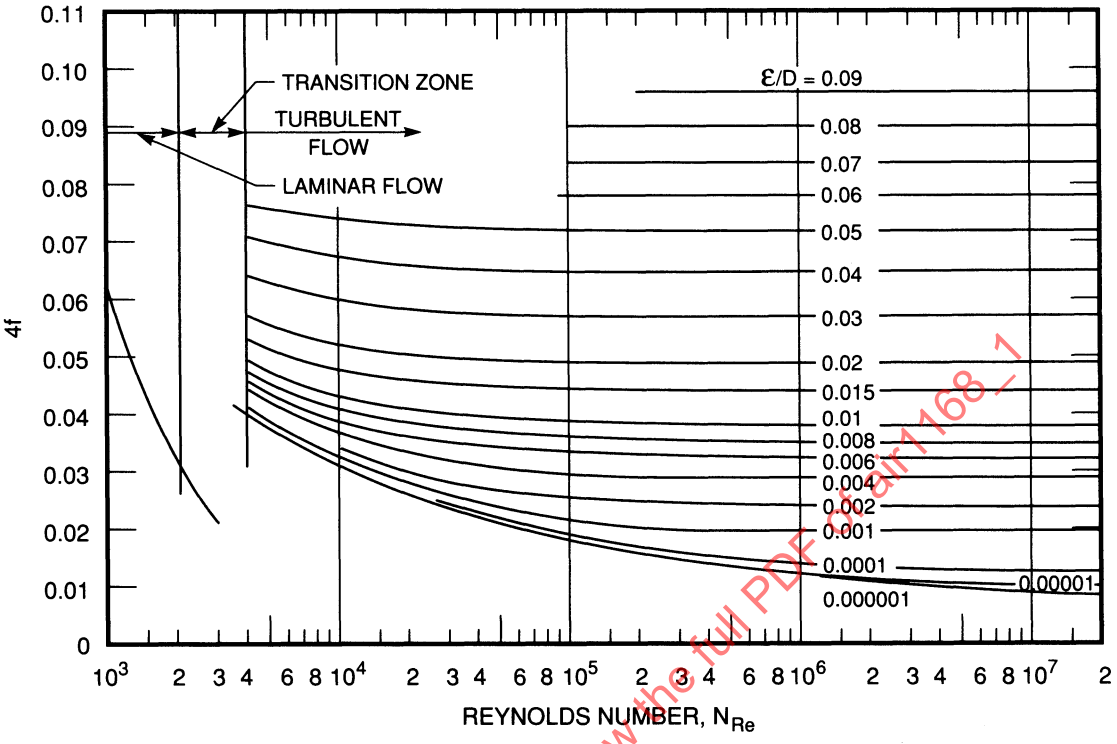

Figure 1A-5 - Friction Factor Versus Reynolds Number (Ref. 14)

For some of the more common shapes the equivalent diameters are:

Square duct: D_e = length of side

Rectangular duct: $D_e = 2ab/(a+b)$ (a and b are sides)

Elliptical duct:

$$D_e = 2ab\left(\frac{2}{a^2+b^2}\right)^{1/2}$$

(a and b are semi-major and semi-minor axes, respectively)

Annular duct: $D_e = D_o - D_i$

where D_o and D_i are the outer and inner duct diameters, respectively.

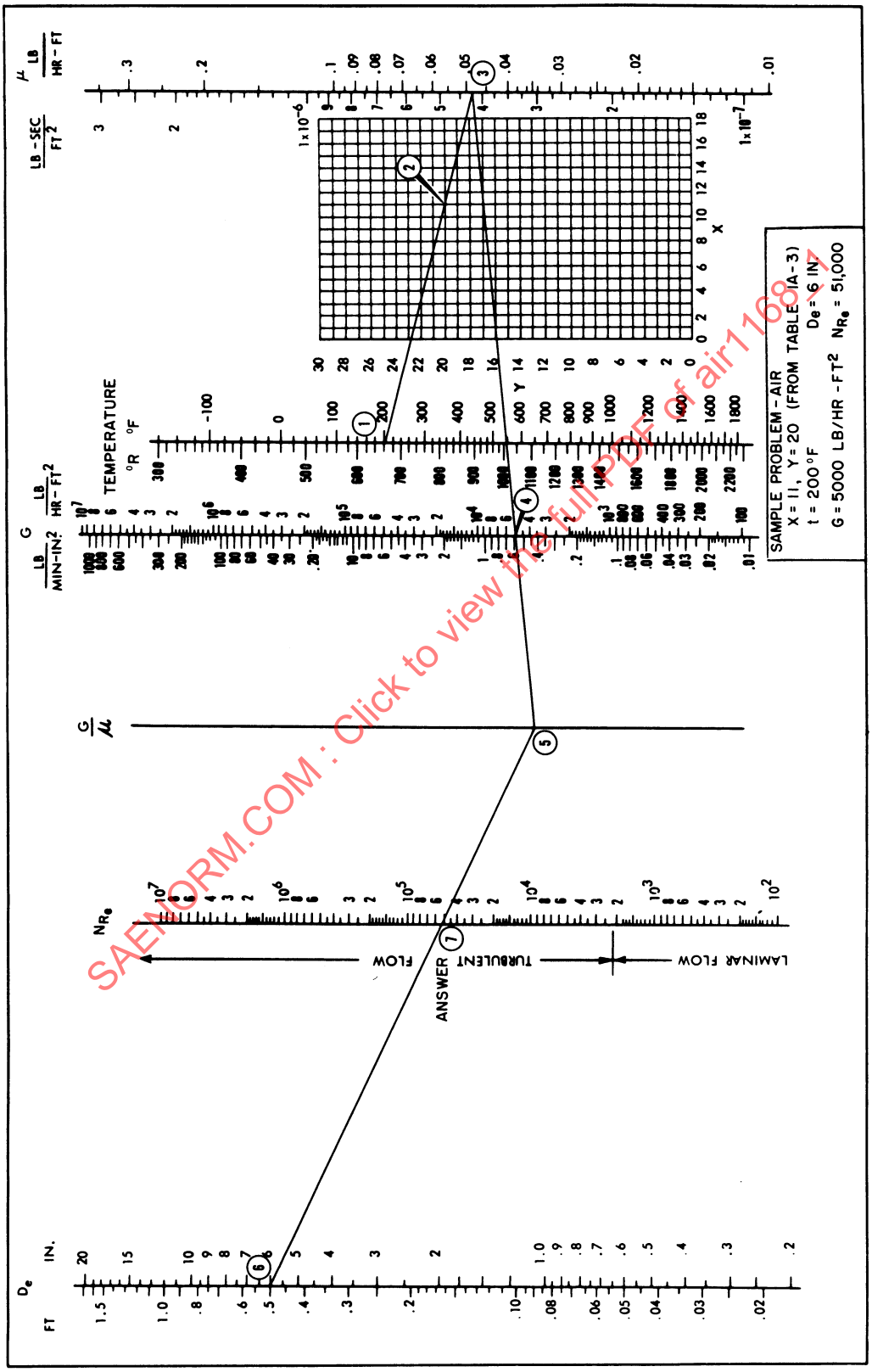

Figure 1A-6 - Reynolds Number in Gases

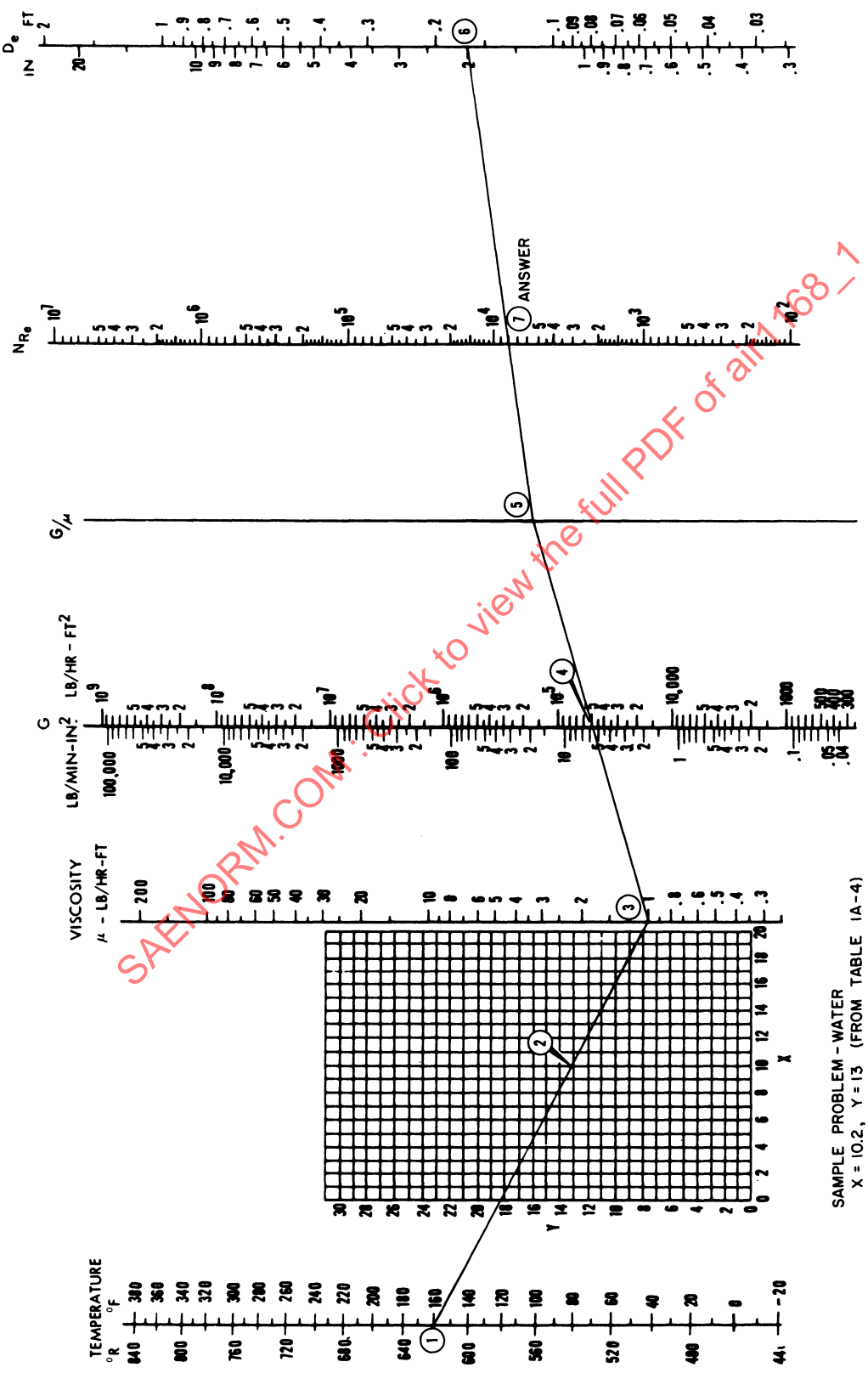

Figure 1A-7 - Reynolds Number in Liquids

Table 1A-3 - Coordinates for Reynolds Number Nomograph for Gases (Fig. 1A-6)[1]

Gas	X	Y	Gas	X	Y
Acetic Acid	7.7	14.3	Freon-113	11.3	14.0
Acetone	8.9	13.0	Helium	10.9	20.5
Acetylene	9.8	14.9	Hexane	8.6	11.8
Air	11.0	20.0	Hydrogen	11.2	12.4
Ammonia	8.4	16.0	3 H_2N_2	11.2	17.2
Argon	10.5	22.4	Hydrogen Bromide	8.8	20.9
Benzene	8.5	13.2	Hydrogen Chloride	8.8	18.7
Bromine	8.9	19.2	Hydrogen Cyanide	9.8	14.9
Butene	9.2	13.7	Hydrogen Iodide	9.0	21.3
Butylene	8.9	13.0	Hydrogen Sulfide	8.6	18.0
Carbon Dioxide	9.5	18.7	Iodine	9.0	18.4
Carbon Disulfide	8.0	16.0	Mercury	5.3	22.9
Carbon Monoxide	11.0	20.0	Methane	9.9	15.5
Chlorine	9.0	18.4	Methyl Alcohol	8.5	15.6
Chloroform	8.9	15.7	Nitric Oxide	10.9	20.5
Cyanogen	9.2	15.2	Nitrogen	10.6	20.0
Cyclohexane	9.2	12.0	Nitrosyl Chloride	8.0	17.6
Ethane	9.1	14.5	Nitrous Oxide	8.8	19.0
Ethyl Acetate	8.5	13.2	Oxygen	11.0	21.3
Ethyl Alcohol	9.2	14.2	Pentane	7.0	12.8
Ethyl Chloride	8.5	15.6	Propane	9.7	12.9
Ethyl Ether	8.9	13.0	Propyl Alcohol	8.4	13.4
Ethylene	9.5	15.1	Propylene	9.0	13.8
Fluorine	7.3	23.8	Sulfur Dioxide	9.6	17.0
Freon-11	10.6	15.1	Toluene	8.6	12.4
Freon-12	11.1	16.0	2,2,3-Trimethylbutane	9.5	10.5
Freon-21	10.8	15.3	Water Vapor	8.0	16.0
Freon-22	10.1	17.0	Xenon	9.3	23.0

[1] Ref. 11.

The following formulas are useful in determining the friction factors of smooth pipes over the ranges listed and approximate the data on Fig. 1A-5.

$$f = \frac{16}{N_{Re}} \quad \text{for } N_{Re} < 2100 \tag{1A-12}$$

$$f = \frac{0.0791}{N_{Re}^{0.25}} \quad \text{for } N_{Re} = 3000 \text{ to } 10{,}000 \tag{1A-12a}$$

$$f = \frac{0.046}{N_{Re}^{0.2}} \quad \text{for } N_{Re} = 10{,}000 \text{ to } 5 \times 10^6 \tag{1A-13}$$

Table 1A-4 - Coordinates for Reynolds Number Nomograph for Liquids (Fig. 1A-7)[1]

Liquid	X	Y	Liquid	X	Y
Acetaldehyde	15.2	4.8	Freon-22	17.2	4.7
Acetic Acid 100%	12.1	14.2	Freon-113	12.5	11.4
Acetic Acid 70%	9.5	17.0	Glycerol 100%	2.0	30.0
Acetic Anhydride	12.7	12.8	Glycerol 50%	6.9	19.6
Acetone 100%	14.5	7.2	Heptane	14.1	8.4
Acetone 35%	7.9	15.0	Hexane	14.7	7.0
Allyl Alcohol	10.2	14.3	Hydrochloric Acid 31.5%	13.0	16.6
Ammonia 100%	12.6	2.0	Isobutyl Alcohol	7.1	18.0
Ammonia 26%	10.1	13.9	Isobutyric Acid	12.2	14.4
Amyl Acetate	11.8	12.5	Isopropyl Alcohol	8.2	16.0
Allyl Alcohol	7.5	18.4	Kerosene	10.2	16.9
Aniline	8.1	18.7	Linseed Oil, Raw	7.5	27.2
Anisole	12.3	13.5	Mercury	18.4	16.4
Arsenic Trichloride	13.9	14.5	Methanol 100%	12.4	10.5
Benzene	12.5	10.9	Methanol 90%	12.3	11.8
Brine, $CaCl_2$, 25%	6.6	15.9	Methanol 40%	7.8	15.5
Brine, NaCl, 25%	10.2	16.6	Methyl Acetate	14.2	8.2
Bromine	14.2	13.2	Methyl Chloride	15.0	3.8
Bromotoluene	20.0	15.9	Methyl Ethyl Ketone	13.9	8.6
Butyl Acetate	12.3	11.0	Naphthalene	7.9	18.1
Butyl Alcohol	8.6	17.2	Nitric Acid 95%	12.8	13.8
Butyric Acid	12.1	15.3	Nitric Acid 60%	10.8	17.0
Carbon Dioxide	11.6	0.3	Nitrobenzene	10.6	16.2
Carbon Disulfide	16.1	7.5	Nitrotoluene	11.0	17.0
Carbon Tetrachloride	12.7	13.1	Octane	13.7	10.0
Chlorobenzene	12.3	12.4	Octyl Alcohol	6.6	21.1
Chloroform	14.4	10.2	Pentachloroethane	10.9	17.3
Chlorosulfonic Acid	11.2	18.1	Pentane	14.9	5.2
Chlorotoluene, ortho-	13.0	13.3	Phenol	6.9	20.8
Chlorotoluene, meta-	13.3	12.5	Phosphorus Tribromide	13.8	16.7
Chlorotoluene, para-	13.3	12.5	Phosphorus Trichloride	16.2	10.9
Cresol, meta-	2.5	20.8	Propionic Acid	12.8	13.8
Cyclohexanol	2.9	24.3	Propyl Alcohol	9.1	16.5
Dibromoethane	12.7	15.8	Propyl Bromide	14.5	9.6
Dichloroethane	13.2	12.2	Propyl Chloride	14.4	7.5
Dichloromethane	14.6	8.9	Propyl Iodide	14.1	11.6
Diethyl Oxalate	11.0	16.4	Sodium	16.4	13.9
Dimethyl Oxalate	12.3	15.8	Sodium Hydroxide 50%	3.2	25.8
Diphenyl	12.0	18.3	Stannic Chloride	13.5	12.8
Dipropyl Oxalate	10.3	17.7	Sulfur Dioxide	15.2	7.1
Ethyl Acetate	13.7	9.1	Sulfuric Acid 110%	7.2	27.4
Ethyl Alcohol 100%	10.5	13.8	Sulfuric Acid 98%	7.0	24.8
Ethyl Alcohol 95%	9.8	14.3	Sulfuric Acid 60%	10.2	21.3
Ethyl Alcohol 40%	6.5	16.6	Sulfuryl Chloride	16.2	12.4
Ethyl Benzene	13.2	11.5	Tetrachloroethane	11.9	15.7
Ethyl Bromide	14.5	8.1	Tetrachloroethylene	14.2	12.7
Ethyl Chloride	14.8	6.0	Titanium Tetrachloride	14.4	12.3
Ethyl Ether	14.5	5.3	Toluene	13.7	10.4
Ethyl Formate	14.2	8.4	Trichloroethylene	14.8	10.5
Ethyl Iodine	14.7	10.3	Turpentine	11.5	14.9
Ethylene Glycol	6.0	23.6	Vinyl Acetate	14.0	8.8
Formic Acid	10.7	15.8	Water	10.2	13.0
Freon-11	14.4	9.0	Xylene, ortho-	13.5	12.1
Freon-12	16.8	5.6	Xylene, meta-	13.9	10.6
Freon-21	15.7	7.5	Xylene, para-	13.9	10.9

[1] Ref. 11.

The following equation approximates data over the entire range of experiments:

$$\frac{1}{\sqrt{f}} = 40\log_{10}\left(N_{Re}\sqrt{f}\right) - 0.40 \qquad \text{(1A-14)}$$

It is recommended for extrapolating to higher Reynolds numbers.

For air, the factor $4f$ versus w/D is presented in Fig. 1A-8 to simplify the calculation of ΔP_t, using Eq. 1A-10.

3.2 Pressure Losses, Elbows

The flow loss in a bend or an elbow is

$$\Delta P_t = \left(4f\frac{L}{D} + CK_{t90}\right)\left(\frac{1}{2}\rho V^2\right) \qquad \text{(1A-15)}$$

where C = Correction factor for bends other than 90 deg, dimensionless
L = Length along centerline of duct

The loss coefficients for all bends and elbows given in the succeeding sections give total pressure loss due to turning only. The wall or straight duct friction loss must be added to this loss to determine the overall loss of the elbow. Fig. 1A-9 illustrates the combined pressure loss, turning plus duct friction, in a circular duct for various radius ratios. It is seen from this figure that the minimum loss occurs at an r/D ratio of 3. While this particular figure is for a Reynolds number equal to 10^6, the principle holds true for other Reynolds numbers. Therefore, considering both pressure drop and fabrication, a bend with a radius ratio between 2 and 3 should be used wherever possible.

Note: The loss coefficients for bends and elbows in Figs. 1A-10 to 1A-21, unless otherwise specified, apply to elbows followed by a length of duct equal to at least four duct diameters. If no duct follows the elbow, the loss coefficient should be corrected as in Par. 3.2.1.

3.2.1 Effect of Discharge Duct

When the discharge duct at the exit of an elbow is removed, the flow pattern through the elbow is changed, and this changes the loss coefficient. For bend angles less than 90 deg, the flow losses are increased by removing the exit duct; for angles greater than 90 deg, the flow losses are decreased by removing the exit duct. This can be explained by the fact that for angles greater than 90 deg, the removal of the exit duct reduces the net turning angle, and this is the predominant loss effect. The effect of the exit duct is plotted in Fig. 1A-22 for 90 deg bends and presents the ratio of the loss factor with and without the exit duct. The loss without the exit duct is for the loss just up to the exit end of the elbow. Therefore, an additional loss for the sudden expansion should be added to the values obtained to determine the total loss of an elbow without an exit duct (3.3). For angles other than 90 deg, Fig. 1A-23 is used to correct the loss factors obtained from Fig. 1A-22 for bend angle. Although the data used to obtain Fig. 1A-22 were obtained from rectangular ducts, they can be applied to elliptical and circular ducts in lieu of specific data for these ducts.

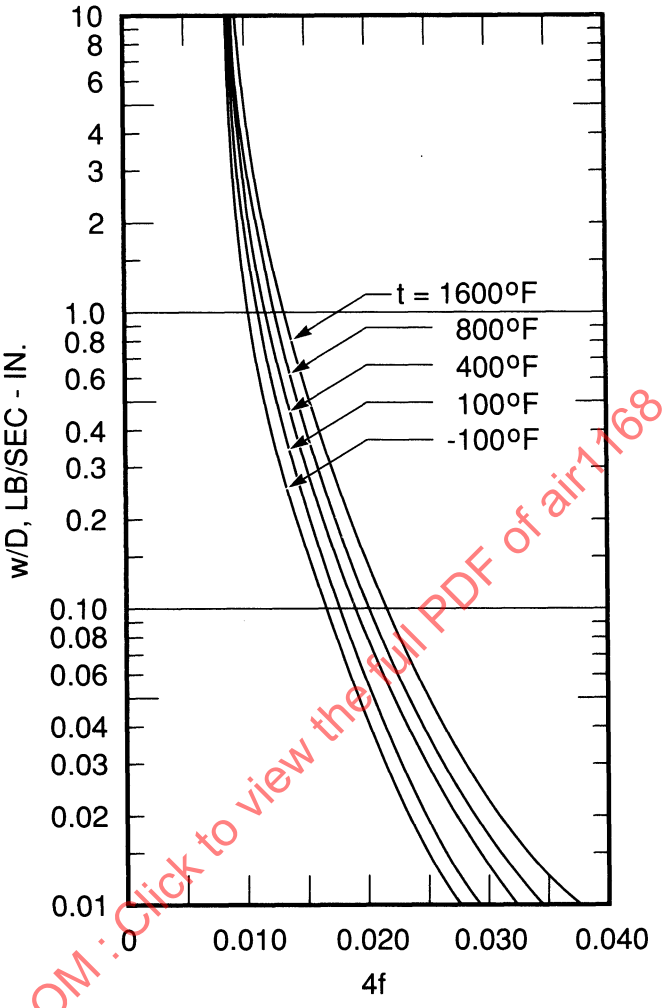

Figure 1A-8 - Friction Factor Versus Weight Flow Per Unit Diameter, Air in Smooth Round Ducts

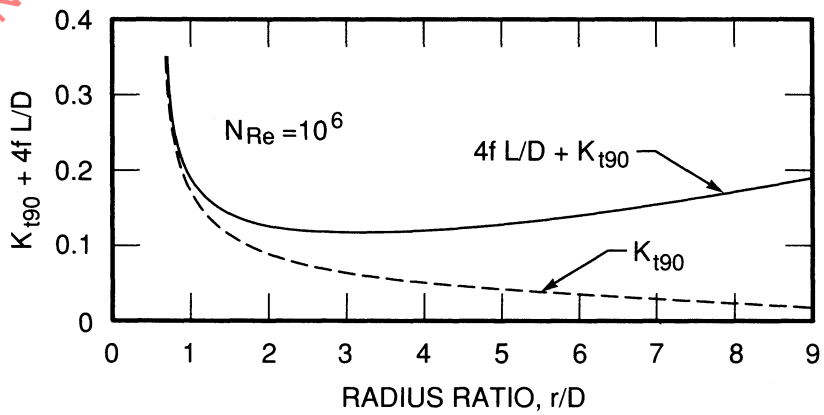

Figure 1A-9 - Bend Loss

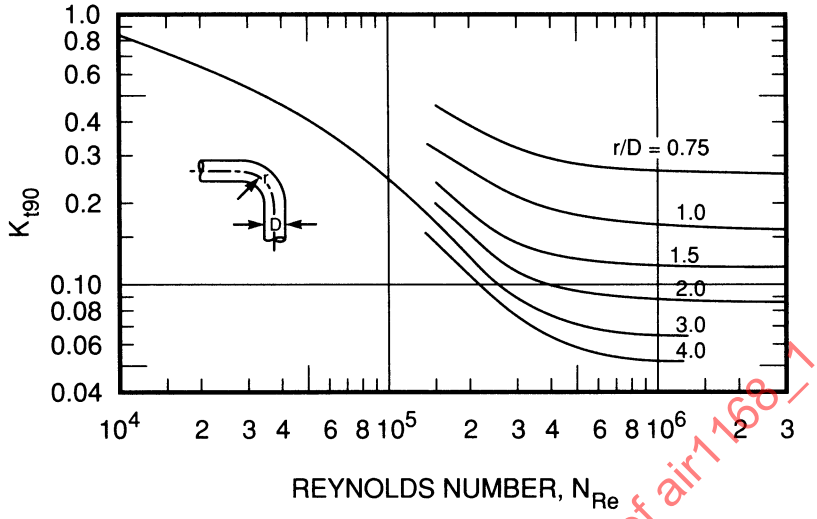

Figure 1A-10 - Loss Coefficient Versus Reynolds Number for 90 deg Radius Bends, Circular Ducts. (Data for $N_{Re} > 10^5$ From Ref. 1, for $N_{Re} < 10^5$ From Ref. 28)

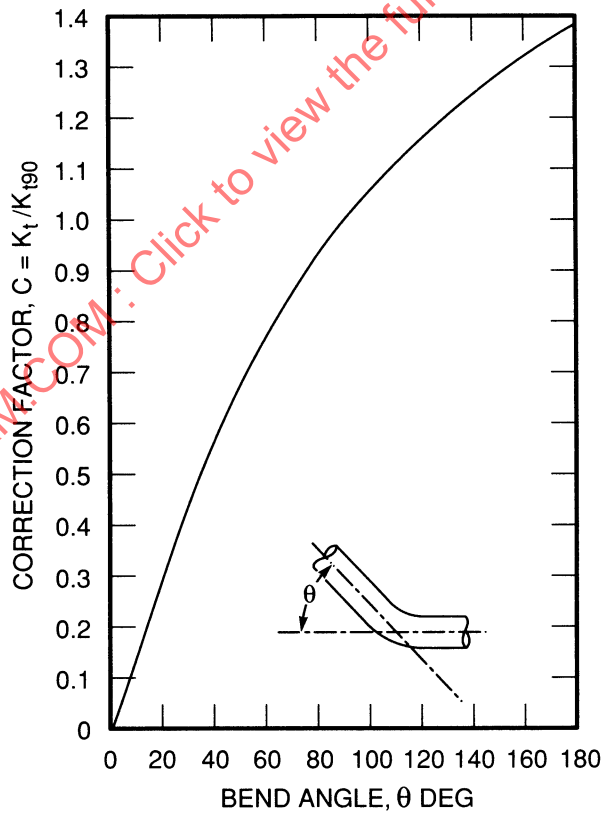

Figure 1A-11 - Correction Factor for Bends Other Than 90 deg for Elliptical and Circular Ducts (From Ref. 12, Fig. 16)

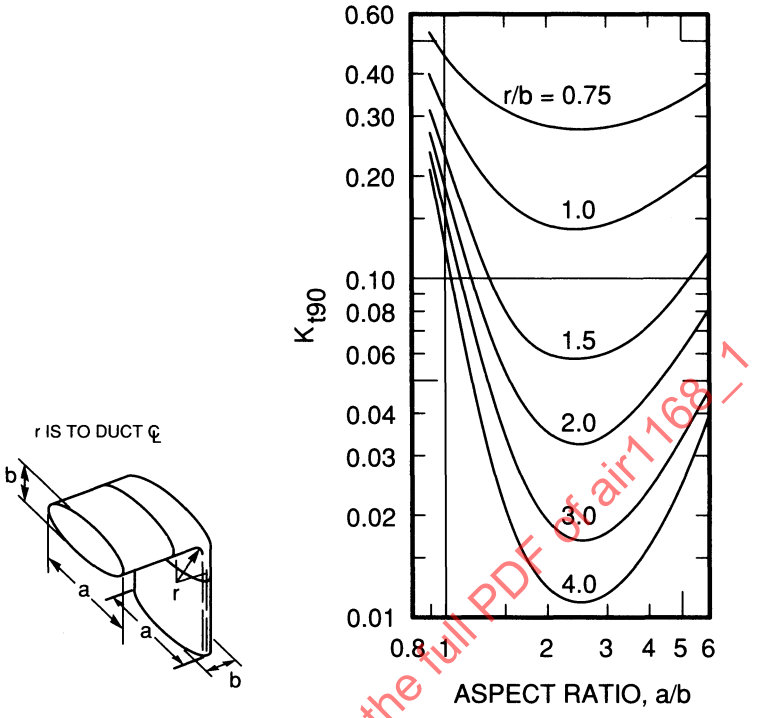

Figure 1A-12 - Loss Coefficient for 90 deg Radius Bends, Elliptical Ducts, N_{Re} = 150,000 (From Ref. 1, Fig. 3a)

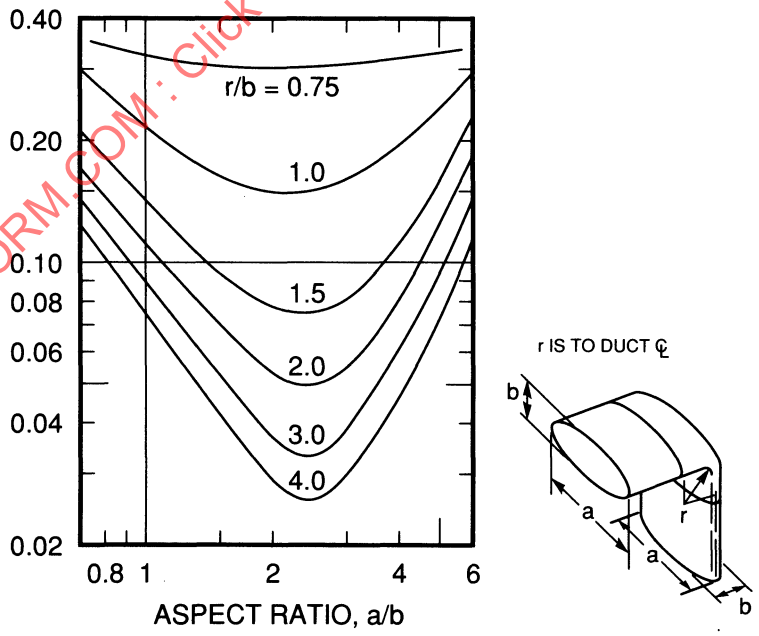

Figure 1A-13 - Loss Coefficient for Radius Bends, Elliptical Ducts, N_{Re} = 300,000 (From Ref. 1, Fig. 3b)

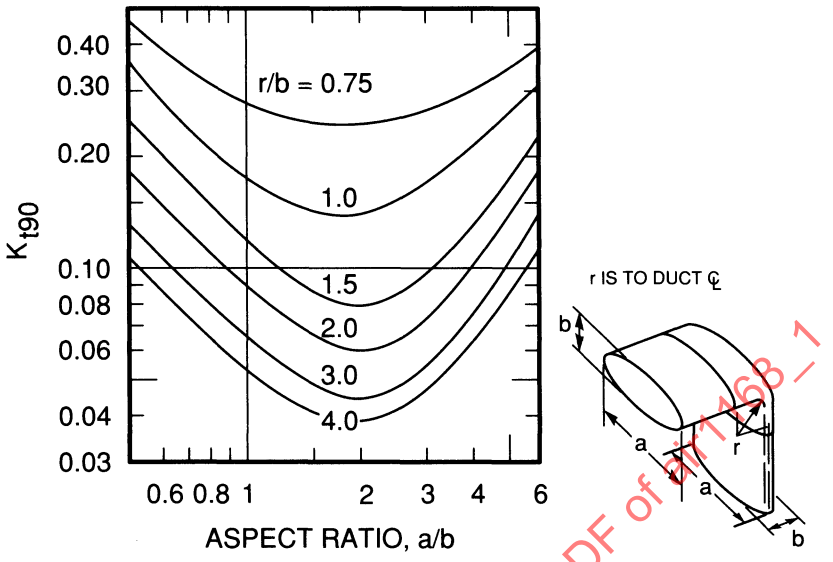

Figure 1A-14 - Loss Coefficient for 90 deg Bends, Elliptical Ducts, N_{Re} = 600,000 (From Ref. 1, Fig. 3c)

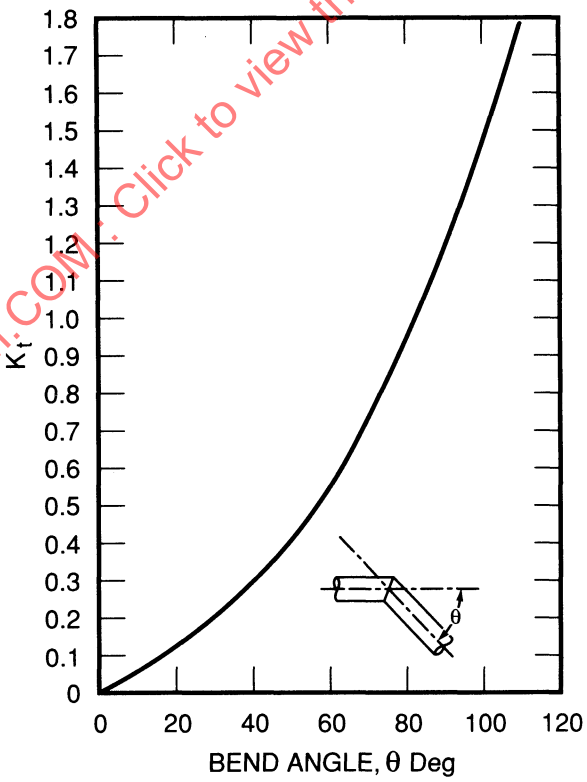

Figure 1A-15 - Loss Coefficient for Miter Bends, Circular Ducts, N_{Re} < 1000 (From Ref. 12)

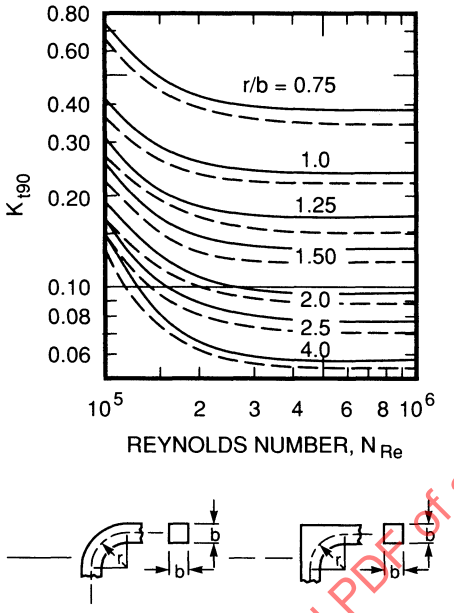

Figure 1A-16 - Loss Coefficient Versus Reynolds Number for 90 deg Radius Elbows, Square Ducts (From Ref. 1, Fig. 2; Ref. 9)

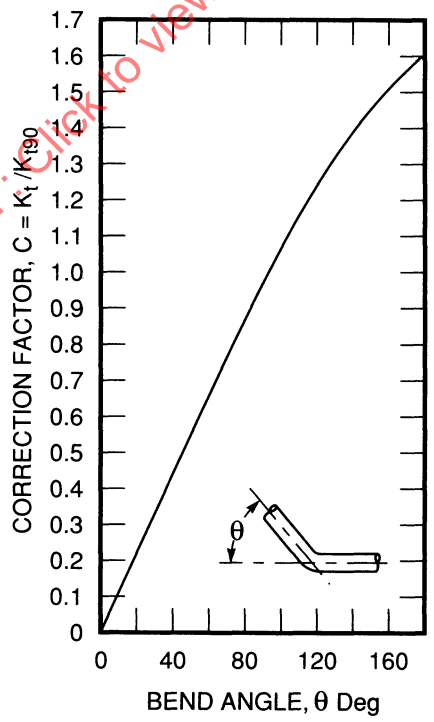

Figure 1A-17 - Correction Factor for Bends Other Than 90 deg, Rectangular and Square Ducts (From Ref. 5)

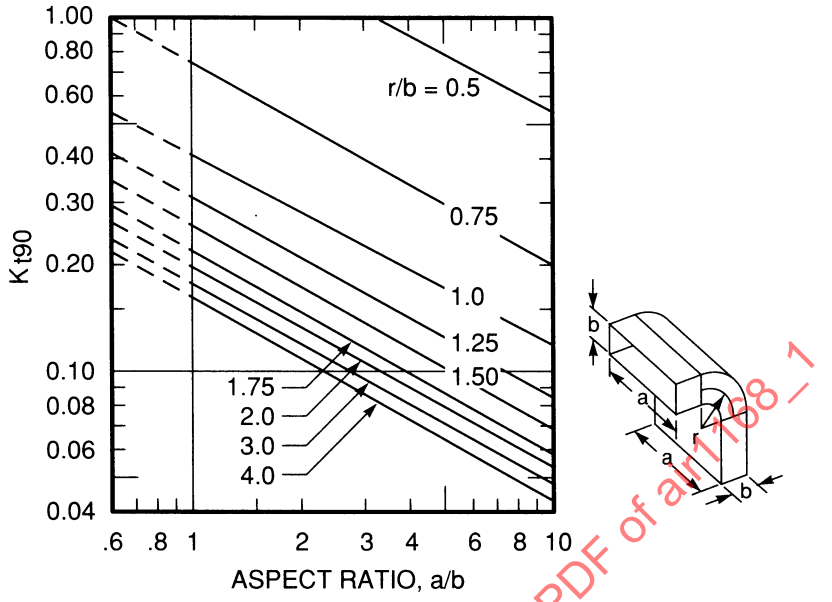

Figure 1A-18 - Loss Coefficient for 90 deg Bends, Rectangular Ducts, N_{Re} = 100,000 (From Ref. 1, Fig. 2a)

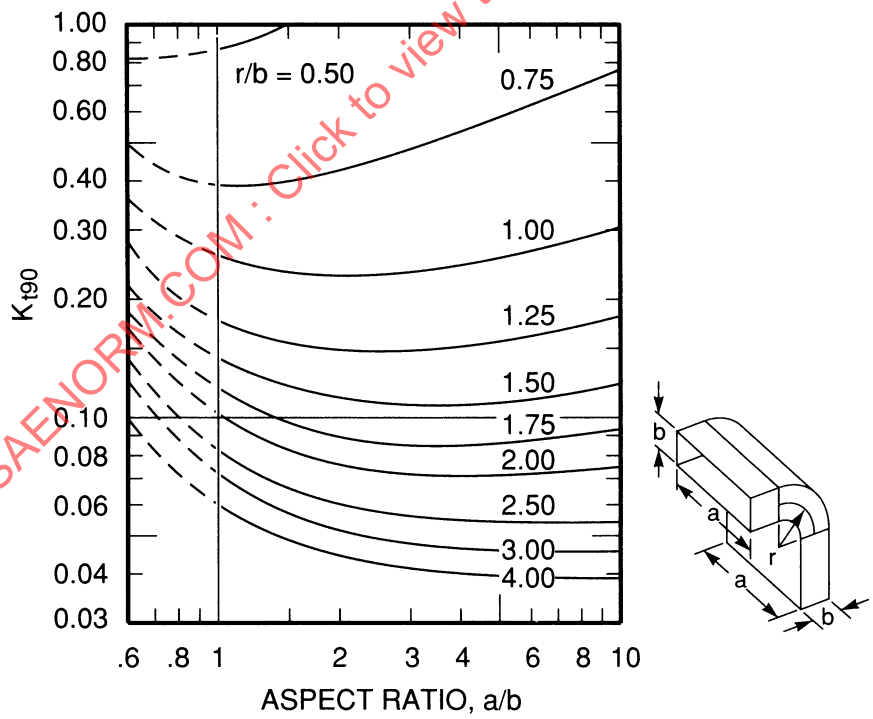

Figure 1A-19 - Loss Coefficient for 90 deg Radius Bends, Rectangular Ducts, N_{Re} = 300,000 (From Ref. 1, Fig. 2b)

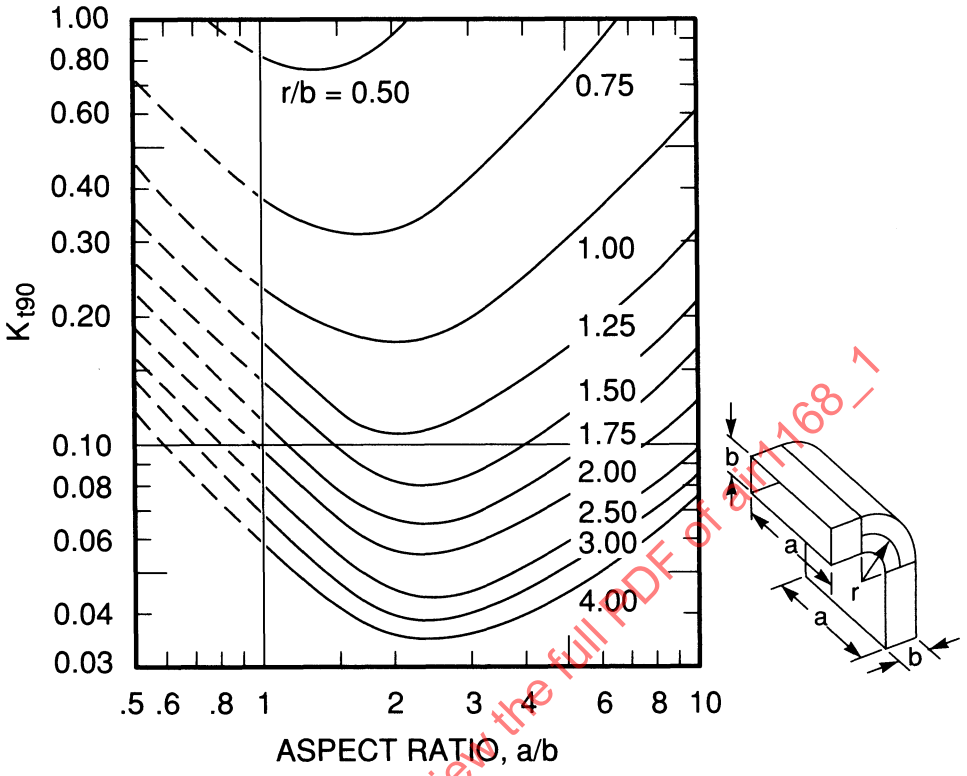

Figure 1A-20 - Loss Coefficient for 90 deg Radius Bends, Rectangular Ducts, N_{Re} = 600,000 (From Ref. 1, Fig. 2c)

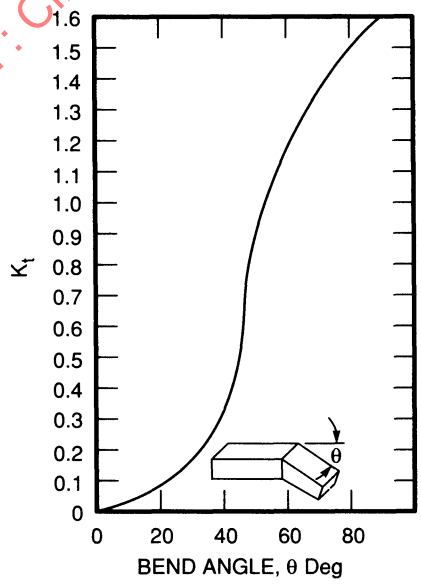

Figure 1A-21 - Loss Coefficient for Square Mitered Elbow (From Ref. 13)

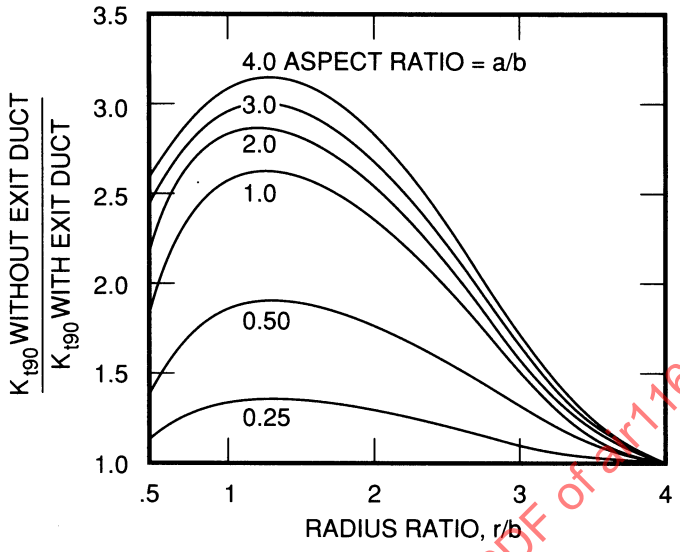

Figure 1A-22 - Effect of Exit Duct on 90 deg Elbow (Data From Ref. 5)

3.2.2 Compound Elbows

Figs. 1A-24 and 1A-25 for circular ducts plot K_t versus r/D for compound U-bends and 90 deg offset bends, respectively. Fig. 1A-26 plots the same values for Z-bends.

3.2.3 Improving Bend Efficiency

3.2.3.1 Turning Vanes

Turning vanes are used in sharp bends to improve the exit velocity distribution and reduce the pressure loss. All the turning vanes in a particular elbow are of the same size and shape as opposed to splitter elbows (3.2.3.2). Eqs. 1A-19 and 1A-20 were obtained from Ref. 1, pages 10 to 13, and the performance data for thin vanes were obtained from Refs. 1, 9, 13, and 15; data for thick vanes are from Ref. 29. The geometry referred to in the following paragraphs is shown in Fig. 1A-27.

$$\Delta\overline{V} = \overline{V}_1\left[1+\left(\frac{A_1}{A_2}\right)^2-\left(\frac{2A_1}{A_2}\right)\cos\theta\right]^{1/2} \tag{1A-16}$$

The actual gap, s, between vanes for all types of vanes is determined from the equation

$$s = \frac{b_1}{(n+1)\cos(\theta/2)} \tag{1A-17}$$

(A) Design

(1) Thin Vanes, Circular Profile: Due to the ease of installation, a thin circular arc vane is recommended for general use. These vanes are equally spaced within the bend. A vane is considered thin when its thickness is less than 1/40 of the inside bend radius (r_i).

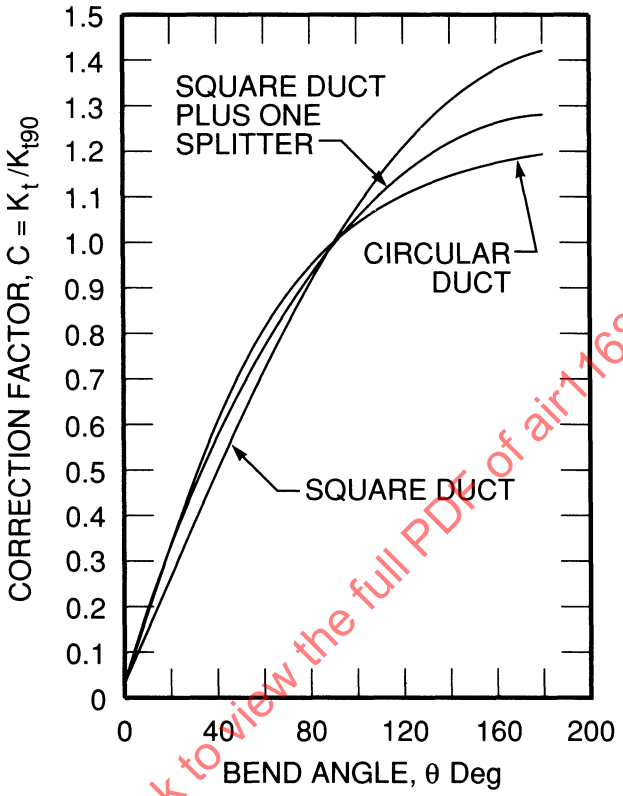

Figure 1A-23 - Correction Factor for Bends Other Than 90 deg for Bends Without Exit Ducts (Data From Refs. 5 and 12)

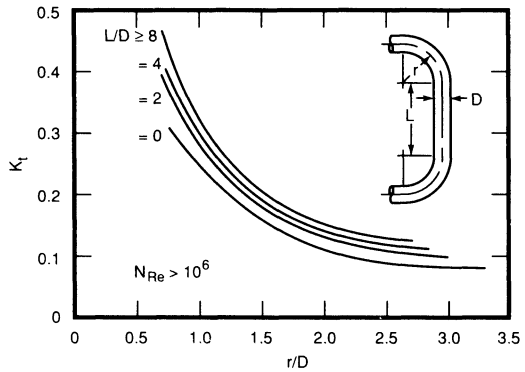

Figure 1A-24 - Loss Coefficient for Compound U-bends, Circular Ducts (Reduced From Ref. 3, Figs. 27-32; Ref. 8, Fig. 30)

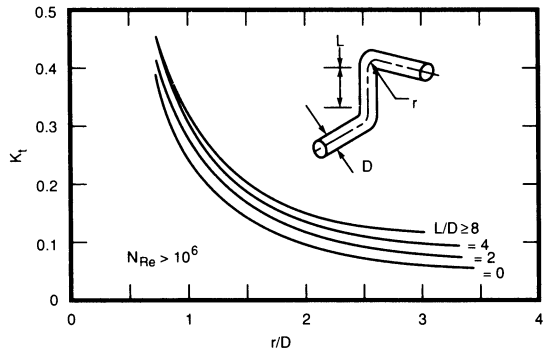

Figure 1A-25 - Loss Coefficient for 90 deg Offset Bends, Circular Ducts (Reduced From Ref. 3, Figs. 39-44; Ref. 8, Fig. 32)

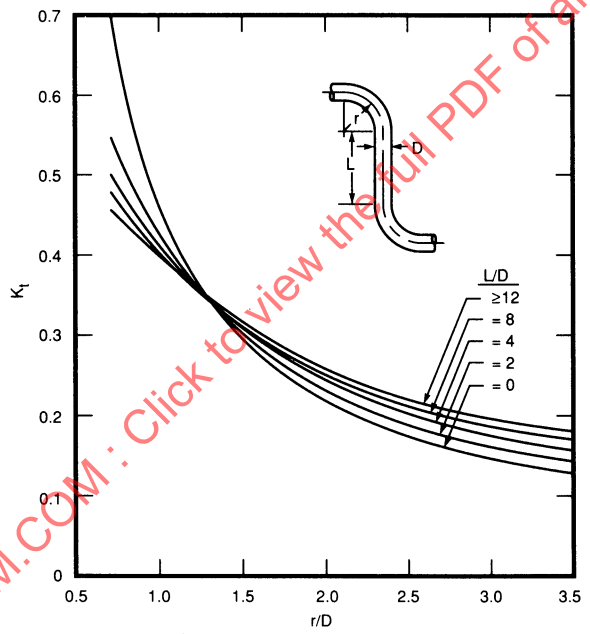

Figure 1A-26 - Loss Coefficient for Z-bends, Circular Ducts (Reduced From Ref. 3, Figs. 33-38; Ref. 8, Fig. 31)

The vane geometry is determined from the duct width, b, the inside bend radius, r_i, the bend angle, θ, and the area ratio, A_1/A_2. The inside bend radius, r_i, should be made as large as space will permit.

Vane bend radius: $r = r_i$

Chord length: $c = 2r \sin(\theta/2)$

Number of vanes $= n$

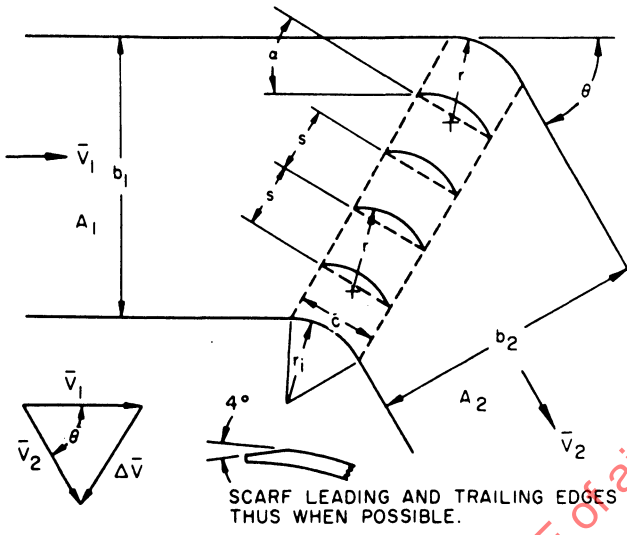

Figure 1A-27 - Turning Vanes Geometry

For all bends (Fig. 1A-27):

$$n = 2.5\left[\frac{\Delta\bar{V}}{\bar{V}_1}\frac{b_1}{c}\right]-1 \qquad \text{(1A-18)}$$

For bends of equal inlet and outlet dimensions, this equation reduces to

$$n = 5\frac{b}{c}\left(\sin\frac{\theta}{2}\right)-1 \qquad \text{(1A-19)}$$

In Fig. 1A-28, n is plotted as a function of r/b for equal inlet and outlet dimensions. The angle of attack is presented in Fig. 1A-29.

(2) Thin Vanes, Noncircular Profile: For use in bends with equal inlet and outlet dimensions, a noncircular thin vane, which is more efficient than the circular arc vane, has been developed. However, since the noncircular arc is more difficult to fabricate, it should be used only where the decreased pressure drop is necessary. The coordinates for this type of vane are shown in Fig. 1A-30, and the angle of attack is presented in Fig. 1A-31.

At the upstream end of the vane, x=0 and y=0. For this type of vane, the shape of the inside and outside corners should be the same shape as the blade instead of having a radius r_i. Therefore, a chord length c should be selected as large as the bend inside-corner clearance will permit. The blade and corner blade locations in the duct are determined from c and the angle of attack, α (Fig. 1A-31). The number of blades is determined from c, the s/c value from Fig. 1A-31, and the following equation:

$$n = \frac{b}{c\,(s/c)\cos(\theta/2)}-1 \qquad \text{(1A-20)}$$

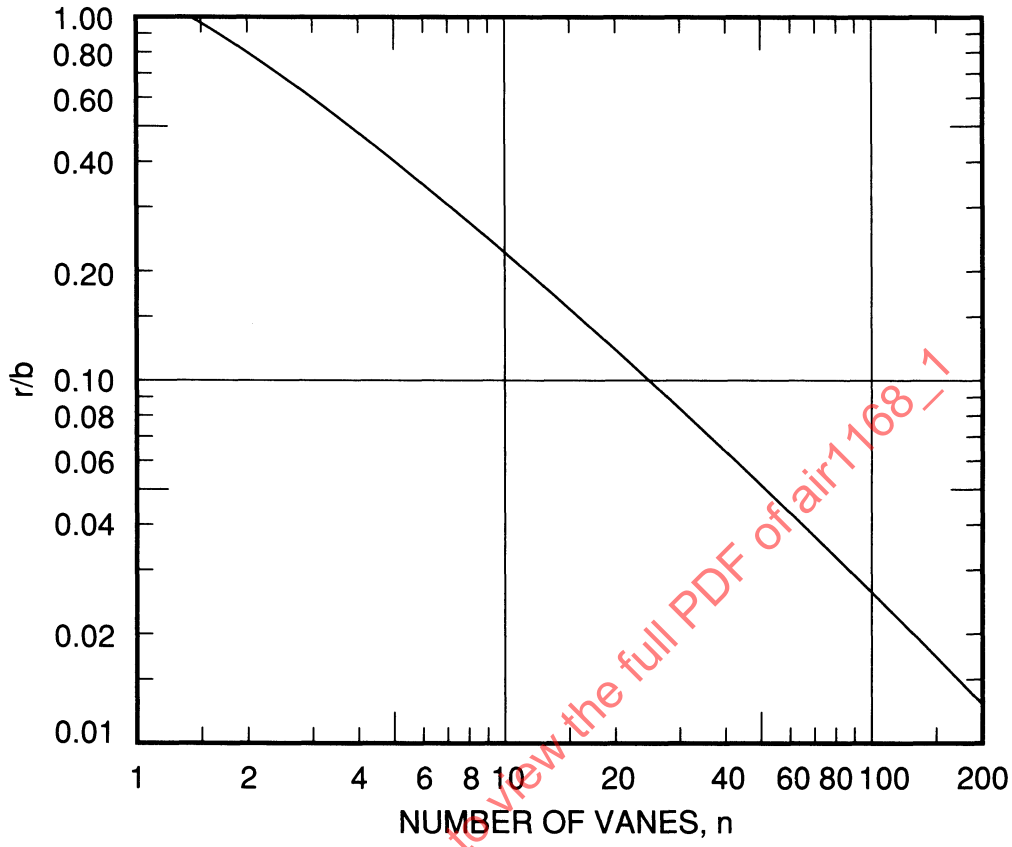

Figure 1A-28 - Number of Vanes for Thin Circular Arc Vanes, $c = 2r \sin(\theta/2)$, $n = (5b/c)[\sin(\theta/2)] - 1$ (From Ref. 1)

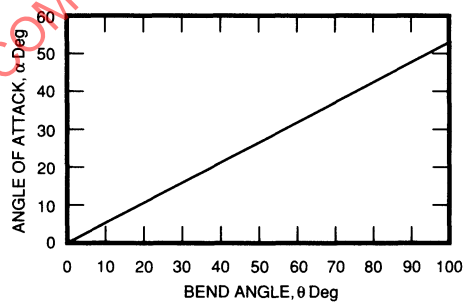

Figure 1A-29 - Angle of Attack for Thin Circular Arc Vanes (Calculated From Ref. 13)

(3) Thick Vanes: Two types of thick vanes are presented and are designated as type A and type B in Fig. 1A-32. Both types are very similar and vary only in the contour of the leading edges.

Number of vanes for both types of vanes

$$n = \left[4\left(\frac{b}{c}\right)\sin\frac{\theta}{2}\right] - 1 \qquad \text{(1A-21)}$$

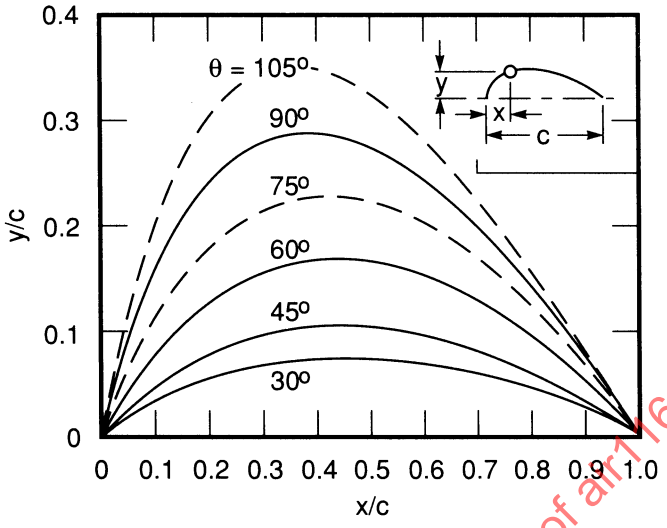

Figure 1A-30 - Thin Vanes, Noncircular Profile, Coordinates. (Data From Ref. 13)

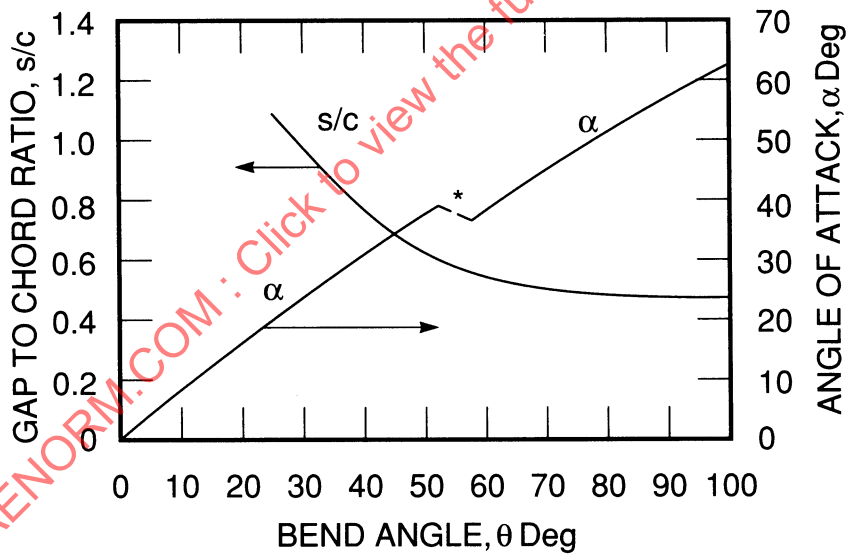

Figure 1A-31 - Bend Angle and Gap to Chord Ratio. *The discrepancy in the angle of attack curve (shown by the broken diagonal line) is apparently a result of different methods used in developing the vane profiles. (From Ref. 1)

Chord length: Type A has the following chord length; type B starts with a type A vane and is shortened by virtue of the leading-edge contour change:

$$c = 2 r_c \sin\frac{\theta}{2} \qquad \text{(1A-22)}$$

where r_c = Inside chord radius.

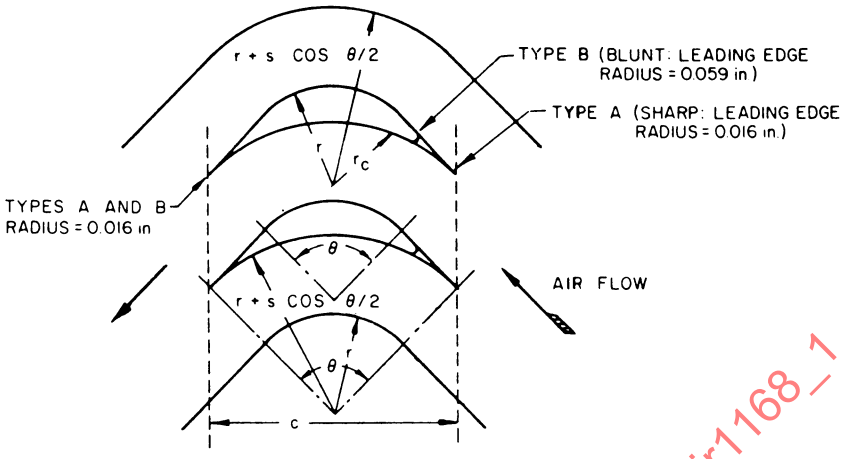

Figure 1A-32 - Thick Vanes (Calculated From Ref. 29)

(B) Pressure Loss: The following pressure loss coefficients are based on the upstream q immediately preceding the vaned bend. The Reynolds number is based on duct velocity and chord length.

(1) Thin Vanes, Circular Profile: Figs. 1A-33 and 1A-34 plot loss coefficients and gap-to-chord ratio versus K_t, respectively.

(2) Thin Vanes, Noncircular Arc: Fig. 1A-35 plots K_t versus bend angle.

(3) Thick Vanes: The pressure loss versus Reynolds number for thick vanes is presented in Fig. 1A-36. The pressure drop data were determined for 90 deg bends with a spacing s equal to 1 in. and a radius, r, equal to 0.743 in. Some of the data were determined with an open duct downstream; therefore, the pressure loss data may be a little low under some flow conditions. The recommended number of vanes as determined in 3.2.3.1 (a) was determined from good turning vane practice and is believed to be good for extrapolating the data to other angles and vane radii. For other angles, the loss coefficient can be determined with reasonable accuracy by applying the bend angle correction factor of Fig. 1A-17 for rectangular elbows.

3.2.3.2 Splitters

The pressure loss in a rectangular elbow may be reduced by dividing the elbow with a number of flow dividers called "splitters." These splitters divide the larger elbow into a number of smaller elbows, each having a larger radius-to-duct width ratio and therefore a smaller loss coefficient. When the splitters are positioned in a manner such that all smaller elbows have the same radius-to-duct width ratio, the loss will be a minimum for a particular number of splitters. This means that the ratio of the inside duct radius, r_i, to the outside duct radius, r_o, of all smaller elbows will be the same and is equal to

$$\left(\frac{r_i}{r_o}\right)_A = (r_i/r_o)^{1/n} \qquad \text{(1A-23)}$$

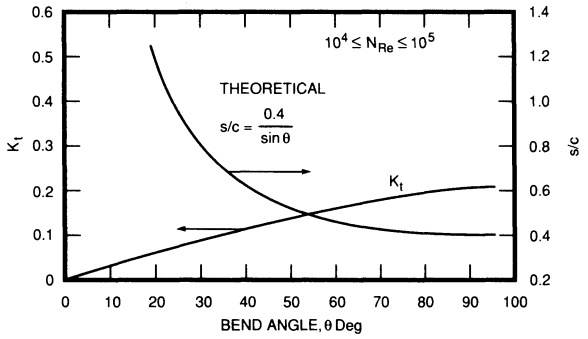

Figure 1A-33 - Loss Coefficient for Thin Circular Arc Vanes

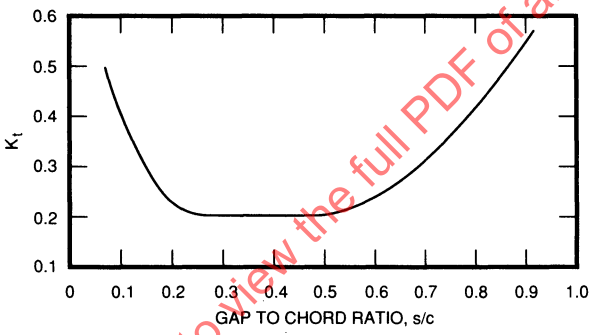

Figure 1A-34 - Effect of Gap to Chord Ratio on Thin Circular Arc Vanes (From Refs. 13 and 15)

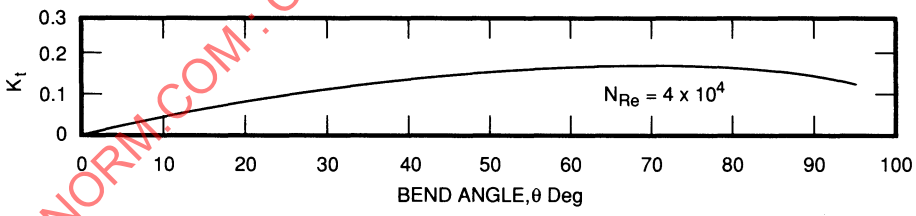

Figure 1A-35 - Loss Coefficient for Thin Noncircular Arc Vanes (From Ref. 1)

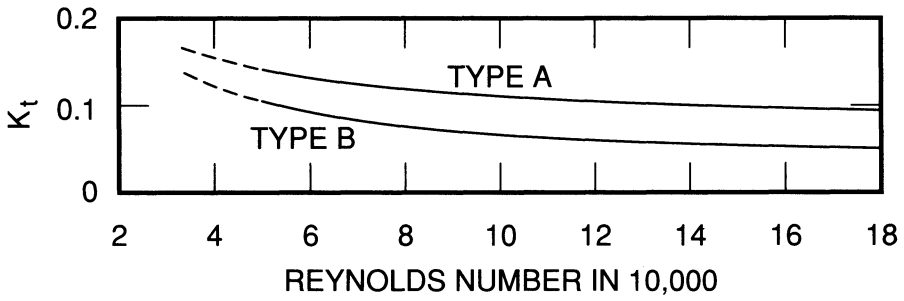

Figure 1A-36 - Loss Coefficient for 90 deg Thick Vane Bends (From Ref. 29)

where $(r_i / r_o)_A$ = Ratio of inside radius to outside radius of any subdivided elbows

r_i / r_o = Ratio of inside to outside radius of original duct before splitters are added (see Fig. 1A-37)

n = Number of splitters plus 1, that is, for one splitter, n=2

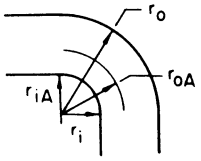

Figure 1A-37 - Sketch of Inside and Outside Radii with Splitters

The pressure loss of the new elbow with splitters is calculated by using a loss coefficient based on the radius-to-duct width ratio of the subdivided elbows. See Figs. 1A-18 through 1A-20 for rectangular elbows. The Reynolds number should also be based on the subdivided elbow. It should be mentioned that turning vanes may be lighter and show an advantage in Reynolds number if a large number of duct divisions is used. Ref. 27 contains additional information on losses in elbows of this type.

3.2.4 Transition Elbows

The loss coefficient for 90 deg rectangular transitional elbows may be otained by using the correction factor of Fig. 1A-38 and the loss factor for 90 deg constant area rectangular elbows (Figs. 1A-18 through 1A-20).

3.3 Pressure Losses, Duct Area Changes

3.3.1 Sudden Expansions or Contractions

The accompanying figure (Fig. 1A-39) represents expansion (a) and contraction (b) in direction of the flow, for which

$$\Delta P = K_t q \tag{1A-24}$$

where q is the dynamic pressure or velocity head in the *smaller* area section.

The loss coefficient K_t is given in Figs. 1A-40 and 1A-41.

3.3.2 Gradual Contractions

Table 1A-5 shows the angular displacement versus pressure loss coefficient for a gradual contraction as diagrammed in Fig. 1A-42 and expressed by

$$\Delta P = \left(K_t + 4f \frac{L}{D_m} \right) q_2 \tag{1A-25}$$

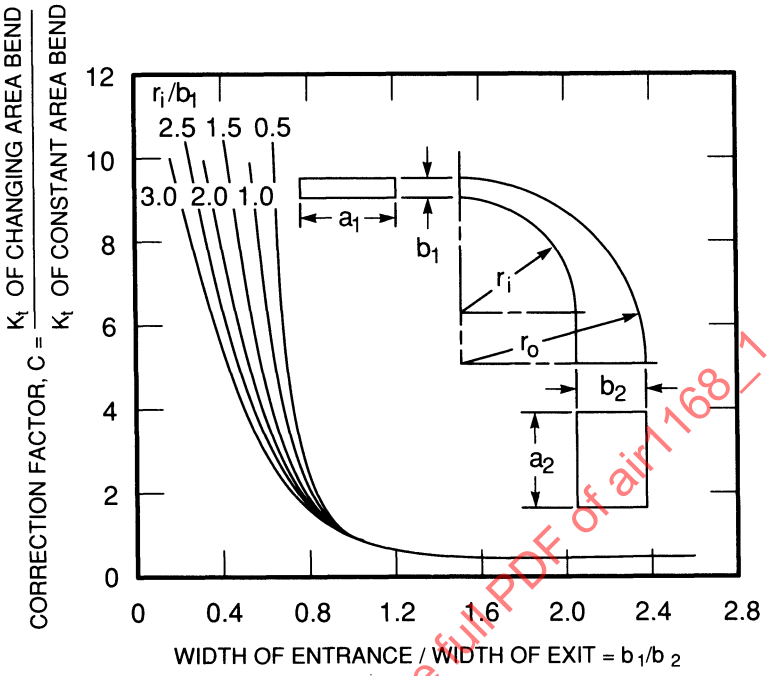

Figure 1A-38 - Pressure Loss Correction Factor for Transitional Elbows. Note: Radius Ratio of Constant Area Bend = $r_i / b_1 + 1/2$, $r_o = r_i + b_2$, $a_1 = a_2$ (From Ref.1)

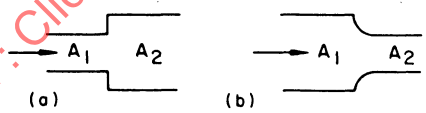

Figure 1A-39 - Sketch of Typical Types of Expansion and Contraction Areas

where $D_m = \dfrac{D_1 + D_2}{2}$

= mean equivalent diameter

3.3.3 Diffusers (Subsonic)

3.3.3.1 Geometry

Whenever possible, a diffuser should be designed symmetrically about its axis, with an expansion angle (2θ) between 7 and 12 deg. Nonsymmetrical flow or too large an expansion angle may cause the flow to separate from the diffuser walls and thereby cause an increase in pressure loss. When space limitations necessitate a large expansion angle (2θ > 15 deg), separation may be prolonged by use of a curved wall or truncated diffuser, by the addition of guide vanes (Refs. 19, 22, and 24), or in extreme cases by the use of boundary layer control (Ref. 23).

Table 1A-5 - Angular Displacement Versus Loss Coefficient[1]

2θ, deg	K_t
0-30	0
30-45	0.05
45-180	Sudden contraction from A_1 to A_2, as shown in Par. 3.3.1

[1] Ref. 27, p. 115.

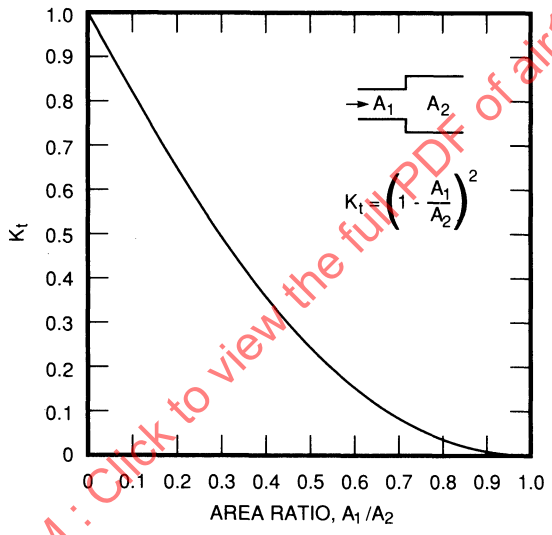

Figure 1A-40 - Loss Coefficient of a Sudden Expansion (From Ref. 24)

The type of intersection (sharp or rounded corner) between inlet duct and diffuser walls appears to have little effect on pressure loss characteristics except at high entrance Mach numbers ($M_1 > 0.7$). (Ref. 21.)

The optimum expansion angle is a function of area ratio, surface roughness, and Reynolds number. For example, for a given area ratio and surface roughness, the expansion angle with minimum pressure loss coefficient (as determined from Table 1A-5 and Eq. 1A-25) varies with inlet Reynolds number as shown in Fig. 1A-43. These curves are based on a smooth, straight-walled conical diffuser with an inlet-to-exit area ratio of 0.36 and a length-to-mean diameter ratio of 0.25 (cot θ).

Some types of diffusers are listed here.

(a) Straight Wall, Conical: For the diffuser shown in the following drawing (Fig. 1A-44)

$$D_2 = 2L \tan\theta + D_1 \qquad (1A\text{-}26)$$

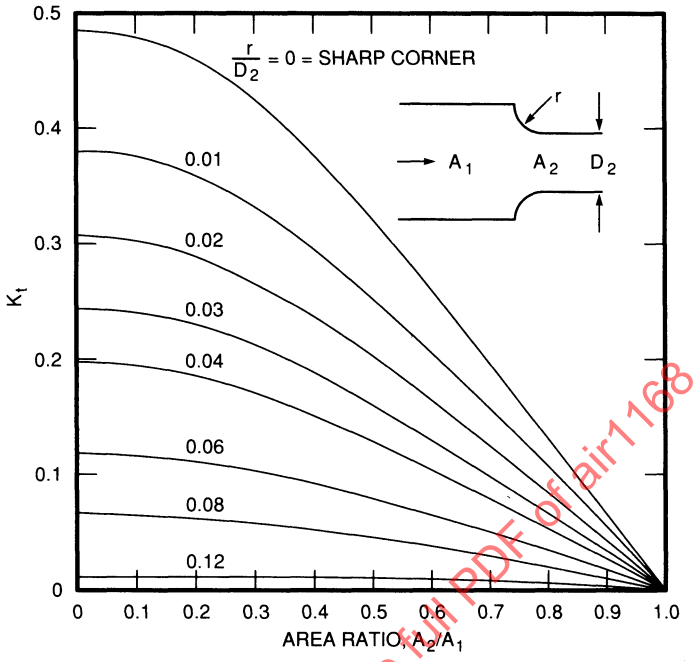

Figure 1A-41 - Loss Coefficient of a Sudden Contraction

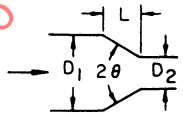

Figure 1A-42 - Sketch of a Typical Gradual Contraction

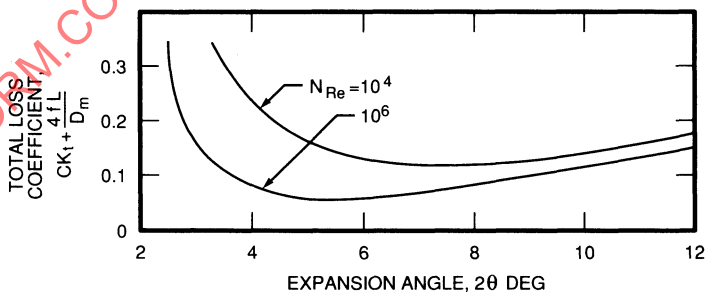

Figure 1A-43 - Total Loss Coefficient Versus Expansion Angle

(b) Straight Wall, Rectangular: Referring to Fig. 1A-45, values are:

Two Dimensions

$$a_2 = a_1 \quad (1A\text{-}27)$$

$$b_2 = b_1 + 2L\tan\theta \quad (1A\text{-}28)$$

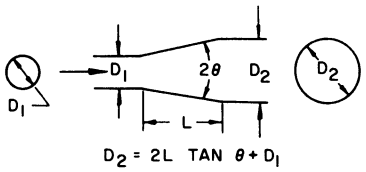

Figure 1A-44 - Sketch of a Straight Wall Conical Diffuser

Square

$$a_2 = a_1 + 2L\tan\theta \quad \text{(1A-29)}$$

$$b_2 = b_1 + 2L\tan\theta \quad \text{(1A-30)}$$

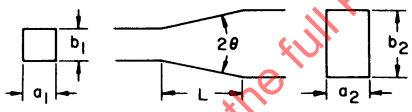

Figure 1A-45 - Sketch of a Straight Wall Rectangular Diffuser

(c) Curved Wall: At large expansion angles, diffusers of the shape shown in Fig. 1A-46 (Ref. 1, Fig. 10) appear to have lower pressure loss than do straight wall diffusers. The equation for the curved section is

$$y = \frac{D_1}{2}\left[\frac{1}{1+(x/L)\sqrt{(A_1/A_2)-1}}\right] \quad \text{(1A-31)}$$

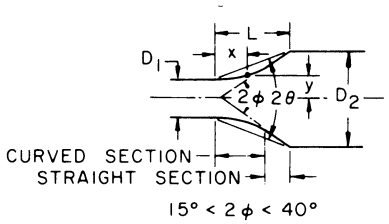

Figure 1A-46 - Curved Wall Diffuser

(d) Truncated: This type is identical to a straight wall diffuser except that there is a sudden enlargement into the downstream pipe (see Fig. 1A-47). This is useful where space is prohibitive and a curved wall diffuser is too expensive to fabricate.

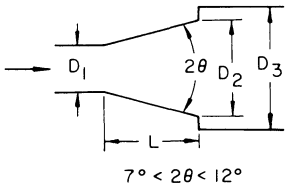

Figure 1A-47 - Sketch of a Truncated Diffuser

3.3.3.2 Pressure Loss

Pressure loss through a straight or curved wall diffuser may be expressed as the sum of expansion loss and friction loss:

$$\Delta P = \left[CK_t + \frac{4fL}{D_m} \right] q_1 \qquad \text{(1A-32a)}$$

where C = Expansion factor (Fig. 1A-48), dimensionless
K_t = Pressure loss coefficient for sudden expansion from A_1 to A_2 (Par. 3.3.1), dimensionless
D_m = Mean equivalent diameter, ft

$$= \frac{D_1 + D_2}{2} \qquad \text{(1A-32)}$$

The loss through a truncated diffuser is equal to that of a straight wall diffuser plus the loss in the sudden enlargement at the exit. Based on the velocity head at A_1, the pressure loss equation becomes

$$\Delta P = \left[CK_{t1} + \frac{4fL}{D_m} + K_{A2} \left(\frac{A_1}{A_2} \right)^2 \right] q_1 \qquad \text{(1A-33)}$$

where K_{t1} is the loss coefficient of the straight wall diffuser, and K_{A2} is the loss coefficient for a sudden expansion from A_2 to A_3.

The pressure loss, determined from the preceding equations, will be less than the actual loss if the diffuser is directly preceded by a bend or a long (L/D>10) straight section of ducting; it will be higher than the actual loss if the diffuser is directly preceded by some installation that produces rotational flow.

3.3.3.3 Pressure Recovery Equations

The equations given below are applicable to incompressible flow only.

(a) Exit Static Pressure

$$P_{s2} = P_{s1} + q_1 \left[1 - \left(\frac{A_1}{A_2} \right)^2 - \sum K_t \right] \qquad \text{(1A-34)}$$

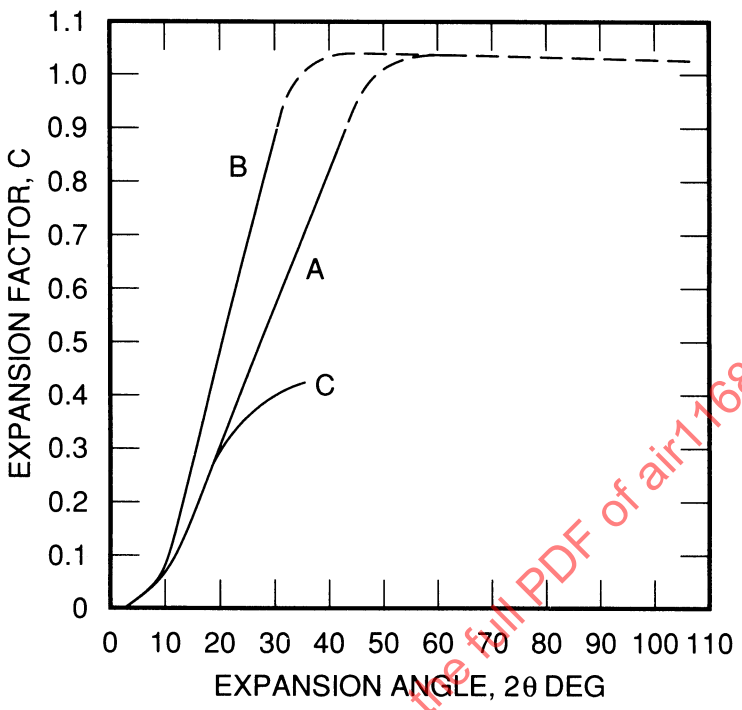

Figure 1A-48 - Diffuser Expansion Factor (curve A-straight wall, conical and square; curve B-straight wall, two dimensional; curve C-curved wall, conical)

(b) Diffuser Efficiency: In some reports, diffuser performance is expressed as a dimensionless term called efficiency (η):

$$\eta = \frac{P_{s2}-P_{s1}}{q_1-q_2} = \frac{P_{s2}-P_{s1}}{q_1[\,1-(A_1/A_2)^2\,]} \tag{1A-35}$$

The loss coefficient in terms of efficiency is expressed as

$$K_i = [1-\eta]\left[1-\left(\frac{A_1}{A_2}\right)^2\right] \tag{1A-36}$$

3.3.3.4 Diffuser Followed by a Resistance Unit

The addition of a resistance unit, such as a heat exchanger, immediately downstream of a diffuser decreases the tendency of flow separation and thereby reduces the pressure losses in wide-angle diffusers.

Ref. 26 recommends the shape shown here (Fig. 1A-49) and gives corresponding pressure loss characteristics for a conical diffuser. This information may also be used as a guide for nonconical diffusers.

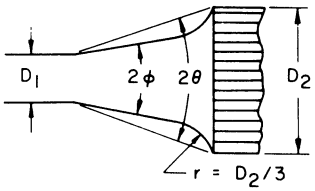

Figure 1A-49 - Sketch of a Diffuser Followed by a Resistance Unit

In this illustration 2φ is the actual expansion angle between walls (Fig. 1A-50) and 2θ is the equivalent expansion angle. Recommended values of 2φ for various area ratios and equivalent expansion angles are given in Fig. 1A-50.

The pressure loss through this type of installation may be estimated from Eq. 1A-33 for diffuser pressure loss and the expansion factor *C* from Fig. 1A-51:

K_{tr} = Pressure loss coefficient of resistance unit following diffuser (see Fig. 1A-51)

Data for other area ratios are not available.

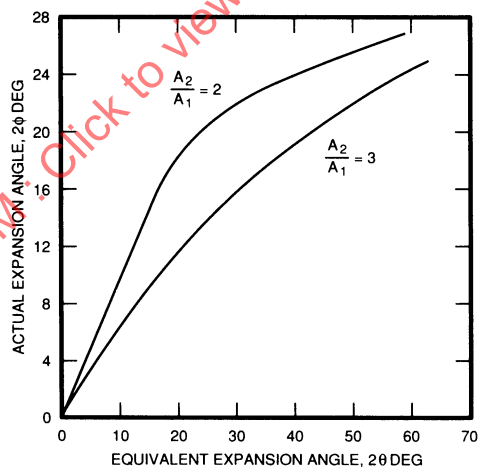

Figure 1A-50 - Equivalent Expansion Angle for a Diffuser Followed by a Resistance Unit (From Ref. 26)

3.3.4 Venturi

The irrecoverable pressure loss through a venturi may be considered to be the sum of the contraction, friction, and expansion losses. With normal venturi design, the contraction losses may be neglected and the pressure loss equation becomes

$$\Delta P_t = \left(\sum \frac{4fL}{D} + CK_t\right) q \quad \text{(throat)} \qquad \text{(1A-37)}$$

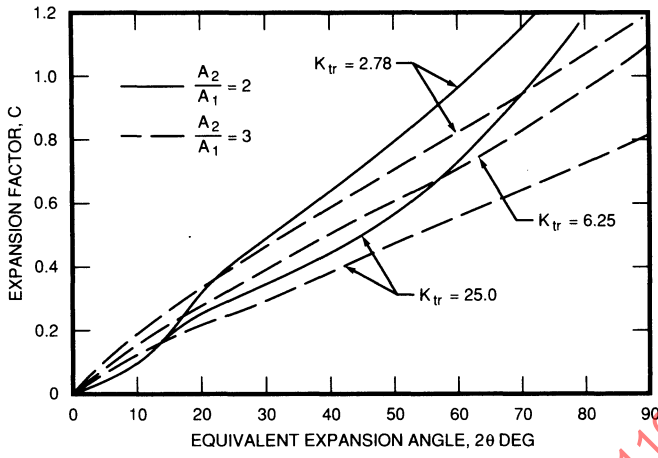

Figure 1A-51 - Expansion Factor for a Diffuser Followed by a Resistance Unit (From Ref. 26)

where $\sum(4fL/D)$ = Sum of friction loss coefficients in entrance, throat, and diffuse sections (see Eqs. 1A-32 and 1A-33), dimensionless

CK_t = Expansion loss coefficient (Eq. 1A-33), dimensionless

A rapid approximation of this pressure loss may be made from Fig. 1A-56, where the pressure loss is shown as a function of the differential static head.

3.3.5 Orifice in a Duct

The irrecoverable pressure loss of an incompressible fluid through an orifice (see Fig. 1A-52) may be calculated from the equation

$$\Delta P_t = K_t q_2 \tag{1A-38}$$

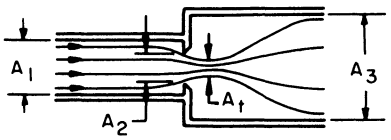

Figure 1A-52 - Sketch of an Orifice in a Duct

When $A_1 = A_3$, K_t may be estimated from Fig. 1A-53. A rapid approximation of ΔP_t may be made from Fig. 1A-56, where ΔP_t is shown as a function of the differential static head.

When $A_1 \neq A_3$, the loss coefficient K_t may be taken as that of an abrupt expansion from the vena contracta (A_t) to A_3, based on the velocity head at the vena contracta. Correcting the loss coefficient at A_t conditions to A_2 conditions results in the same equation as Eq. 1A-38:

$$\Delta P_t = K_t q_2 \tag{1A-39}$$

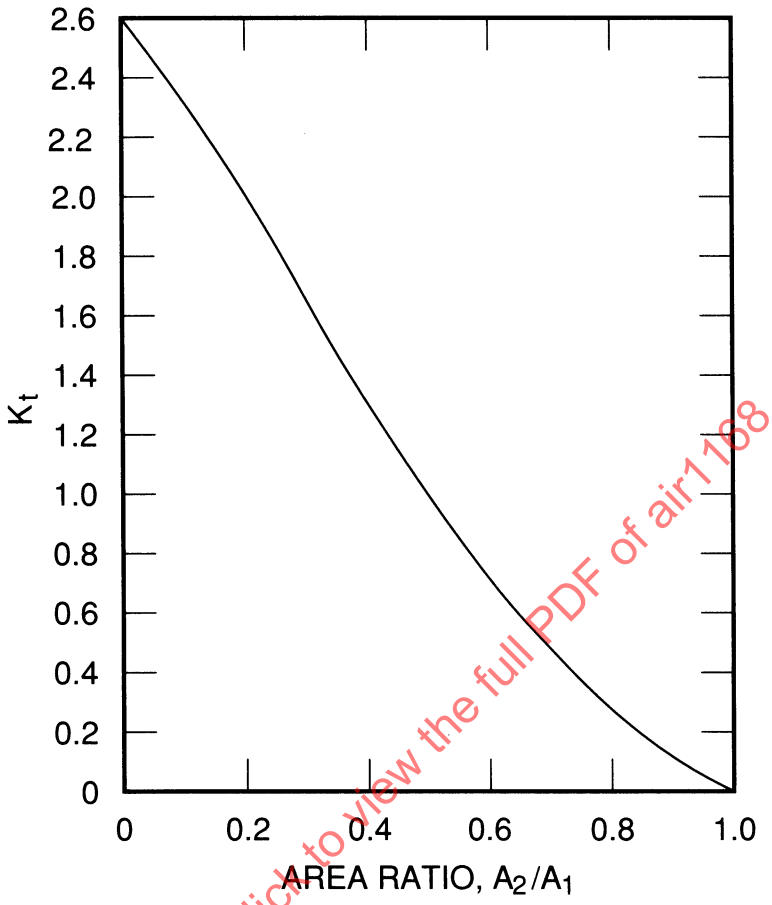

Figure 1A-53 - Loss Coefficient for an Orifice in a Duct; $A_1 = A_3$ (From Ref. 45, Table 11)

$$\text{where } K_t = \left[\frac{1}{C_C} - \frac{A_2}{A_3}\right]^2 \qquad \text{(1A-40)}$$

$$C_C = \frac{A_t}{A_2} \qquad \text{(1A-41)}$$

q_2 = Velocity head based on A_2

K_t can be determined from Figs. 1A-54 and 1A-55, knowing A_2/A_1 and A_2/A_3.

3.4 Pressure Losses, Duct Branches

The pressure loss due to mixing in converging and diverging branch ducts is

$$\Delta P_t = K_t q_1 \qquad \text{(1A-42)}$$

The loss coefficients discussed below do not include wall friction.

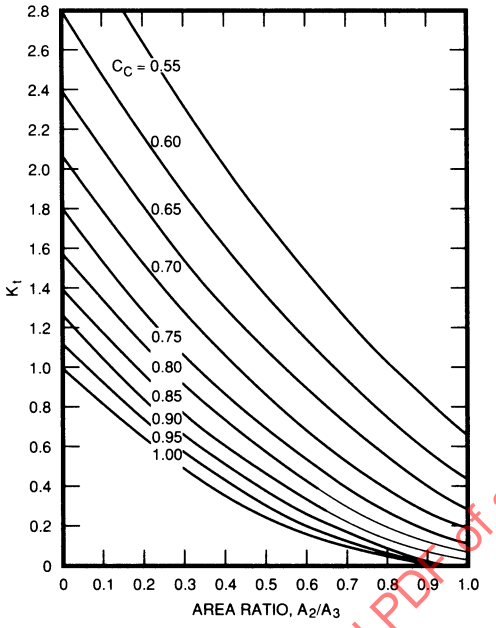

Figure 1A-54 - Loss Coefficient for an Orifice in a Duct: $K_t = [(1/C_c)-(A_2/A_3)]^2$

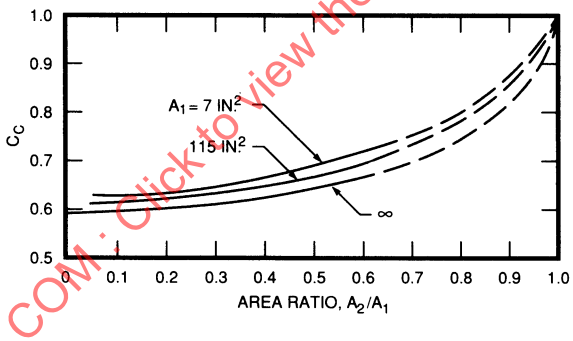

Figure 1A-55 - Contraction Coefficient of an Orifice (From Ref. 45, Tables 8 and 13)

3.4.1 Diverging Branches

The loss coefficients (K_t) may be estimated from the equation taken from Ref. 7:

$$ {}_1K_{t2} = \lambda_2 + \left(2\lambda_2 - \lambda_3\right)\left(G_2/G_1\right)^2 - 2\lambda_3\left(G_2/G_1\right)\cos\alpha' \qquad \text{(1A-43)} $$

where ${}_1K_{t2}$ = Loss coefficient from 1 to 2, based on q_1

λ_2 = Function of α for branch 2 (from Fig. 1A-57)

λ_3 = Function of α for branch 3 (from Fig. 1A-57)

α' = $\alpha(1.39-5.84\times10^{-3}\alpha)$ (This is a curve-fit made from Fig. 3 of Ref. 7)

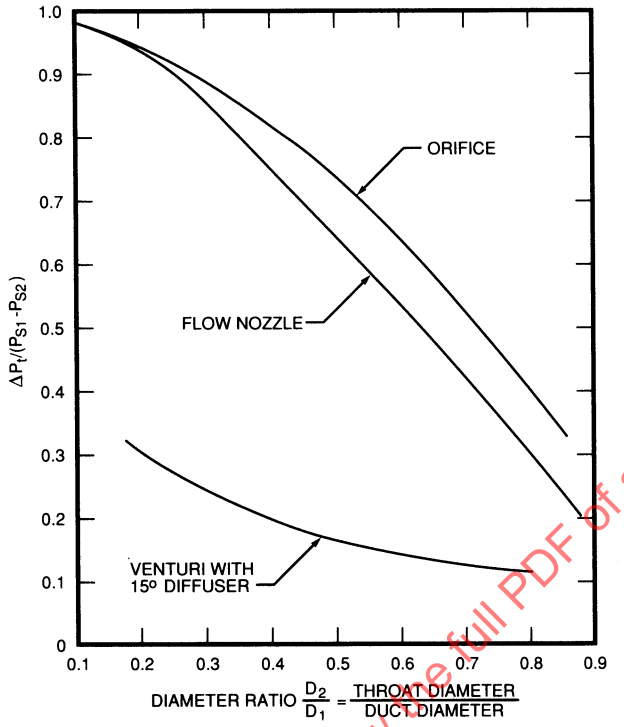

Figure 1A-56 - Approximate Pressure Loss Through Several ASME Flow Metering Devices
P_{s1} = Upstream Static Pressure; P_{s2} = Throat Static Pressure (From Ref. 35, Fig. 5)

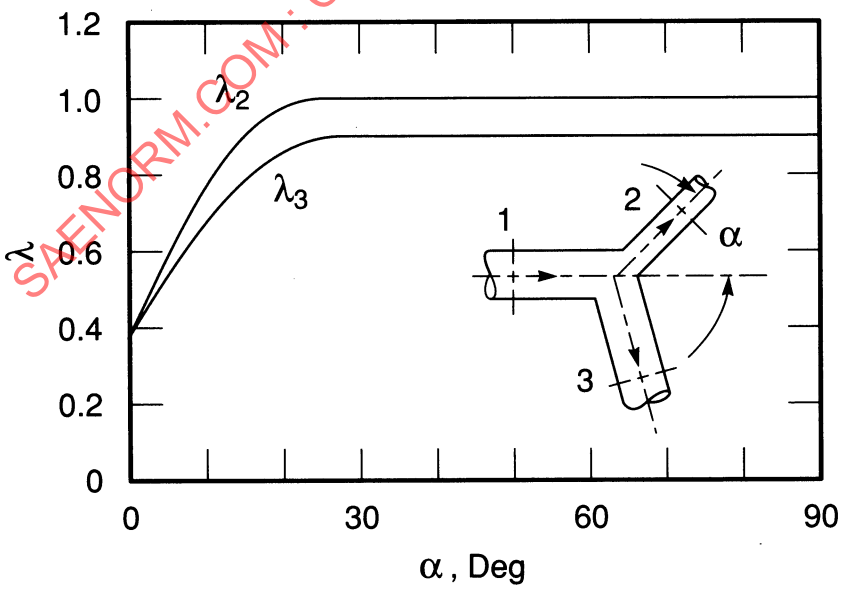

Figure 1A-57 - Diverging Branch, Functions for Computing Loss Coefficient (Ref. 7)

3.4.2 Converging Branches

The loss coefficients (K_t) may be estimated from the following equations:

$$ {}_1K_{t3} = \lambda + \left(\frac{G_3}{G_1}\right)^2 - 2\frac{A_1}{A_3}\cos\beta' - \left(\frac{G_2}{G_1}\right)^2\left(2\frac{A_2}{A_3}\cos\delta'\right) \quad \text{(1A-44)} $$

$$ {}_2K_{t3} = \lambda + \left(\frac{G_3}{G_2}\right)^2 - 2\frac{A_2}{A_3}\cos\delta' - \left(\frac{G_1}{G_2}\right)^2\left(2\frac{A_1}{A_3}\cos\beta'\right) \quad \text{(1A-45)} $$

where ${}_1K_{t3}$ = Loss coefficient from 1 to 3, based on q_1 (Fig. 1A-58), dimensionless

${}_2K_{t3}$ = Loss coefficient from 2 to 3, based on q_2 (Fig. 1A-58), dimensionless

λ = Function of β (Fig. 1A-58)

For ${}_2K_{t3}$, λ = Function of δ (Fig. 1A-58)

$2\frac{A_1}{A_3}\cos\beta'$ = Function of β and A_1/A_3 (Fig. 1A-58)

$2\frac{A_2}{A_3}\cos\delta'$ = Function of δ and A_2/A_3 (Fig. 1A-58)

3.4.3 Manifolds

The symbols used in this paragraph pertain to Fig. 1A-59:

Three of the variables that influence the rate of discharge from the ports of a manifold are the manifold cross-sectional area, port area, and port spacing. Flow regulation may be accomplished by varying one of these while keeping the other two constant, or by any other combination. These variables may be estimated by solving the following equations. It should be noted, however, that values of K_t and $4f\Delta L/D$ are only approximate, and exact sizing or flow distribution should be determined by test.

The total pressure loss from any one port of a manifold through the next port is equal to

$$ \Delta P_t = \left[K_t + \frac{4f\Delta L}{D}\right]q \quad \text{(1A-46)} $$

where K_t = Entrance pressure loss coefficient into the port (Fig. 1A-57), dimensionless

$4f$ = Friction factor based on the Reynolds number in the manifold (Fig. 1A-4), dimensionless

ΔL = Center-to-center distance between ports, ft

D = Manifold equivalent diameter, ft

q = Velocity head in the manifold between ports, lb/ft^2

This relationship is applied as follows to determine the flow through the various ports:
First Port (Ref. 66):

$$ P_{ta} - P_{t1} = K_{t1}\,q_a \quad \text{(1A-47)} $$

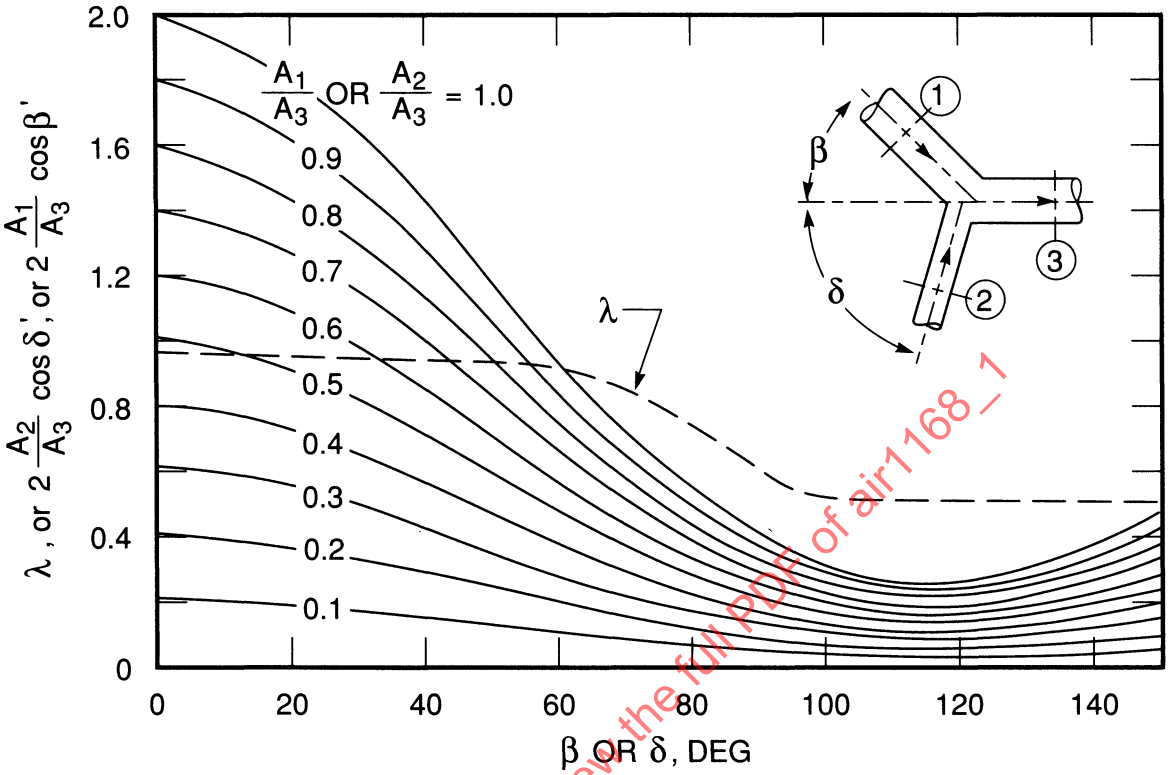

Figure 1A-58 - Converging Branch, Functions for Computing Loss Coefficient (From Ref. 7)

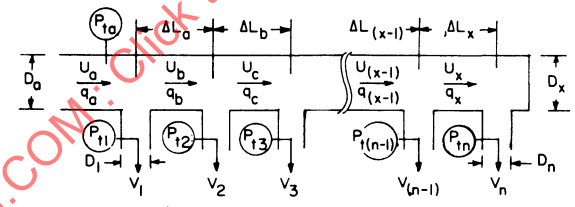

Figure 1A-59 - Sketch of a Typical Manifold

Second Port:

$$P_{ta} - P_{t2} = \left[K_{t2} + \frac{4f\Delta L_a}{D}\right] q_b \tag{1A-48}$$

$$w_a = w_1 + w_b \tag{1A-49}$$

Third Port:

$$P_{ta} - P_{t3} = \left[\frac{4f\Delta L_a}{D}\right] q_b + \left[K_{t3} + \frac{4f\Delta L_b}{D}\right] q_c \tag{1A-50}$$

$$w_a = w_1 + w_2 + w_c \tag{1A-51}$$

nth Port:

$$P_{ta} - P_{tn} = \left[\frac{4f\Delta L_a}{D}\right] q_b + \cdots + \left[\frac{4f\Delta L_{(x-1)}}{D}\right] q_{(x-1)} + \left[K_{tn} + \frac{4f\Delta L_x}{D}\right] q_x \qquad \text{(1A-52)}$$

$$w_a = w_1 + w_2 + \cdots + w_{(n-1)} + w_x \qquad \text{(1A-53)}$$

These equations may be solved simultaneously or by substituting various assumed values of w_x. The quantities w_a and P_{ta} may then be calculated and compared with the known conditions.

If the flow is determined by assuming values of w_x, values of K_t may be determined from Fig. 1A-57. If the equations are solved simultaneously, assumed values of K_t may be used. A recommended value for assumption is $K_t = A_{manifold}/A_{port}$ at G_n/G_x. In an open-end manifold, this assumption gives reasonable results along the entire length of the manifold; however, in a closed-end manifold, the weight flows will be in error near the closed end. Ref. 66, pages 120-122, makes the following assumptions for calculating manifold characteristics:

(a) Equal weight flow through each port ($w_1 = w_2 = \cdots = w_n$).

(b) Equal static pressure in all ports ($P_{s1} = P_{s2} = \cdots = P_{sn}$).

(c) Equal friction loss coefficients between ports

$$\frac{4f\Delta L_a}{D} = \frac{4f\Delta L_b}{D} = \cdots = \frac{4f\Delta L_x}{D}$$

(d) Constant manifold cross-sectional area ($A_a = A_x$).

The various port areas may then be calculated from the following equation:

For the (n - y)th port:

$$A^2_{(n-y)} = \left\{ \frac{K_{tn} + (4f\Delta L/D)\,[(y/6)(y+1)(2y+1)]}{A_a^2} - \frac{[y+1]^2\,[K_{t(n-y)} + (A_a/A_n)^2]}{A_a^2} \right\}^{-1} \qquad \text{(1A-54)}$$

that is, $y=4$ for the $(n-4)$th port, $y=(n-1)$ for the first port (continuing for all ports) where n is the total number of ports.

If the port areas are proportioned according to the preceding equation, the total weight flow or upstream total pressure may be calculated from

$$q_a = \left\{ \frac{(1/n^2)K_{tn}}{P_{ta} - P_{s1}} + \frac{(1/n^2)\,(4f\Delta L/D)\,(n/6)\,(n-1)\,(2n-1)}{P_{ta} - P_{s1}} + \frac{(1/n^2)\,(A_a/A_n)^2}{P_{ta} - P_{s1}} \right\}^{-1} \qquad \text{(1A-55)}$$

A manifold may be treated as an infinite reservoir ($P_{ta} = P_{tb} = \cdots P_{tx}$) when the velocity head in the manifold is small compared with the static pressure, $q/P_s < 0.01$.

3.5 Pressure Losses, Internal Installations

3.5.1 Valves

In most variable geometry components, the pressure loss characteristics may vary considerably with size and manufacturer. Additional information on valves is contained in SAE AIR 1168/6, Par. 7. The following loss coefficients should be used only in lieu of the absence of manufacturer's data.

3.5.1.1 Gate Valves

Refer to Fig. 1A-60.

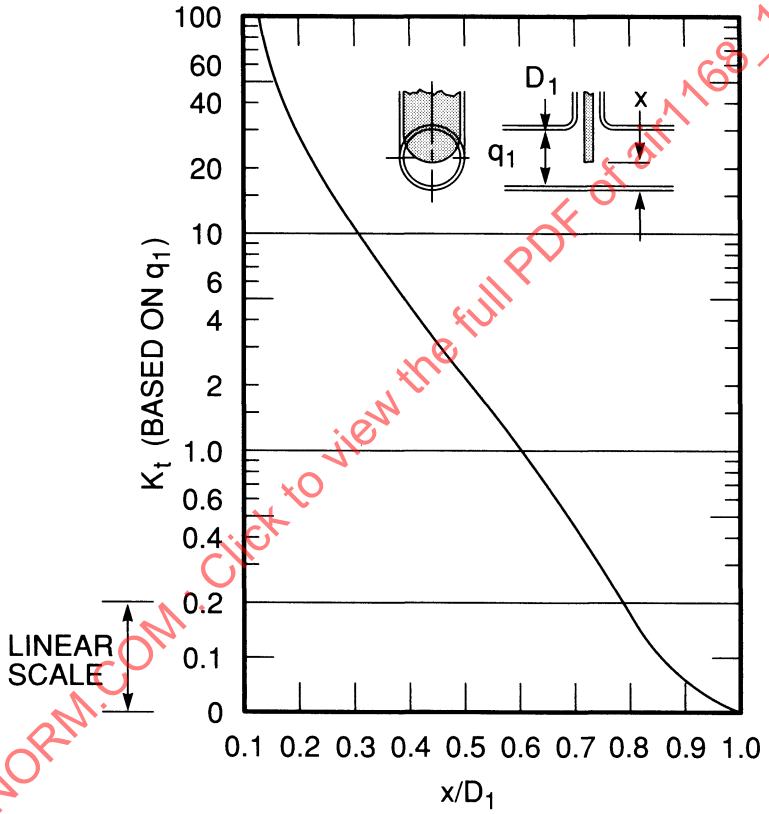

Figure 1A-60 - Loss Coefficients, Gate Valves (From Ref. 12)

3.5.1.2 Butterfly Valves

Fig. 1A-61 gives loss coefficients for a butterfly valve that is fully closed when $\alpha = 0$. A slightly different valve is one that is fully closed when α equals some angle α_o. The loss coefficient for this type of valve can be estimated from the same figure:

$$\alpha = \cos^{-1} \frac{\cos(\alpha_0+\alpha_1)}{\cos \alpha_0} \qquad (1A\text{-}56)$$

where $\alpha_o < 20°$ and α_1 is the valve opening from the closed position α_o.

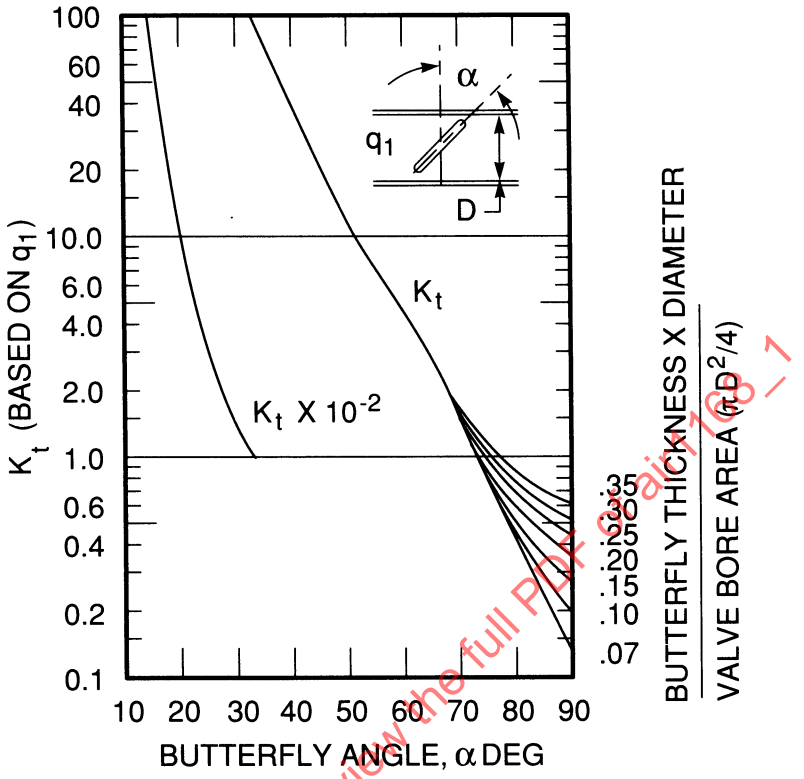

Figure 1A-61 - Loss Coefficient, Butterfly Valves (From Ref. 65)

3.5.2 Screens and Grids

The pressure loss coefficients shown in Fig. 1A-62 (based on upstream velocity head) are for screens mounted in a duct where the upstream and the downstream areas are the same. The loss coefficients are for Reynolds numbers (based on the screen open area and velocity) greater than 400. At lower Reynolds numbers, the loss coefficient increases rapidly (Refs. 48, 53, and 56).

The solidity, ϕ, is defined as the ratio of the solid (no-flow) area divided by the total (no-flow plus flow) area of the screen.

3.5.3 Heat Exchangers

3.5.3.1 Installation Angle

Where space is limited, diffusion and turning may be accomplished with minimum increase in pressure loss by setting the axis of the heat exchanger or similar resistance unit at an angle to the centerline of the entrance duct, as shown in Fig. 1A-63.

This makes the effective area of the duct at the face of the heat exchanger equal to $A_1/\cos\alpha$. Fig. 1A-64 was obtained for air but should hold reasonably well for other fluids. For this graph:
K_t = Loss coefficient of heat exchanger plus turning angle at approach angle α, dimensionless
K_{tr} = Loss coefficient of the resistance unit at zero angle of approach, dimensionless.

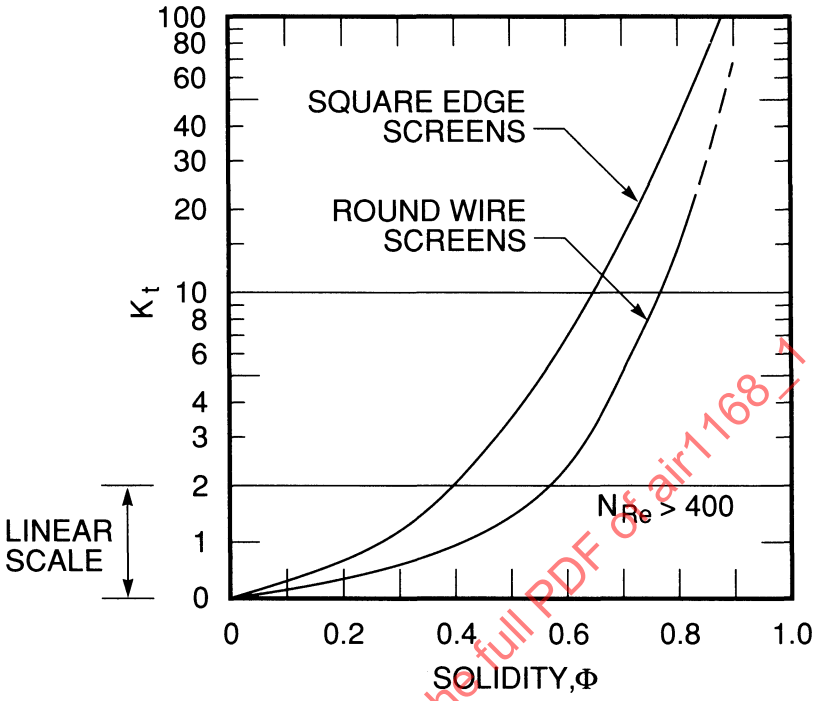

Figure 1A-62 - Loss Coefficients for Screens and Grids (From Ref. 56)

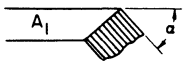

Figure 1A-63 - Sketch of Heat Exchanger Set at an Angle to the Entrance Duct Centerline

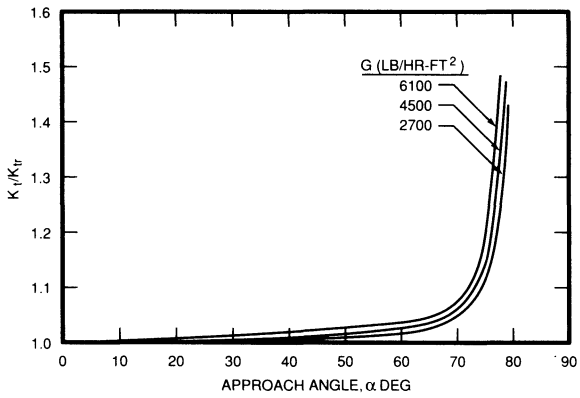

Figure 1A-64 - Effect of Angle on Heat Exchangers (From Ref. 6)

3.6 Pressure Losses, Exits To Compartments

3.6.1 General

Exits from duct systems into compartments are extremely varied and there are probably no two alike. Exits are usually one of three types: nondiffusing (grills, slots, and screens), diffusing (most circular overhead types), and ejector.

3.6.2 Grills and Perforations

In the absence of specific manufacturer's data, the pressure loss for grills and perforations can be estimated by adding the pressure loss for a screen (Fig. 1A-62) and the pressure loss for an abrupt expansion from the total area of the exit to the flow area of the enclosure into which the air is discharging. Perforated plates will match the square edge data, and screen type grills will match the round wire screen data. Round wire screen exits produce less noise than perforated grills. The noise level of perforated grills can be reduced by putting round wire screens behind them.

3.6.3 Slots and Nozzles

The pressure drop for slot type exits that have well rounded entrances can be determined by using a loss coefficient for an abrupt expansion from the exit area to the flow area of the enclosure (see 3.3.1). When the entrance is not well rounded, the loss can be determined by using a loss coefficient based on an abrupt expansion from the vena contracta area to the flow area of the enclosure (vena contracta area = free flow area of exit multiplied by discharge coefficient). Nozzle type exits have the same loss coefficients as the well-rounded slot type of exits.

In all subsonic types of exits where there is no vena contracta, the static pressure at the exit plane of the exit is equal to the static pressure of the enclosure into which the exit is discharging. When a vena contracta is present, the static pressure at the vena contracta is equal to the pressure in the enclosure. For sonic or supersonic flow, see Section 1B of this AIR.

3.6.4 Diffusing Exits

Manufacturer's pressure drop data should be used for diffusing outlets because designs of these outlets are so varied. An approximate pressure drop can be obtained by applying loss coefficients based on the diffusion angle (see 3.3.3).

3.6.5 Velocity Distribution in Enclosures

To have a comfortable environment in an occupied enclosure, the velocity distribution should be such that the air velocity on personnel is less than 50 ft/min. A velocity between 25 and 30 ft/min is desirable. The following discussion is confined to free air jets except where noted. A free jet is one in which the flow area of the jet is less than one-fifth the flow area of the enclosure. The velocity from an exit into an enclosure is constant for a distance of about four effective diameters and is equal to the exit velocity. The effective diameter for rectangular slots is equal to the diameter of a circular area which is equal to the free flow area of the rectangular slot times its discharge coefficient. For distances from $4D_{ef}$ to $8D_{ef}$, the centerline velocity can be calculated from

$$\frac{V_x}{V_0} = \frac{\sqrt{C'b}}{x} \qquad \text{(1A-57)}$$

where b = Width of jet of air at outlet or vena contracta, ft
x = Distance from the face of the outlet, ft
V_o = Initial velocity of the jet = $V_c / C_d R_{fa}$, ft/min
V_x = Velocity at x distance from outlet face, ft/min
C_d = Coefficient of discharge of the exit, dimensionless
R_{fa} = Ratio of free area to total area of exit, dimensionless
D_{ef} = Effective diameter of the outlet, ft
C' = Constant from Table 1A-6, dimensionless

For greater distances than 8 D_{ef} from the exit face, the following equation can be used to calculate the centerline velocity down to a V_x equal to 150 ft/min. When V_x is between 150 and 50 ft/min, the same equation can be used, but C' should be reduced by 20%.

$$V_x = \frac{C' Q}{x\sqrt{A_t C_d R_{fa}}} \qquad (1A\text{-}58)$$

$$= \frac{C' Q}{x\sqrt{A_{ef}}} \text{ for } x > 8 D_{ef} \qquad (1A\text{-}59)$$

where Q = Air flow, ft^3/min
A_t = Total area of exit, ft^2
A_{ef} = Effective area of exit = $A_t C_d R_{fa}$, ft^2

Table 1A-6 - Values of C' = Constant

Type of Outlet	V_0 = 500 - 1000	V_0 = 2000 - 10,000
Free Openings		
Round or square	5.7	7.0
Rectangular, large aspect ratio < 40	4.9	6.0
Annular slots, axial or radial	3.9	4.8
Grills and Grids		
Free area 40% or more	4.7	5.7
Perforated Panels		
Free area 3-5%	3.0	3.7
Free area 10-20%	4.0	4.9

If we define a distance x at which the centerline velocity is 50 ft/min and call this the throw of the exit, it can be determined from

$$\text{Throw} = \frac{C' Q}{50\sqrt{A_{ef}}} \qquad (1A\text{-}60)$$

The velocity at locations other than on the centerline may be obtained for distances greater than $8D_{ef}$ from the exit, using the following equation:

$$\frac{r}{r_{0.5}} = 3.3 \log \frac{V_x}{V} \qquad (1A\text{-}61)$$

where V_x = Centerline velocity at plane of r, ft/min
r = Radius from the centerline of jet, ft
$r_{0.5}$ = Radius at which $V = 0.5\,V_x$, ft

The radius $r_{0.5}$ occurs at an angle equal to one-half the angle of divergence. The angle of divergence is equal to 20 – 24 deg for slots and nozzle types, and 18 deg for grills and screens.

When a jet discharges along a wall, the jet behaves the same as a free jet that has a width or diameter twice as large as the jet discharging along the wall and whose centerline velocity is at the wall. The C' values must also be multiplied by $\sqrt{2}$.

3.7 Example of Pressure Loss Calculations

Calculate the flow losses in the example illustrated in Fig. 1A-65, and determine the proper number of thin circular turning vanes for the minimum flow loss in the 7-in. square elbow. The discharge through the exit screen is into a very large enclosure ($A = \infty$).

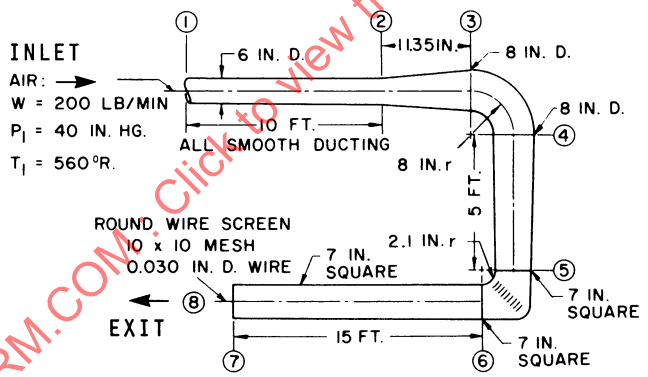

Figure 1A-65 - Example of a Duct System for Flow Loss Calculations

The calculations and a recommended calculation format are given in Table 1A-7. Most of the calculations are self-explanatory except for the following:

(a) For areas ② to ③ in Fig. 1A-65, numbers in column (9) are determined at the inlet, column (16) numbers are based on the Reynolds number of column (9), and column (17) numbers are based on the arithmetic average diameter.

(b) For areas at location ④ to ⑤, all calculations are based on average equivalent diameter of the inlet and the outlet.

(c) To check the applicability of the data, for locations ⑤ to ⑥, D_e is equal to the chord length of the turning vanes, and the Reynolds number is based on this length.

(d) To check the applicability of the data, for location ⑦, the second line of calculation determines the Reynolds number, based on the free flow area of the screen.

Table 1A-7 - Example of Flow Loss Calculation

Location and/or Description (See Fig. 1A-65)	(1) P Inlet, in. Hg	(2) T, °R	(3) w, lb/min	(4) D or D_e, in.	(5) A, Inlet or Exit, in.^{2}	(6) G, lb/min-in.^{2}	(7) ρg, lb/ft^3	(8) q, in. H_2O	(9) N_{Re}	(10) r/D or Area Ratio or ϕ	(11) K_{t90} or K_t	(12) θ (bend) or 2θ (diff.)	(13) C	(14) CK_t	(15) L, in.	(16) 4 f	(17) 4 fl/D_e or 4 fl/D_m	(18) CK_t +4fl/D_e	(19) ΔP_t, in. H_2O
① to ② [1]	40	560	200	6	28.3	7.06	0.0948	9.05	7×10^5	...	...	...	...	...	120	0.0123	0.246	0.246	2.22
② to ③ Diffuser	39.84	560	200	6	28.3	7.06	0.0943	9.10	7×10^5	0.563	0.19	10	0.075	0.0143	11.35	0.0123	0.020	0.034	0.31
③ to ④ circ. elbow	39.81	560	200	8	50.3	3.97	0.0943	2.87	5.3×10^5	1.0	0.18	90	1.0	0.18	12.56	0.013	0.020	0.20	0.57
④ to ⑤ Transition, ○ to □	39.78	560	200	7.5av	50.3	3.97	0.0942	2.87	4.98×10^5	...	...	...	...	...	60	0.013	0.104	0.104	0.30
⑤ to ⑥ Vaned Elbow [2]	39.74	560	200	2.97	49	4.08	0.0942	3.04	2×10^5	0.3	0.2	90	...	...	...	...	...	0.20	0.61
⑥ to ⑦	39.71	560	200	7	49	4.08	0.0940	3.04	4.7×10^5	...	...	...	...	...	180	0.0132	0.340	0.340	1.03
⑦	39.63	560	200	7	49	4.08	0.0939	3.04	...	0.51	1.63	...	...	...	...	...	...	1.63	4.95
Across Grill	...	...	...	0.64	25	8.00	0.0939	...	8.4×10^5										
⑦ to ⑧ Abrupt Expansion	39.27	560	200	7	49	4.08	0.0930	3.08	...	0	1.0	...	...	...	...	...	...	1.0	3.08
Total																			13.07

[1] Example calculations for ① to ② :

For columns 1, 2, and 3 assume given values

$G = (3)/(5) = 200/28.3 = 7.06$

$\rho g = 1.326\, P_e/T = 0.0948$ (Table 1A-2)

$q = G^2/\rho g C = 7.06^2/(0.0948 \times 58.14) = 9.05$ (Table 1A-1)

$4f = 0.0123$ for $w/D = 0.555$ (from Fig. 1A-8)

$4\, fl/D = 0.0123 \times 120/6 = 0.246$ (in column 17)

$\Delta P_t = (8) \times (18) = 9.05 \times 0.246 = 2.22$ in. H_2O

[2] Example Calculation for finding K_t for vaned elbow given r = 2.1, b = 7, e = 90°

Vane chord $c = 2r \sin\theta/2 = 2.98$

$n = 5\,(b/c)\,(\sin\theta/2) - 1$ (from Eq. 1A-19)

$= 7.33$, use 7

$$s = \frac{b}{(n+1)\cos(\theta/2)} = 1.24 \text{ (from Eq. 1A-17)}$$

$$s/c = \frac{1.24}{2.98} = 0.41$$

From Figs. 1A-33 and 1A-34, $K_t = 0.20$

4. REFERENCES

1. J. R. Henry, "Design of Power Plant Installations, Pressure-Loss Characteristics of Duct Components." NACA Wartime Report L-208, June 1944.
2. J. T. Higgenbotham, C. C. Wood, and E. F. Valentine, "A Study of the High-Speed Performance Characteristics of 90° Bends in Circular Ducts." NACA TN 3696, June 1956.
3. O. P. Lamb and J. S. Holdhusen, "Investigation of Aircraft Ducting Components at High Subsonic Speeds." Fluidyne Report WADC TR 56-187, ASTIA Document 97321, September 1956.
4. C. H. McClellan and W. A. Bartlett, Jr., "Investigation of Air Flow in Right Angle Elbows in a Rectangular Duct." NACA Wartime Report L-328, October 1941.
5. R. D. Madison and J. R. Parker, "Pressure Losses in Rectangular Ducts," Trans. ASME, Vol. 38 (1936), pp. 167-176.
6. M. R. Nichols, "Investigation of Flow Through an Intercooler Set at Various Angles to the Supply Duct." NACA Wartime Report L-408, April 1942.
7. A. Vazsonyi, "Pressure Loss in Elbows and Duct Branches," Trans. ASME, Vol. 66 (1944), pp. 177-183.
8. J. R. Weske, "Pressure Loss in Ducts with Compound Elbows." NACA Wartime Report W-39, February 1943.
9. L. Wirt, "New Data for the Design of Elbows in Duct Systems," General Electric Review, Vol. 30 (June 1927), pp. 286-296.
10. W. H. McAdams, Heat Transmission. New York: McGraw-Hill Book Company Inc., 2nd ed., 1942, p. 118.
11. J. H. Perry, Chemical Engineers' Handbook. New York: McGraw-Hill Book Company Inc., 3rd ed., 1950, pp. 370-373.
12. "Airplane Heating and Ventilating Equipment Engineering Data." SAE Information Report No. 23, October 1951.
13. G. N. Patterson, "Note on the Design of Corners in Duct Systems." R & M 1773 (British), October 1936.
14. L. F. Moody, "Friction Factors for Pipe Flow," Trans. ASME, Vol. 66 (1944), pp. 671-677.
15. C. Salter, "Experiments on Thin Turning Vanes." R & M 2469 (British), 1952.
16. H. Peters, "Conversion of Energy in Cross-Sectional Divergences Under Different Conditions of Inflow." NACA TM 737, 1934.

17. A. N. Vedernikoff, "An Experimental Investigation of the Flow of Air in a Broadening Channel." NACA TM 1059, 1944.

18. J. Persh, "The Effect of Surface Roughness on the Performance of a 23° Conical Diffuser at Subsonic Mach Numbers." NACA CR 3737, 1952.

19. E. G. Reid, "Performance Characteristics of Plane-Wall Two-Dimensional Diffusers." NACA TN 2888, February 1953.

20. B. H. Little and S. W. Wilbur, "Performance and Boundary-Layer Data from 12° and 23° Conical Diffusers of Area Ratio 2.0 at Mach Numbers Up to Choking and Reynolds Numbers Up to 7.5×10^6." NACA TR 1201, 1954.

21. M. R. Copp, "Effects of Inlet Wall Contour on the Pressure Recovery of a 10° 10-Inch-Inlet-Diameter Conical Diffuser." NACA CR 3569, September 5, 1951.

22. C. A. Moore, Jr., and Stephen J. Kline, "Some Effects of Vanes and of Turbulence in Two-Dimensional Wide-Angle Subsonic Diffusers." NACA TN 4080, June 1958.

23. W. J. Biebel, "Low-Pressure Boundary Layer Control in Diffusers and Bends." NACA WR L-84, 1945.

24. G. N. Patterson, "Modern Diffuser Design," Aircraft Engineering, Vol. X, No. 115, September 1938, pp. 267-273.

25. R. Scherrer and W. E. Anderson, "Preliminary Investigation of a Family of Diffusers Designed for Near Sonic Inlet Velocities." NACA TN 3668, February 1956.

26. C. H. McLellan and M. R. Nichols, "Investigation of Diffuser Resistance Combinations in Duct Systems." NACA WR L329, February 1942.

27. "Fan Engineering." New York: Buffalo Forge Co., 4th ed., 1938.

28. C. P. Kittredge and D. S. Rawley, "Resistance Coefficients for Laminar and Turbulent Flow Through One-Half-Inch Valves and Fittings," Trans. ASME, Vol. 79 (1957), pp. 1759-1766.

29. A. R. Collar, "Some Experiments with Cascades of Aerofoils." R & M No. 1768, 1937.

30. K. J. Bell and O. P. Bergelin, "Flow Through Annular Orifices," Trans. ASME, Vol. 79 (1957), pp. 593-599.

31. E. J. O. Brandt, "How You Can Measure Airflow," Product Eng. (June 1957), pp. 145-150.

32. E. Buckingham, "Notes on Some Recently Published Experiments on Orifice Meters," Trans. ASME, Vol. 78 (1956), pp. 379-387.

33. R. G. Cunningham, "Orifice Meters with Supercritical Compressible Flow," Trans. ASME, Vol. 73, July 1951, pp.625-638.

34. A. L. Ducoffe, J. R. Bennett, and C. G. Ray, "Subcritical and Critical Flow Through Straight-Through Elbow, and Tee A-N Fittings and Sharp-edged Orifices at Elevated Temperatures," Trans. ASME, Vol. 80, October 1958, pp. 1349-1357.

35. "Flow Measurement, 1959."~ ASME Power Test Codes, PTC 19.5.4, 1959.

36. H. P. Grace and C. E. Lapple, "Discharge Coefficients of Small Diameter Orifices and Flow Nozzles," Trans. ASME, Vol. 73 (1951), pp. 639-648.

37. H. W. Iversen, "Orifice Coefficients for Reynolds Numbers from 4 to 50,000," Trans. ASME, Vol. 78 (1956), pp. 359-364.

38. A. L. Jorissen, "Discharge Coefficients of Herschel Type Venturi Tubes," Trans. ASME, Vol. 74 (1952), pp. 905-913.

39. A. L. Jorissen, "Discharge Measurements at Low Reynolds Numbers - Special Devices," Trans. ASME, Vol. 78 (1956), pp. 365-372.

40. A. L. Jorissen, "Discharge Measurements by Means of Venturi Tubes," Trans. ASME, Vol. 73 (1951), pp. 403-411.

41. A. L. Jorissen and H. T. Newton, "Discharge Measurements by Means of Cylindrical Nozzles," Trans. ASME, Vol. 74 (1952), pp. 825-835.

42. I. O. Miner, "The Dall Flow Tube," Trans. ASME, Vol. 78 (1956), pp. 475-479.

43. J. A. Perry, "Critical Flow Through Sharp-edged Orifices," Trans. ASME, Vol. 71 (1949), pp. 757-764.

44. M. Rivas, Jr., and A. Shapiro, "On the Theory of Discharge Coefficients for Rounded-entrance Flow Meters and Venturis," Trans ASME, Vol. 78 (1956), pp. 489-497.

45. J. M. Spitzglass, "Orifice Coefficients - Data and Results of Tests," Trans. ASME, Vol. 44 (1922), pp. 919-974.

46. J. Warren, "A Study of Head Loss in Venturi Meter Diffuser Sections," Trans. ASME, Vol. 73 (1951), pp. 399-402.

47. A. Weir, Jr., J. L. York, and R. B. Morrison, "Two and Three Dimensional Flow of Air Through Square Edged Sonic Orifices," Trans. ASME, Vol. 78 (1956), pp. 481-488.

48. B. Eckert and F. Pfluger, "The Resistance Coefficent of Commercial Round Wire Grids." NACA TM 1003, January 1942.

49. A. A. Adler, "Variation With Mach Number of Static and Total Pressures Through Various Screens." NACA CR 2007 (L23), February 1946.

50. S. F. Hoerner, "Pressure Losses Across Screens and Grids." AFTR 6289, November 1950.

51. W. D. Baines and E. G. Peterson, "An Investigation of Flow Through Screens," Trans. ASME, Vol. 73 (1951), pp. 467-480.

52. L. L. Repko, "Pressure Drop Across Various Commercial Screens," Design News, January, 1951, pp.51-53.

53. W. G. Cornell, "Losses in Flow Normal to Plane Screens," Trans. ASME, Vol. 80 (1958), pp. 791-799.

54. R. E. Dannenberg, B. J. Gambucci, and J. A. Weiberg, "Perforated Sheets as a Porous Material for Distributed Suction and Injection." NACA TN 3669, April 1956.

55. L. F. G. Simmons and C. F. Cowdrey, "Measurements of the Aerodynamic Forces Acting on Porous Screens." R & M 2276, British R.A.E., 1945.

56. G. B. Schubauer, W. G. Spangenberg, and P. S. Klebanoff, "Aerodynamic Characteristics of Damping Screens." NACA TN 2001, January 1950.

57. P. Jonas, "The Changes Produced in an Air Stream by Wire Gauze," Engineers Digest, Vol. 18, May 1957, pp. 191-193.

58. A. L. Loeffler, Jr., and M. Perlmutter, "Turbulent Flow Through Porous Resistances Slightly Inclined to the Flow Direction." NACA TN 4221, February 1958.

59. "Flexible Components for Pneumatic Ducting Systems," Arrowhead Products, Technical Bulletin 516, 1959, pp. 1-8.

60. C. M. Daniels, "Pressure Losses in Flexible Metal Tubing," Product Engineering, April 1956, pp. 223-227.

61. "Pressure Drop in Convoluted Hoses," Douglas Aircraft Co. Testing Division, Technical Memorandum TM-DC8-P & M-L0284, October 1957.

62. Douglas Aircraft Co. Testing Division Memorandum A851-JNS-M55, January 20, 1956 and Memorandum A851-JNS-M148, February 22, 1956.

63. R. C. Martinelli, E. B. Weinberg, E. H. Morrin, and L. M. K. Boelter, "An Investigation of Aircraft Heaters III - Measured and Predicted Performance of Double Tube Heat Exchangers", NACA WR W-98, October 1942.

64. L. M. K. Boelter, E. H. Morrin, R. C. Martinelli, and H. F. Poppendiek, "An Investigation of Aircraft Heaters IV - An Air and Heat Flow Analysis of a Ram-Operated Heater and Duct System", NACA WR W-21, March 1949.

65. B. Dahle, "Butterfly Valves for High Performance Applications", Machine Design, Volume 30, December 25, 1958, pp. 105-109.

66. J. Allen and B. Albinson, "An Investigation of the Manifold Problem for Incompressible Fluids with Special Reference to the Use of Manifolds for Canal Locks", Proceedings of the Institution of Civil Engineers, Vol. 4, April 1955, pp. 114-138.

67. W. M. Dow, "The Uniform Distribution of Fluid Flowing Through a Perforated Pipe", Journal of Applied Mechanics, Vol. 17, 1950, pp. 431-438.

68. J. H. Horlock, "An Investigation of the Flow in Manifolds with Open and Closed Ends", Journal of the Royal Aeronautical Society, Vol. 60, 1956, pp. 749-753.

69. E. Markland, "The Analysis of Flow From Pipe Manifolds", Engineering, January 30, 1959, pp. 150-151.

SECTION 1B - THERMODYNAMICS AND COMPRESSIBLE FLOW

1. INTRODUCTION

1.1 Definition and Scope

Thermodynamics is a branch of engineering concerned primarily with systems and processes for converting thermal energy into mechanical energy or mechanical energy into thermal energy. In aircraft these processes are used for:

(a) Generation of mechanical power.

(b) Refrigeration (reversed power cycles).

(c) Compression of air for control of cabin atmosphere, and for power and heat distribution systems.

In these, and other similar processes, the engineer deals with relations between heat and work in a system fluid and is guided by two general laws of nature, the first and second laws of thermodynamics.

1.2 Nomenclature

a = Constant, atm-ft^6/mole^2 (Eq. 1B-39)
a_o = Speed of sound, ft/sec
a_0^* = Speed of sound when M=1, ft/sec
A = Area, ft^2, in.^{2}
A_* = Streamtube area for sonic flow, in.^{2}
b = Constant, ft^3/mole (Eq. 1B-39)
c = Constant, dimensionless
c = Specific heat, Btu/lb - °F
C = Constant, dimensionless
D = Diameter, ft, in.
E = Internal energy, Btu
f = Friction coefficient, dimensionless
F = Force, lb
F = Impulse function, lb
g = Gravitational acceleration, ft/sec^2
h = Scoop height, in.
h = Specific enthalpy, Btu/lb
J = Joule's constant, 778 ft-lb/Btu
K = Pressure loss coefficient, dimensionless
K = Outlet discharge coefficient, dimensionless
L = Length, ft, in.
m = Mass (W/g), lb-sec^2/ft, lb
M = Mach number, dimensionless
M = Molecular weight
N = Boundary layer profile parameter, dimensionless
N_{Re} = Reynolds number ($VD\rho g/\mu$, $Vx\rho g/\mu$), dimensionless

P = Pressure, lb/ft^2, in. Hg
P_s = Static pressure, psi, lb/ft^2, in. Hg
P_t = Total pressure, psi, lb/ft^2, in. H_2O
q = Dynamic pressure, $(1/2)\rho V^2$, lb/ft^2, in. Hg, in. H_2O
Q = Heat, Btu
R = Characteristic gas constant, ft-lb/lb - °R
R_u = Universal gas constant, ft-lb/lb - °R
S = Entropy, Btu/°F
T = Temperature, absolute, °R
T_s = Static temperature, °R
T_t = Total temperature, °R
u = Specific internal energy (E/W), Btu/lb
U = Velocity, ft/sec
v = Specific volume, ft^3/lb
V = Volume, ft^3
w = Mass flow rate, lb/sec
W = Weight, lb
W = Mass flow rate, lb/min
W_k = Work, ft-lb
x,y = Distance, ft
Y = Pressure ratio function (See Eq. 1B-20)
z = Elevation, ft
Z = Compressibility factor, dimensionless
γ = Ratio of specific heats, dimensionless
δ = Boundary layer thickness, ft, in.
δ = Body angle, deg
δ^* = Boundary layer displacement thickness, in.
η = Efficiency, dimensionless
θ = Mach turning angle, deg
ν = Kinematic viscosity, $\mu/\rho g$, ft^2/sec
μ = Mach angle, deg
ρ = Mass density, lb-sec^2/ft^4
ρg = Specific weight (density), lb/ft^3
τ = Time, sec
τ_w = Wall shear stress, lb/ft^2

Subscripts:

am = Arithmetic mean
c = Compression
c = Cold
cr or *CR* = Critical point
h = Hot
isen = Isentropic
m = Mixture
max = Maximum
o = Freestream

o	= Outside
p	= Pressure
r or *R*	= Reduced
s	= Static
st	= Storage
t	= Total
t	= Expander
thr	= Throat
tr	= Triple point
v	= Volume
1	= Point 1
2	= Point 2
3	= Point 3

Superscripts:

—	= Average
*	= (See Fig. 1B-20)

2. FIRST LAW OF THERMODYNAMICS

The first law of thermodynamics states that various forms of energy are convertible and, in the conversion processes, energy is neither created nor destroyed but is conserved. This law pertains to all forms of energy such as mechanical, chemical, electrical, and thermal. Thermodynamics engineering is concerned primarily with mechanical and heat energy.

A list of conversion factors useful in dealing with problems involving changes from one form of energy to another is given in Table 1B-1.

A general equation that accounts for most of the forms of energy of interest in a conversion process is

$$\frac{Wz_1}{J} + \frac{WU_1^2}{2gJ} + Wu_1 + \frac{WP_1v_1}{J} + Q = \frac{Wz_2}{J} + \frac{WU_2^2}{2gJ} + Wu_2 + \frac{WP_2v_2}{J} + \frac{W_k}{J} \qquad \text{(1B-1)}$$

where W = Weight of fluid being considered (usually per unit time), lb
z = Elevation, ft
J = Joule's constant, 778 ft-lb/Btu
g = Acceleration of gravity, 32.2 ft/sec^2
U = Velocity, ft/sec
u = Specific internal energy, Btu/lb
P = Pressure, lb/ft^2
v = Specific volume, ft^3/lb

Q = Heat energy, Btu
W_k = Work, ft-lb

Table 1B-1 - Conversion Factors

778.16 ft-lb	=	1 Btu
550 ft-lb/sec	=	1 hp
33,000 ft-lb/min	=	1 hp
2544.48 Btu/hr	=	1 hp
42.408 Btu/min	=	1 hp
3412.76 Btu	=	1 kW-hr
745.578 watts	=	1 hp
1 joule/sec	=	1 watt
10^7 ergs	=	1 joule
252 cal	=	1 Btu
1.8 Btu/lb	=	1 cal/gram

This version of the energy equation represents a steady flow equilibrium process. The first four terms of each side are quantities related to the working fluid and the last terms on each side are system characteristics. The first four terms are respectively:

(a) Potential energy due to physical elevation, z

(b) Kinetic energy of motion

(c) Internal (molecular) energy due to temperature

(d) Flow work required to produce fluid movement down a pipe

The fifth term on the left side, Q, is the heat energy transferred to the system through a boundary. On the right side, W_k is the mechanical energy delivered as work from the system. If this were a nonequilibrium flow process, terms would have to be added to account for storage of energy if some of the heat transferred into the system were not immediately available to the process (for example, a Q_{st} term). In most practical problems, the potential energy terms are negligible and are usually omitted.

From this general form of the energy equation, several simpler and more restricted forms can be derived. First, however, certain properties of the working fluids are discussed.

3. IDEAL OR PERFECT GASES AS WORKING FLUIDS

3.1 Equation of State

All three phases of substances (solid, liquid, and gas) are of interest in thermodynamics. The gaseous or vaporous phase is of primary significance. A greatly simplifying assumption in the discussion of thermodynamic fundamentals is that the working fluids have certain idealized properties. It is a fortunate fact that a number of common gases, particularly diatomic gases, do behave over moderate ranges of temperature and pressure as ideal gases.

The most important characteristic of an ideal gas is that it conforms to certain simple relationships with respect to pressure, temperature, and density, namely:

$$PV = WRT \tag{1B-2}$$

$$\text{or: } P = \rho g R T \tag{1B-3}$$

where Eq. 1B-3 is the characteristic equation of an ideal gas. Here, T is the absolute temperature in degrees Rankine; R is a characteristic constant for each particular gas and is related to the molecular weight by the so-called universal gas constant R_u, which is equal to 1545.33 ft-lb/lb-°R, so that:

$$R = \frac{R_u}{M} = \frac{1545.33}{\text{molecular weight}} \tag{1B-4}$$

The extent to which common gases conform to the ideal gas equation can be noted in Table 1B-2.

3.2 Energy Equations of a Ideal Gas

3.2.1 Nonflow Processes

A special case of the general steady flow energy equation is the case in which no flow occurs, so that the energy is transferred to or from a fixed (or trapped) quantity of working fluid, as, for example, in the compression stroke of a reciprocating air compressor. In this form, the energy equation is simplified to the following form by the omission of the kinetic energy terms and the flow work terms:

$$Q = W\left(u_2 - u_1\right) + \frac{W_k}{J} \tag{1B-5}$$

The evaluation of the terms of this simplified energy equation depends on a knowledge of the type of process involved. In the case of the compressor cylinder and piston, the general expression for the nonflow work is:

$$W_k = \int_1^2 P\,dV \quad \text{ft-lb} \tag{1B-6}$$

as illustrated in Fig. 1B-1

3.2.2 Specific Heat

By definition, specific heat is:

$$c = \frac{dQ}{W dT} \quad \frac{\text{Btu}}{\text{lb-°F}} \tag{1B-7}$$

Table 1B-2 - Characteristic Constants for Gases

Gas	M	c_p	c_v	γ	$R=PV/WT$	R_u/M
Air	29	0.24	0.1715	1.4	53.3	53.28
Carbon Monoxide (CO)	28.011	0.2487	0.1779	1.398	55.1	55.169
Hydrogen (H_2)	2.016	3.421	2.4354	1.405	767	766.54
Nitric Oxide (NO)	30.008	0.2378	0.1717	1.384	51.4	51.498
Nitrogen (N_2)	28.016	0.2484	0.1776	1.4	55.1	55.159
Oxygen (O_2)	32	0.2193	0.1573	1.394	48.25	48.292
Argon (A)	39.944	0.125	0.0751	1.668	38.7	38.688
Helium (He)	4.003	1.25	0.754	1.659	386	386.05
Carbon Dioxide (CO_2)	44.011	0.202	0.157	1.29	34.9	35.113
Hydrogen Sulfide (H_2S)	34.082	0.328	0.270	1.21	44.8	45.342
Nitrous Oxide (N_2O)	44.016	0.211	0.166	1.27	34.9	35.109
Acetylene (C_2H_2)	26.038	0.409	0.333	1.23	58.8	59.350
Ethane (C_2H_6)	30.07	0.422	0.357	1.18	50.8	51.392
Ethylene (C_2H_4)	28.054	0.374	0.304	1.23	54.7	55.085
Isobutane (C_4H_{10})	58.124	0.420	0.387	1.09	25.8	26.587
Methane (CH_4)	16.043	0.533	0.409	1.30	96.2	96.325
Propane (C_3H_8)	44.097	0.404	0.360	1.12	34.1	35.042

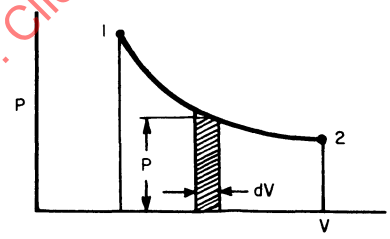

Figure 1B-1 - Nonflow Work, Compressor Cylinder and Piston

The value of c depends on the process by which heat Q is added. At constant volume $c = c_v$; at constant pressure $c = c_p$. Note that c_p is always larger than c_v, owing to the work of expansion at constant pressure. The ratio of c_p/c_v is designated γ, which is an important characteristic parameter of gases and vapors.

3.2.3 Internal Energy of a Gas

Joule determined experimentally that a change of internal energy was a function of the change of temperature only. To evaluate the relationship between temperature change and internal energy change, consider a constant volume process in which heat is added to a fluid. Since the work term is zero, the simplified energy equation becomes:

$$Q = W\left(u_2 - u_1\right) \tag{1B-8}$$

and by definition of c_v,

$$Q = W\int_{T_1}^{T_2} c_v\, dT \tag{1B-9}$$

so that $W(u_2-u_1) = Wc_v(T_2-T_1)$. (1B-9a)

3.2.4 c_p, c_v, and R Relationship

Consider a constant pressure-temperature change in which the work is:

$$W_k = \int PdV = P\left(V_2-V_1\right) = WR\left(T_2-T_1\right) \tag{1B-10}$$

and the heat added is

$$Q = Wc_p\left(T_2-T_1\right) \tag{1B-11}$$

and the change in internal energy is

$$W\left(u_2-u_1\right) = Wc_v\left(T_2-T_1\right) \tag{1B-12}$$

Substituting in Eq. 1B-5,

$$Wc_p\left(T_2-T_1\right) = Wc_v\left(T_2-T_1\right) + W\frac{R}{J}\left(T_2-T_1\right) \tag{1B-13}$$

which yields

$$c_p = c_v + \frac{R}{J} \quad \text{or} \quad c_p - c_v = \frac{R}{J}$$

or

$$c_v = \frac{1}{\gamma-1}\frac{R}{J} \quad \text{and} \quad c_p = \frac{\gamma}{\gamma-1}\frac{R}{J} \tag{1B-14}$$

3.2.5 Enthalpy

The property of a fluid called specific enthalpy (or generally, enthalpy) is arbitrarily defined as

$$h = u + \frac{Pv}{J} \text{ or } u + \frac{P}{J\rho} \tag{1B-15}$$

This property bears the same relationship to heat added in a constant pressure process as internal energy added in a constant volume process. Like internal energy, enthalpy is a property of a fluid that depends on the state point and not on the process by which a given value of enthalpy is reached. Only the change in value, not the absolute magnitude, is significant to any process under study. Thus, for an ideal gas:

$$\Delta h = \Delta u + \Delta\left(\frac{Pv}{J}\right) = c_v\left(T_2-T_1\right) + \frac{R}{J}\left(T_2-T_1\right)$$

$$= c_p\left(T_2-T_1\right) \tag{1B-16}$$

3.2.6 Reversibility

In dealing with conversion processes between heat and work, work can always be converted completely into heat energy (for example, by friction, turbulence, magnetic hysteresis, or eddy current). However, heat can never be completely converted to work, except in hypothetical processes referred to as "ideal," "perfect," or "reversible." This would indicate that work is a "higher grade" of energy than heat (as electrical and chemical energy also are).

Thus the "reversible" process can be considered a goal (unattainable in nature) by which to measure the degree of perfection actually achieved by a given process under study. In another sense, a reversible process is one in which no energy is irreversibly lost by friction and turbulence.

3.2.7 Entropy

It has been found very useful to define another thermodynamic property of a working fluid to describe the reversible or "ideal" transfer of heat (or its equivalent) to or from a system. This property is called entropy and, like enthalpy, its magnitude does not depend on the process being considered. Its definition does, however, refer to a reversible transfer of heat. Also like enthalpy, entropy is important only in terms of changes in its value rather than in its absolute magnitude. The definition of a change in entropy is

$$\Delta S = S_2 - S_1 = \int_1^2 \frac{dQ}{T} \tag{1B-17}$$

where dQ is the heat (or its equivalent) reversibly added to or subtracted from a working fluid at an absolute temperature, T.

A process involving a change in temperature with no change in entropy is an "ideal" or reversible process and is normally referred to as isentropic.

3.2.8 Isentropic Processes

A process in which no heat is added or subtracted from the fluid (perfectly insulated against heat transfer) is called adiabatic. Only a reversible adiabatic change, however, is also isentropic. In such processes,

$$P_1 V_1^{\gamma} = P_2 V_2^{\gamma} \tag{1B-18}$$

where $\gamma = c_p / c_v$.

From equation 1B-18 and the equation of state, Eq. 1B-2, the following equations can be derived:

$$\frac{T_2}{T_1} = \left(\frac{P_2}{P_1}\right)^{(\gamma-1)/\gamma} \tag{1B-19}$$

If $P_2/P_1 > 1$,

$$T_2 - T_1 = T_1\left[\left(\frac{P_2}{P_1}\right)^{(\gamma-1)/\gamma} - 1\right] = T_1 Y \tag{1B-20}$$

$$\text{where } Y = \left[\left(\frac{P_2}{P_1}\right)^{(\gamma-1)/\gamma} - 1\right], \text{ for } P_2/P_1 > 1 \tag{1B-20a}$$

If $P_1/P_2 > 1$,

$$T_1 - T_2 = T_1\left[1 - \left(\frac{P_2}{P_1}\right)^{(\gamma-1)/\gamma}\right] = T_1\left[\frac{Y}{Y+1}\right] \tag{1B-21}$$

$$\text{where } Y = \left[\left(\frac{P_1}{P_2}\right)^{(\gamma-1)/\gamma} - 1\right], \text{ for } P_1/P_2 > 1 \tag{1B-21a}$$

Y in this case is evaluated for $P_1/P_2 > 1$.

3.2.9 Nonisentropic Processes

The two most common energy conversion processes encountered in aerothermodynamics are compression and expansion of gases. With the widespread use of turbo machinery, these processes are generally adiabatic, or nearly so (small external heat transfer). Being real rather than ideal, however, they are never reversible or isentropic but are carried out at some finite efficiency less than 100%. For these conditions, Eqs. 1B-20 and 1B-21 become

$$T_2 - T_1 = \frac{T_1 Y}{\eta_c} \quad \text{for compression} \tag{1B-21b}$$

and

$$T_1 - T_2 = \eta_t T_1\left[\frac{Y}{Y+1}\right] \quad \text{for expansion} \tag{1B-21c}$$

where

$$\eta_c = \text{Compressor isentropic efficiency} = \frac{T_1 Y}{T_2 - T_1} \tag{1B-22}$$

$$\eta_t = \text{Expander isentropic efficiency} = \frac{(T_1 - T_2)(Y+1)}{T_1 Y} \tag{1B-23}$$

Note that in any nonisentropic compression or expansion process, there is always an increase in entropy resulting from irreversibility.

3.2.10 Work in Nonflow Compression or Expansion

Table 1B-3 presents a summary of ideal gas equations for nonflow processes.

3.2.10.1 Isentropic

$$PV^{\gamma} = C$$

$$W_k = \int_{V_1}^{V_2} P\,dV = C\int_{V_1}^{V_2} \frac{dV}{V^\gamma}$$

$$= \frac{P_2V_2 - P_1V_1}{1-\gamma} \text{ ft-lb} \qquad \text{(1B-24)}$$

$$W_k = WR\frac{T_2 - T_1}{1-\gamma}$$

$$= WJc_v\left(T_1 - T_2\right) \text{ ft-lb} \qquad \text{(1B-25)}$$

For compression, W_k is negative (work done on fluid). For expansion, W_k is positive (work done by fluid).

Table 1B-3 - Summary of Ideal Gas Equations for Nonflow Processes (for a unit weight of fluid)

Quantity Description	Symbols	Processes: Constant Volume	Constant Pressure	Constant Temperature	Constant Entropy
			$\frac{T_2}{T_1} = \frac{V_2}{V_1}$		$P_1V_1^\gamma = P_2V_2^\gamma$
Perfect Gas Relations	P, V, T	$\frac{T_2}{T_1} = \frac{P_2}{P_1}$	$\frac{T_2}{T_1} = \frac{\rho_1}{\rho_2}$	$P_1V_1 = P_2V_2$	$\frac{T_2}{T_1} = \left(\frac{\rho g_2}{\rho g_1}\right)^{\gamma-1} = \left(\frac{V_1}{V_2}\right)^{\gamma-1}$
		Charles' Law	Charles' Law	Boyle's Law	$\frac{T_2}{T_1} = \left(\frac{P_2}{P_1}\right)^{(\gamma-1)/\gamma}$
Work in a Nonflow Expansion or Compression	$\int_1^2 P\,dv$	0	$P(V_2 - V_1)$	$P_1V_1 \log_e \frac{V_2}{V_1}$	$\frac{P_2V_2 - P_1V_1}{1-\gamma}$ $\frac{RT_1}{1-\gamma}\left[\left(\frac{P_2}{P_1}\right)^{(\gamma-1)/\gamma} - 1\right]$
Change in Internal Energy	$u_2 - u_1$	$c_v(T_2 - T_1)$	$c_v(T_2 - T_1)$	0	$c_v(T_2 - T_1)$
Heat Transferred to or from System	Q	$c_v(T_2 - T_1)$	$c_p(T_2 - T_1)$	$\frac{P_1V_1}{J} \log_e \frac{V_2}{V_1}$	0
Change in Enthalpy	$h_2 - h_1$	$c_p(T_2 - T_1)$	$c_p(T_2 - T_1)$	0	$c_p(T_2 - T_1)$
Change in Entropy	$S_2 - S_1$	$c_v \log_e \frac{T_2}{T_1}$	$c_p \log_e \frac{T_2}{T_1}$	$\frac{R}{J} \log_e \frac{V_2}{V_1}$	0

3.2.10.2 Nonisentropic

For compression:

$$W_k = \frac{WR(T_2 - T_1)}{\eta_c\,(1-\gamma)}$$

$$= \frac{WJc_v(T_1 - T_2)}{\eta_c} \text{ ft-lb} \qquad \text{(1B-26)}$$

For expansion:

$$W_k = \frac{W\eta_t R\,(T_2 - T_1)}{1-\gamma}$$

$$= W\eta_t J c_v\,(T_1 - T_2) \text{ ft-lb} \qquad \text{(1B-27)}$$

where η_c and η_t are efficiencies of the compressor and expander.

3.2.11 Work in Steady-Flow Compression or Expansion

When the complete cycle of a reciprocating compressor or expander is considered, and the inflow and exhaust strokes are taken into account, the work equations are identical to those of turbo noncyclic machines. This fact permits using the nonflow cyclic equations for steady-flow machines.

3.2.11.1 Isentropic Steady-Flow Compression (or Expansion)

Fig. 1B-2 and the following equations represent isentropic steady-flow compression.

$$W_k = \frac{P_2V_2 - P_1V_1}{1-\gamma} + P_2\left(V_3 - V_2\right) + P_1\left(V_1 - V_4\right) \qquad \text{(1B-28)}$$

$$W_k = \frac{P_2V_2 - P_1V_1}{1-\gamma} - P_2V_2 + P_1V_1 \text{ (because } V_3 \text{ and } V_4 \text{ equal 0)} \qquad \text{(1B-29)}$$

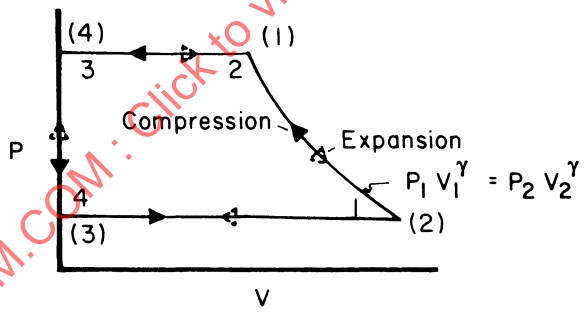

Figure 1B-2 - Steady-Flow Compression or Expansion

$$W_k = \frac{\gamma\,(P_2V_2 - P_1V_1)}{1-\gamma}$$

$$= \frac{W\gamma R(T_2 - T_1)}{1-\gamma} \text{ ft-lb} \qquad \text{(1B-30)}$$

$$W_k = WJc_p\,(T_1 - T_2)$$

$$= -WJc_pT_1Y \text{ ft-lb} \qquad \text{(1B-31)}$$

For noncyclic machines, the general energy equation becomes, after dropping the potential and kinetic energy terms,

$$W_k = WJ\left(h_1 - h_2\right) + JQ \tag{1B-32}$$

For the adiabatic case, $Q = 0$, and

$$W_k = WJ\left(h_1 - h_2\right)$$

$$= WJc_p\left(T_1 - T_2\right) \quad \text{ft-lb} \tag{1B-33}$$

where W_k is negative for compression and positive for expansion, and again

$$W_k = -WJc_pT_1\left[\left(\frac{p_2}{p_1}\right)^{(\gamma-1)/\gamma} - 1\right]$$

$$= -WJc_pT_1Y \quad \text{ft-lb} \tag{1B-34}$$

3.2.11.2 Nonisentropic Steady-Flow Compression or Expansion

For compression:

$$W_k = \frac{-WJc_pT_1Y}{\eta_c} \tag{1B-35}$$

For expansion:

$$W_k = \eta_t WJc_pT_1\left[\frac{Y}{Y+1}\right] \tag{1B-36}$$

3.3 Equations for Mixtures of Ideal Gases

In a mixture of gases, each constituent gas behaves as though it alone occupied the total volume of the mixture. The total pressure of the mixture, P_m, is, according to Dalton's law, the sum of the individual constituent or partial pressures of each gas. For gases a, b, and c

Total pressure $= P_m = P_a + P_b + P_c$

Total volume $= V = V_a = V_b = V_c$

Temperature $= T = T_a = T_b = T_c$

If the composition of the mixture is known by weight, $W_a + W_b + W_c = W_m$. Then the partial pressures can be determined from the following relationship:

$$\frac{P_a}{P_m} = \frac{W_aR_a}{W_mR_m}, \quad \frac{P_b}{P_m} = \frac{W_bR_b}{W_mR_m}, \quad \text{and} \quad \frac{P_c}{P_m} = \frac{W_cR_c}{W_mR_m} \tag{1B-37}$$

where R_a, R_b, and R_c are the constituent gas constants and R_m is the apparent gas constant of the mixture obtained from

$$R_m = \frac{W_aR_a + W_bR_b + W_cR_c}{W_m}$$

Similar weight relationships among constituent properties and mixture properties can be found for specific heat, enthalpy, internal energy, temperature, and entropy.

4. THE SECOND LAW OF THERMODYNAMICS

Although the first law is concerned with the equivalence of various forms of energy, it sheds no light on the extent to which such conversions actually can be achieved. The second law, however, is concerned with the inherent limitations of the heat engine as a means of converting heat into work. Experience has indicated that while work can easily be completely converted into heat (J = 778 ft-lb/Btu), heat cannot be completely converted into work. This experience has resulted in the second law, which, although it has been presented in many ways, essentially states the following:

No heat engine, however perfect, operating in a closed cycle, can convert all the heat supplied to its working fluid into work. Some part of the heat supplied is rejected uselessly to a sink and is therefore unavailable as work.

4.1 Carnot Cycle and Available Energy

To illustrate this principle, consider one of the most ideal heat engine cycles yet devised, that of the Carnot cycle. The Carnot cycle consists of two isothermal and two isentropic steps as indicated in Fig. 1B-3, and expressed as

$$\text{Input heat} = T_h\left(S_2 - S_1\right)$$

$$\text{Rejected heat} = T_c\left(S_2 - S_1\right)$$

$$\text{Net work out} = \left(T_h - T_c\right)\left(S_2 - S_1\right)$$

$$\text{Cycle efficiency} = \frac{\text{Net work out}}{\text{Input heat}}$$

$$= \frac{(T_h - T_c)(S_2 - S_1)}{T_h(S_2 - S_1)} = \frac{T_h - T_c}{T_h} \qquad \text{(1B-38)}$$

Thus the efficiency of this ideal cycle could approach 100% only if T_c approached absolute zero or if T_h approached infinity. Of the total heat input, only the heat input above the sink temperature is available for conversion to work.

4.2 Methods of Graphical Representations

Heat engine or reversed heat engine (refrigeration) cycles are commonly plotted on several different and useful coordinate systems. The most useful of these are presented as follows:

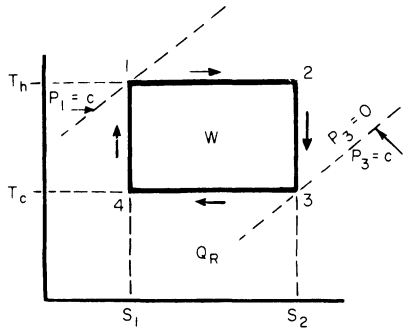

Figure 1B-3 - T-S Diagram

4.2.1 Pressure-Volume Diagram

In Fig. 1B-4, the area enclosed by the cycle represents the net work performed.

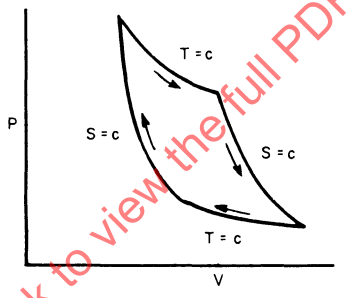

Figure 1B-4 - Carnot Cycle

4.2.2 Temperature-Entropy Diagram

In the highly superheated range, *h* is dependent primarily on temperature; so the T-S diagram is also an h-S, or Mollier, diagram as shown in Figs. 1B-5 and 1B-6.

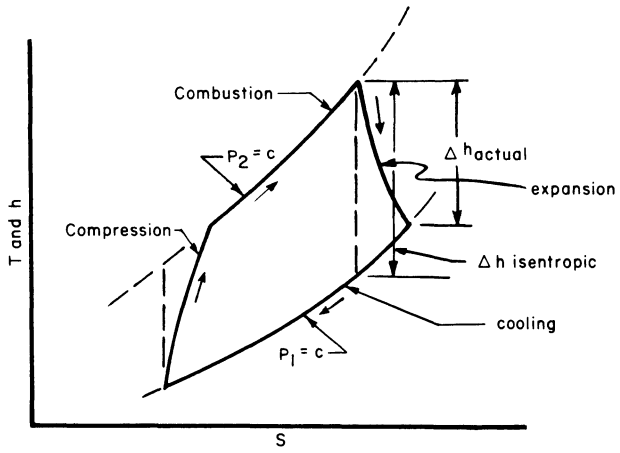

Figure 1B-5 - Brayton Cycle

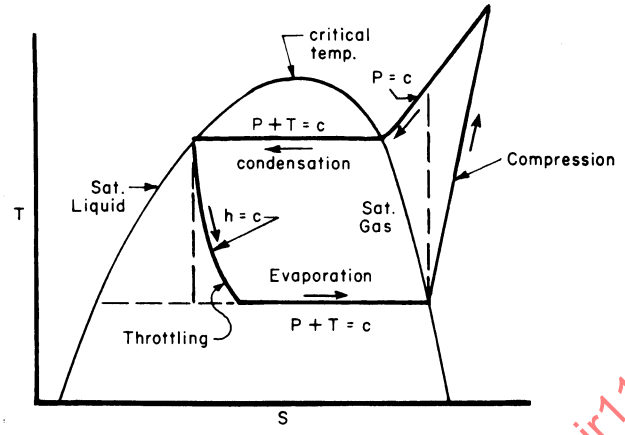

Figure 1B-6 - Rankine Vapor Cycle in Refrigeration

4.2.3 Pressure-Enthalpy Diagram

Fig. 1B-7 illustrates the third type of diagram.

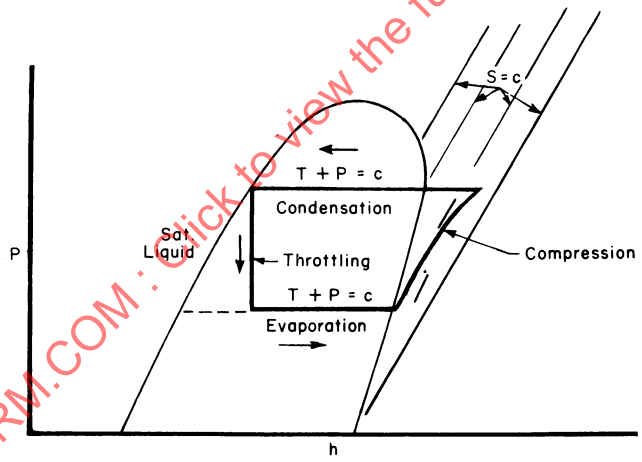

Figure 1B-7 - Vapor Cycle in Refrigeration

5. REAL GAS CHARACTERISTICS

Over the normally moderate range of pressure and temperature, the diatomic gases behave reasonably like ideal gases. As the density is increased, however, their characteristics deviate appreciably from the simple equation of state.

A number of approaches may be used to determine real gas properties. Among these are:

(a) Real gas tables

(b) Mollier or pressure-enthalpy charts

(c) Van der Waals equation

(d) Beattie-Bridgeman equation

(e) Reduced pressure or generalized compressibility chart

Some of the charts mentioned in (b) are available in SAE AIR 1168/10. Methods (c), (d), and (e) will be discussed briefly in the following paragraphs.

5.1 Van der Waals Equation

One of the early equations proposed for correlation of gas characteristics was that of Van der Waals:

$$\left(P + \frac{a}{v^2}\right)(v-b) = RT \qquad \text{(1B-39)}$$

where constant a in atm-ft^6/mole^2 and constant b in ft^3/mole are tabulated for each gas in Table 1B-4.

Table 1B-4 - Constants a and b for Gases, Van der Waals

Gas	a	b	Gas	a	b
Air	343.8	0.585	CH_4	578.9	0.684
O_2	349.5	0.510	C_3H_8	2374.0	1.446
N_2	346.0	0.618	C_4H_{10}	3675.0	1.944
H_2O	1397.1	0.487	NH_3	1076.0	0.598
CO	374.7	0.630	H_2	63.02	0.427
CO_2	924.2	0.685	Hg	5100.0	1.070

5.2 Beattie-Bridgeman

A more recent and more accurate equation of state for real gases is the Beattie-Bridgeman equation:

$$P = \frac{RT(1-e)}{v^2}(v+B) - \frac{A}{v^2} \qquad \text{(1B-40)}$$

where

$$A = A_0\left(1-\frac{a}{v}\right), \quad B = B_0\left(1-\frac{b}{v}\right), \quad e = \frac{c}{vT^3}$$

The constants for this equation are tabulated in Table 1B-5.

Table 1B-5 - Beattie-Bridgeman Constants

Gas	A_0 $\frac{\text{atm-ft}^6}{\text{lb-mole}^2}$	B_0 $\frac{\text{ft}^3}{\text{lb-mole}}$	a $\frac{\text{ft}^3}{\text{lb-mole}}$	$10^{-4}c$ $\frac{\text{ft}^3\text{-}^\circ\text{R}^3}{\text{lb-mole}}$	b $\frac{\text{ft}^3}{\text{lb-mole}}$
Air	334.1	0.739	0.309	406	-0.176
O_2	382.5	0.741	0.410	448	0.0674
N_2	344.3	0.809	0.419	391.7	-0.111
H_2	50.57	0.336	-0.0811	4.7	-0.698
He	5.6	0.224	0.958	0.37	0.0
CO_2	1248.9	1.678	1.143	165	1.159
NH_3	613.9	0.547	2.729	44,560	3.062

5.3 Generalized Reduced Coordinate System

By means of a system in which "reduced properties" are utilized, it is possible to plot a set of curves that approximate the deviations of all gases from the ideal gas equation of state. These reduced properties are

$$P_r = \frac{P}{P_{cr}} \quad \text{and} \quad T_r = \frac{T}{T_{cr}} \tag{1B-41}$$

where the subscript "*cr*" refers to the critical point.

Values of P_{cr} and T_{cr} for some common gases are listed in Table 1B-6, and the generalized plot of gas properties in terms of P_r, T_r, and Z is given in Figure 1B-8.

Table 1B-6 - P_{cr} and T_{cr} for Some Common Cases

Gas	T_{cr} °R	P_{cr} atm	V_{cr} ft³/lb-mole
Air	239	37.2	1.33
O_2	278	50.1	1.19
N_2	227	33.5	1.44
H_2	59.8	12.8	1.04
He	9.33	2.26	0.93
CO_2	548	72.9	1.53
H_2O	1165	218.2	0.91
NH_3	730	111.3	1.16

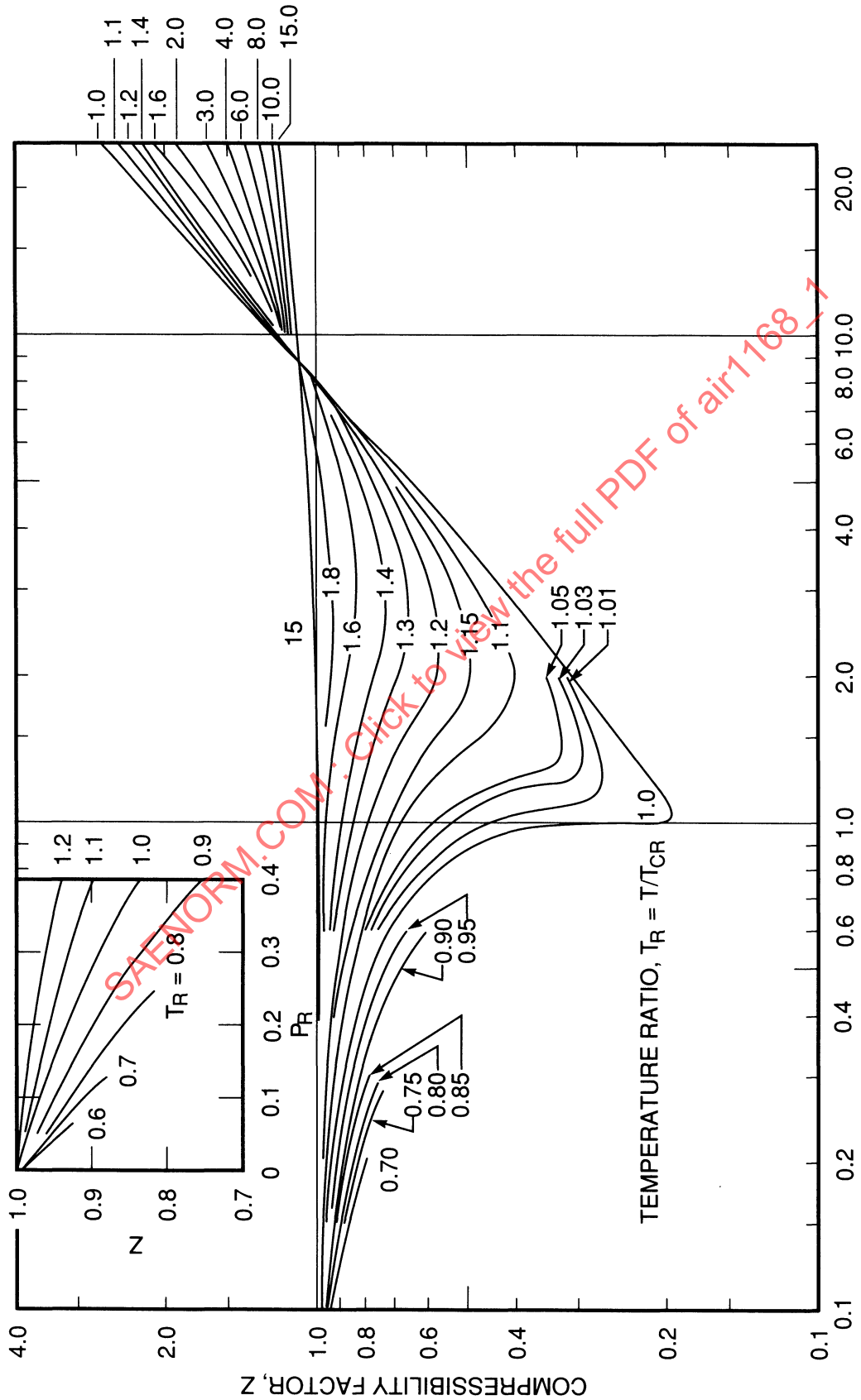

Figure 1B-8 - Compressibility Factor

The generalized equation in which Z is then used is

$$Pv = ZRT \qquad \text{(1B-42)}$$

Note that for low pressures ($P_r < 0.1$), Z approaches 1, and the ideal gas equation applies with little error. By using Fig. 1B-8, the properties of any gas can be determined with accuracies of 1-2%.

5.4 Changes of Phase

Real substances exist in the gas phase only at sufficiently high temperatures and low pressures. At low temperature and high pressure, transition occurs to the liquid phase and the solid phase. Fig. 1B-9 shows typical "pressure versus temperature" and "pressure versus volume" curves of a real substance.

5.5 Triple Point and Triple Line

Figs. 1B-9(a) and 1B-9(b) show regions labeled solid, liquid, and gas. In other regions, labeled solid-liquid, solid-gas, and liquid-gas, both phases can exist simultaneously in equilibrium. Along the line labeled "triple line," all three phases can coexist. In Fig. 1B-9(a), there is a single temperature-pressure point at which all three phases exist. This temperature-pressure point is called the "triple point." Table 1B-7 gives triple points for various substances.

5.6 Latent Heat

When a substance undergoes a change of phase, heat is either absorbed or rejected by the substance. Heat is absorbed when a solid transforms to a liquid, when a liquid transforms to a gas, and when a solid transforms to a gas. The corresponding quantities of heat absorbed per unit mass are called, respectively, the latent heat of fusion, latent heat of vaporization, or evaporation, and the latent heat of sublimation.

5.7 Critical Point

The point on a P-T or P-V diagram labeled "critical point" is the point above which there is no liquid phase. The corresponding pressure, temperature, and volume are called the "critical constants." Table 1B-6 includes critical constants for several gases.

6. THERMODYNAMICS OF HIGH-VELOCITY GAS FLOWS

6.1 Introduction

This section introduces fundamental concepts and working relations for use in the analysis of high-velocity gas flow systems. The majority of information is based on one-dimensional compressible flow concepts, although a brief introduction to shock waves in two-dimensional flow is included. Certain important consequences of heat transfer and viscosity in high-velocity flows are also discussed. Emphasis is placed on flow problems amenable to solution by application of ideal gas concepts. A brief review of real gas effects is included.

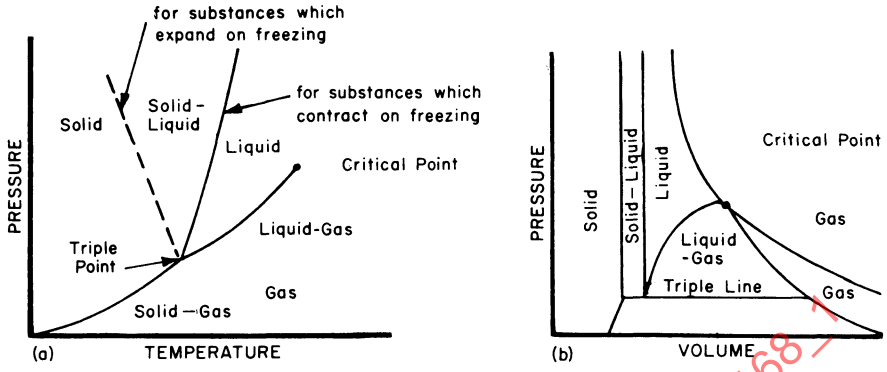

Figure 1B-9 - Solid and Liquid Phases with Changing *P*, *V*, *T*

Table 1B-7 - Triple Point Data

Substance	T_{tr}, °R	P_t, psia
Oxygen	108.7	0.03866
Nitrogen	114.2	1.8634
Carbon Dioxide	389.8	75.000
Hydrogen	25.2	0.99356
Helium	14.2	0.7471
Argon	151.2	9.901
Sulfur Dioxide	361.2	0.3151
Water	491.72	0.0885

6.2 Steady-Flow Energy Equation

Consider the one-dimensional steady flow of a gas to which heat dQ is added and on which mechanical work $(1/J)\,dW_k$ is performed. The sum of the heat added and the work done on the gas must appear as an increase in internal energy dE, as a change in flow work $(W/gJ)\,d(P/\rho)$, or as increased kinetic energy $(W/gJ)\,d(U^2/2)$, as indicated in the steady-flow energy equation (Ref. 1, which defines Q as *positive* for heat *added to* the gas, and W_k as *positive* for work *done on* the gas):

$$dQ + \frac{1}{J}dW_k = dE + \frac{W}{gJ}d\left(\frac{P_s}{\rho_s}\right) + \frac{W}{gJ}d\left(\frac{1}{2}U^2\right) \qquad \text{(1B-43)}$$

$$\text{or:}\quad dQ + \frac{1}{J}dW_k = d\left[E + \frac{W}{gJ}\left(\frac{P_s}{\rho_s}\right)\right] + \frac{W}{gJ}U\,dU = Wd\left[\frac{E}{W} + \frac{1}{gJ}\left(\frac{P_s}{\rho_s}\right)\right] + \frac{W}{gJ}U\,dU \qquad \text{(1B-44)}$$

The quantity $[E/W+(1/gJ)(P_s/\rho_s)]$ is commonly defined as the specific enthalpy h (Ref. 2). Accordingly, the energy equation for steady flow can be expressed in differential form as:

$$dQ + \frac{1}{J}dW_k = Wdh + \frac{W}{gJ}U\,dU \tag{1B-45}$$

Integrating, and considering the flow between the two stations 1 and 2, yields the following form of the energy equation:

$$Q + \frac{W_k}{J} = W\left(h_2 - h_1\right) + \frac{W}{gJ}\left(\frac{U_2^2}{2} - \frac{U_1^2}{2}\right) \tag{1B-46}$$

where Q is the heat added and W_k/J is the work done on the gas between stations 1 and 2. The enthalpy h can be shown to depend only on the temperature for a thermally perfect gas (Ref. 2). Furthermore, for a calorically perfect gas, the specific heats c_p and c_v are constant. Thus, assuming a thermally perfect ($P = g\rho RT$) and calorically perfect gas, the enthalpy can be expressed as

$$h = c_pT + \text{constant}$$

Thus the integrated form of the energy equation is written as

$$Q + \frac{W_k}{J} = Wc_p\left(T_{s2} - T_{s1}\right) + \frac{W}{gJ}\left(\frac{U_2^2}{2} - \frac{U_1^2}{2}\right) \tag{1B-47}$$

6.3 Sonic Velocity and Mach Number

6.3.1 Sonic Velocity

Combining the one-dimensional momentum and continuity equations yields the following expression for the speed of a weak wave, (that is, a sound wave) propagating into an undisturbed gas, as described in Ref. 3.

$$a_o = \left(\frac{dP_s}{d\rho_s}\right)^{1/2} \tag{1B-48}$$

The rate of change of pressure with density, $dP_s/d\rho_s$, is a measure of the compressibility of the gas. The disturbances produced in a gas by a sound wave are weak enough that the process can be assumed isentropic. The isentropic relation

$$\frac{P_s}{\rho_s^{\gamma}} = \text{constant}$$

can therefore be applied to evaluate the derivative in Eq. 1B-48 for the speed of sound, yielding

$$a_o = \left[\gamma\left(\frac{P_s}{\rho_s}\right)\right]^{1/2} \tag{1B-49}$$

or, using the equation of state, $P_s = g\rho_s RT_s$, in conjunction with Eq. 1B-49, the local speed of sound can be shown to be a function only of the local static temperature of a gas:

$$a_o = \sqrt{\gamma g R T_s}$$

$$= 49.0\sqrt{T_s} \quad \text{ft/sec, for air} \qquad \text{(1B-50)}$$

6.3.2 Mach Number

The Mach number, defined as the ratio of the flow velocity to the local velocity of sound, is probably the most important single parameter in the analysis of high-velocity gas flows. The Mach number can be expressed as

$$M = \frac{U}{\sqrt{\gamma g R T_s}} \qquad \text{(1B-51)}$$

The physical significance of Mach number is more readily appreciated, however, by squaring Eq. 1B-51 and interpreting the result as

$$M^2 = \frac{U^2}{\gamma g R T_s} \qquad \text{(1B-52)}$$

It is known from the kinetic theory of gases that the temperature T_s is a measure of the random energy (translation and rotation of molecules) of the gas, whereas the velocity squared (U^2) is a measure of the directed kinetic energy of the gas flow. Thus the Mach number squared indicates the ratio of the directed kinetic energy of gas flow to the random kinetic energy of the individual molecules. Since the equations of high-velocity gas flow include the effects of both thermal energy and directed kinetic energy, the Mach number plays a significant role in the equations describing compressible gas flows.

6.4 One-Dimensional Energy Equation for Steady Flow Without Heat Transfer

In a steady-gas flow in which no heat transfer occurs (adiabatic) and in which no mechanical work is performed, the energy equation, Eq. 1B-45,

$$dQ + \frac{dW_k}{J} = W dh + \frac{W}{gJ} U\, dU \qquad \text{(1B-45)}$$

reduces to

$$dh + \frac{1}{gJ} U\, dU = 0$$

This is integrated to yield

$$h + \frac{1}{gJ}\frac{U^2}{2} = \text{constant}$$

When the velocity U is zero, the temperature and the corresponding enthalpy are defined as total temperature T_t and total enthalpy h_t, repectively. Thus the constant is evaluated as h_t and the energy equation can be written as

$$h + \left(\frac{1}{gJ}\frac{U^2}{2}\right) = h_t$$

$$\text{or} \quad c_p T_s + \left(\frac{1}{gJ}\frac{U^2}{2}\right) = c_p T_t \tag{1B-53}$$

for steady one-dimensional flow of a thermally and calorically perfect gas without heat transfer. The energy equation can be applied to analyze the flow between the two streamwise stations 1 and 2; in this case the differential energy equation is integrated to yield

$$c_p T_{s1} + \left(\frac{1}{gJ}\frac{U_1^2}{2}\right) = c_p T_{s2} + \left(\frac{1}{gJ}\frac{U_2^2}{2}\right) \tag{1B-54}$$

6.5 Total Temperature, Static Temperature, Velocity, and Mach Number Relations

The one-dimensional energy equation for steady flow without heat transfer can be used in conjunction with perfect gas relations and the speed of sound relations to arrive at useful relationships among total temperature, static temperature, and Mach number. From the one-dimensional adiabatic energy equation (Eq. 1B-53):

$$c_p T_s + \left(\frac{1}{gJ}\frac{U^2}{2}\right) = c_p T_t \tag{1B-55}$$

Dividing this equation (after converting units to ft^2/sec^2) by the speed of sound squared, $a_o^2 = \gamma g R T_s$, using the definition of Mach number, and employing the perfect gas relations

$$c_p - c_v = R \quad \text{and} \quad \gamma = \frac{c_p}{c_v}$$

the important relationship among total temperature, static temperature, and Mach number is obtained as follows:

$$\frac{T_t}{T_s} = 1 + \left(\frac{\gamma - 1}{2}\right) M^2 \tag{1B-56}$$

This temperature ratio is plotted in Fig. 1B-10. Solving Eq. 1B-56 for static temperature in terms of Mach number and total temperature, and substituting the result in the Mach number expression, Eq. 1B-52,

$$M^2 = \frac{U^2}{\gamma g R T_s} \tag{1B-57}$$

yields the following relationship among velocity, Mach number, and total temperature:

$$\frac{U}{\sqrt{T_t}} = \frac{M\sqrt{\gamma g R}}{\sqrt{1 + [(\gamma - 1)/2] M^2}} \tag{1B-58}$$

A plot of this parameter as a function of Mach number is presented in Fig. 1B-11.

Another relationship frequently useful and readily derived by manipulations generally similar to those above is that between U/a_0^* and Mach number, where a_0^* is the speed of sound when the Mach number is 1.0:

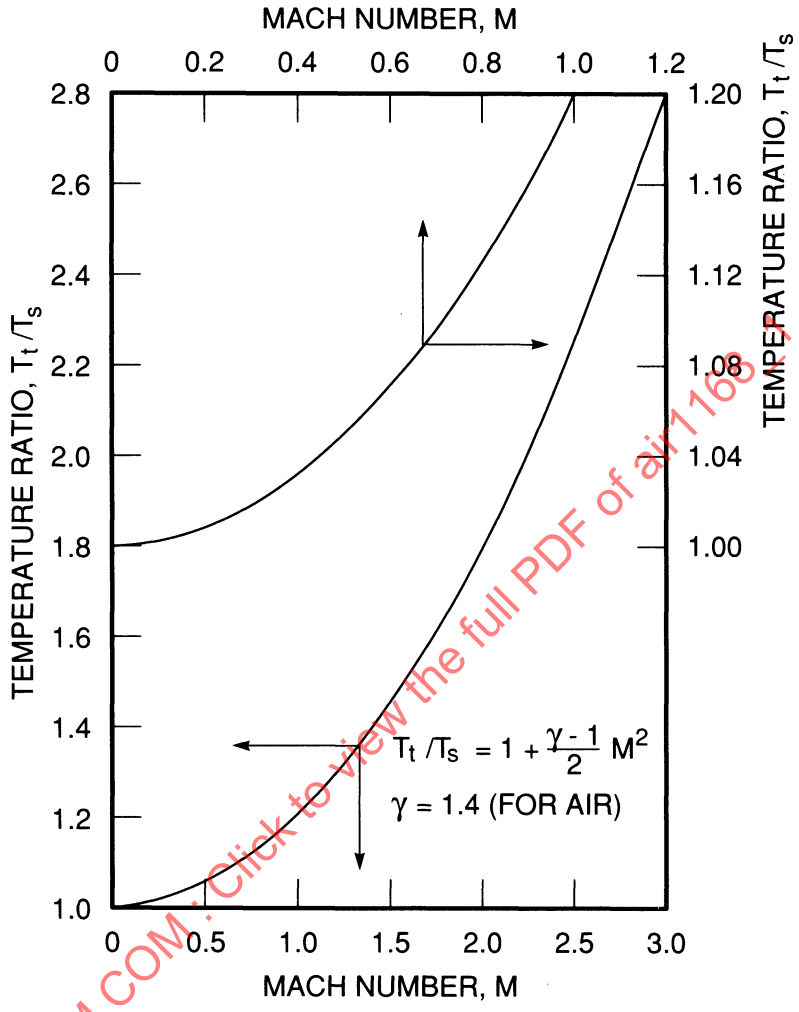

Figure 1B-10 - Temperature Ratio as a Function of Mach Number

$$\frac{U}{a_0^*} = \left[\frac{[(\gamma+1)/2]\,M^2}{1+[(\gamma-1)/2]\,M^2}\right]^{1/2} \tag{1B-59}$$

It is important to note that the speed of sound when the Mach number is 1, a_0^*, is constant throughout a stream-tube for adiabatic flow (that is, T_t = constant) and depends only on total temperature. The expression for the speed of sound when the Mach number is unity, as a function of total temperature, is

$$a_0^* = \left(\frac{2}{\gamma+1}\right)^{1/2} \sqrt{\gamma g R T_t} \tag{1B-60}$$

Many useful compressible flow parameters, including U/a_0^*, have been computed as functions of Mach number and are tabulated in Ref. 4.

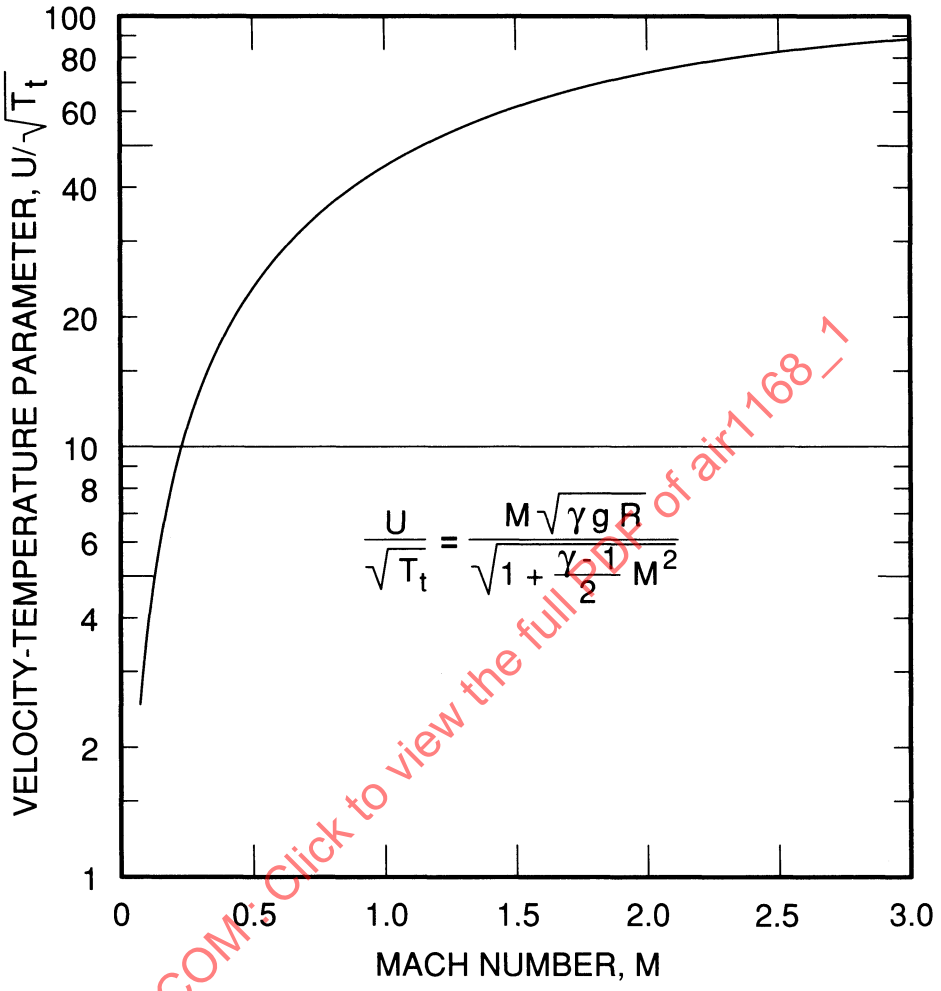

Figure 1B-11 - Velocity-Temperature Parameter as a Function of Mach Number

6.6 Pressure Ratio, Density Ratio, and Mach Number Relations

The relationship among total and static pressure ratio and Mach number at a point in compressible flow is obtained by using the isentropic perfect gas relation

$$\frac{T_t}{T_s} = \left(\frac{P_t}{P_s}\right)^{(\gamma-1)/\gamma} \tag{1B-61}$$

in conjunction with the total to static temperature ratio from Eq. 1B-56.

The resulting relationship is

$$\frac{P_t}{P_s} = \left(1 + \frac{\gamma-1}{2} M^2\right)^{\gamma/(\gamma-1)} \tag{1B-62}$$

This parameter is plotted as a function of Mach number in Fig.1B-12.

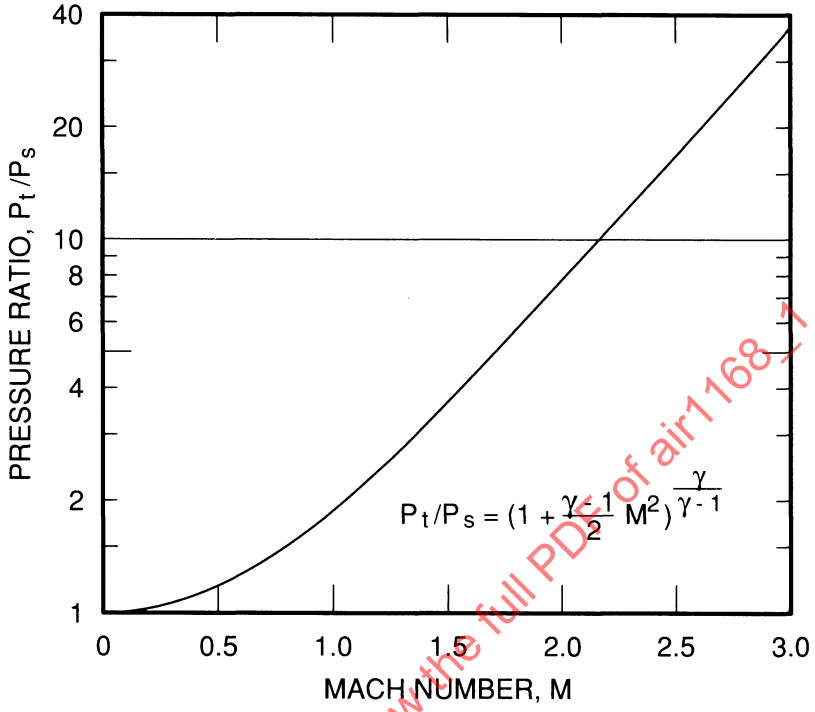

Figure 1B-12 - Pressure Ratio as a Function of Mach Number

Rearranging Eq. 1B-62 yields Mach number as a function of total pressure to static pressure ratio:

$$M = \left\{ \frac{2}{\gamma-1} \left[\left(\frac{P_t}{P_s} \right)^{(\gamma-1)/\gamma} - 1 \right] \right\}^{1/2} \tag{1B-63}$$

The density ratio and Mach number relationship is found in a manner similar to that used to determine the pressure ratio, yielding

$$\frac{\rho_t}{\rho_s} = \left(1 + \frac{\gamma-1}{2} M^2 \right)^{1/(\gamma-1)} \tag{1B-64}$$

It can be noted that both the pressure ratio, P_t/P_s, and the density ratio, ρ_t/ρ_s, were derived from the adiabatic one-dimensional flow energy equation in conjunction with the isentropic perfect gas relationship. Accordingly, these relationships are restricted to processes in which the flow is reversible and adiabatic. In practice, when the flow is being analyzed between two streamwise stations, 1 and 2, this restriction means that the total pressure, P_{t2}, must be equal to P_{t1}. Similarly, the total density, ρ_t, must be constant between the two stations. The temperature ratio T_t/T_s, having been derived directly from the adiabatic one-dimensional flow energy equation in conjunction with the perfect gas relations, did not require the use of isentropic relations and hence is restricted only to adiabatic flow behaving as a perfect gas.

6.7 Continuity Relations

Relationships between weight flow, temperature, pressure, area, and Mach number are of considerable value in the analysis of a large number of practical problems arising in compressible gas flows. Using the equation of continuity:

$$\frac{w}{gA} = \rho_s U = \frac{P_s U}{gRT_s}$$

$$= \frac{P_s U}{\sqrt{\gamma g R T_s}} \left(\frac{\gamma}{gR}\right)^{1/2} \left(\frac{T_t}{T_s}\right)^{1/2} \left(\frac{1}{T_t}\right)^{1/2}$$

$$= \left(\frac{\gamma}{gR}\right)^{1/2} \left(\frac{P_s}{\sqrt{T_t}}\right) M \left(1 + \frac{\gamma-1}{2} M^2\right)^{1/2} \qquad \text{(1B-65)}$$

or

$$\frac{w\sqrt{T_t}}{P_s A} = M\left[\frac{g\gamma}{R}\left(1 + \frac{\gamma-1}{2} M^2\right)\right]^{1/2} \qquad \text{(1B-66)}$$

A similar expression in terms of total pressure is obtained by employing the isentropic relationship between total pressure to static pressure ratio and Mach number to eliminate static pressure from Eq. 1B-66, yielding

$$\frac{w\sqrt{T_t}}{P_t A} = \frac{M\sqrt{g\gamma/R}}{(1+[(\gamma-1)/2]M^2)^{(\gamma+1)/2(\gamma-1)}} \qquad \text{(1B-67)}$$

These continuity expressions, in terms of static pressure and total pressure, are plotted as functions of Mach number in Figs. 1B-13 and 1B-14, respectively. These figures can be used to determine the Mach number when values of w, A, T_t, and P_t or P_s are known. It is of interest to note that the second continuity function, $w\sqrt{T_t}/P_t A$, attains a maximum value at a Mach number of 1.0. The physical significance of this characteristic is that, for a given total pressure and total temperature, the maximum flow per unit area always occurs at a Mach number of unity.

Another expression that is often useful in the analysis of compressible flows is the relationship between the local streamtube area and the streamtube area at sonic conditions. This area ratio is readily determined by using Eq. 1B-67 and assuming that the flow is isentropic between the station of local streamtube area, A, and the sonic flow station having streamtube area A_*:

$$\left.\frac{A}{A_*}\right]_{isen} = \frac{\left(\frac{w\sqrt{T_t}}{P_t A}\right)_{M=1}}{\left(\frac{w\sqrt{T_t}}{P_t A}\right)_M} = \frac{1}{M}\left[\left(\frac{2}{\gamma+1}\right)\left(1+\frac{\gamma-1}{2}M^2\right)\right]^{(\gamma+1)/2(\gamma-1)} \qquad \text{(1B-68)}$$

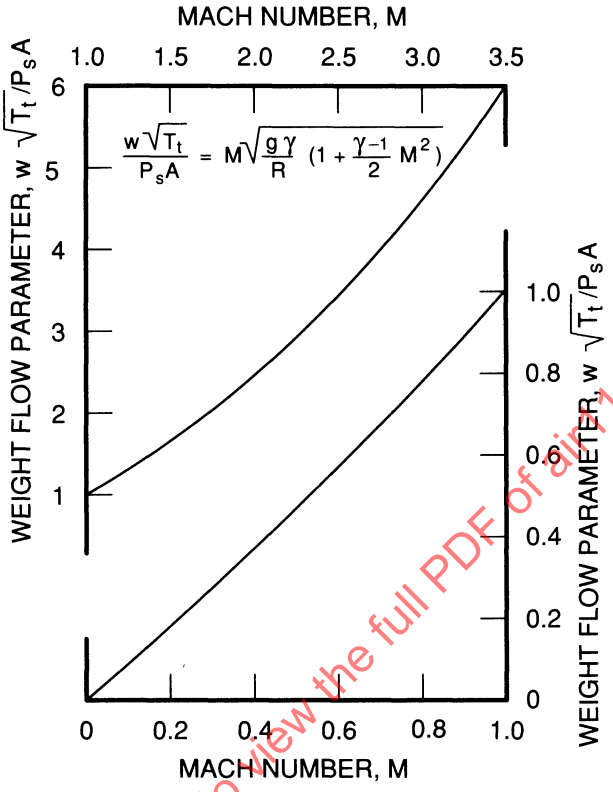

Figure 1B-13 - Weight Flow Parameter, $w\sqrt{T_t}/P_s A$, as a Function of Mach Number

Numerical values have been calculated and tabulated for this relationship in Ref. 4.

One application of the continuity relations that is of special significance is the relationship between two successive sonic throat areas between which a loss in total pressure has occurred. This relationship is derived from Eq. 1B-67.

The resulting expression relating areas between successive sonic throats with total pressure loss is

$$\frac{A_{*2}}{A_{*1}} = \frac{P_{t*1}}{P_{t*2}} \qquad \text{(1B-69)}$$

This relation indicates that in order to pass the same mass flow through the second throat of two successive sonic throats, between which a loss in total pressure has occurred, the second throat must be enlarged relative to the first throat, inversely proportional to the total pressure ratio between throats.

6.8 Illustrative Examples

The application of some of the foregoing concepts and relationships is demonstrated in the examples below.

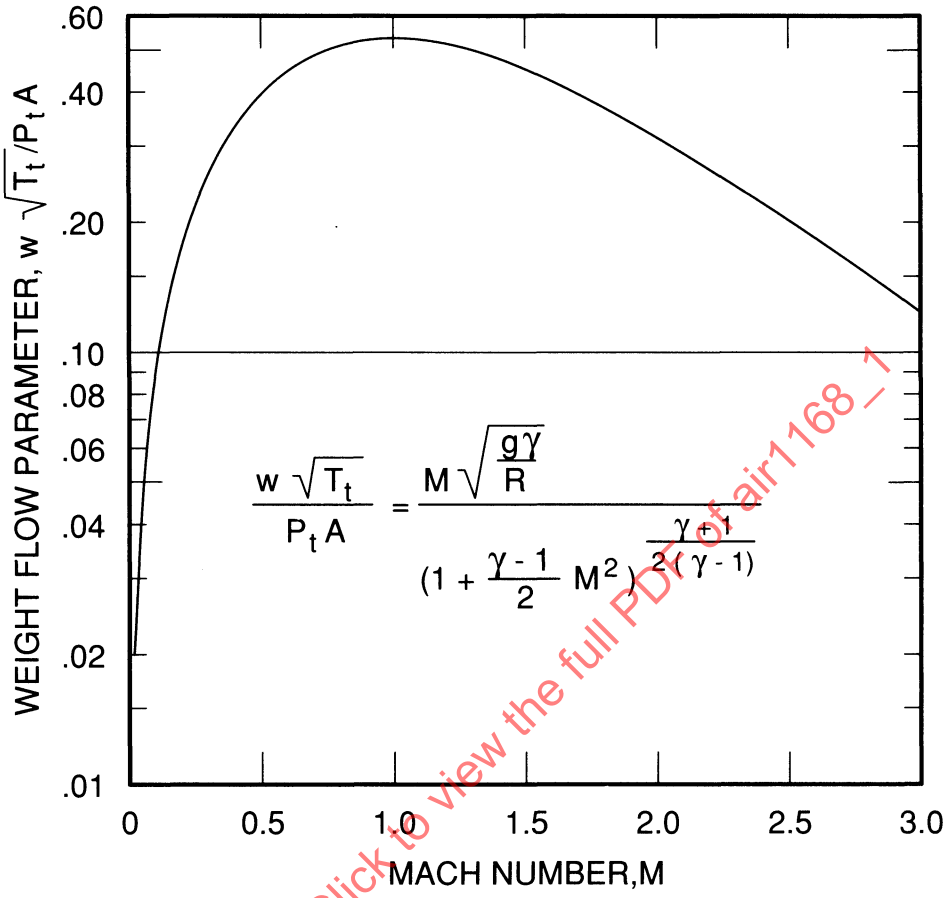

Figure 1B-14 - Weight Flow Parameter, $w\sqrt{T_t}/P_t A$, as a Function of Mach Number

Example 1: An airplane is flying at a Mach number of 0.9 and is taking air aboard through the throat of the engine inlet at a Mach number of 0.7. The atmospheric ambient temperature is 400°R. (a) What is the ratio of engine inlet throat velocity to flight velocity? (b) What are the flight and throat velocities? (c) What is the ratio of throat to free stream static pressure?

Solution: (a) Fig. 1B-11 is entered at a Mach number of 0.7 at which a value of $U_{inlet}\sqrt{T_t} = 33$ is read corresponding to the engine inlet throat conditions. Fig. 1B-11 is next entered at a Mach number of 0.9 at which a value of $U_{airplane}\sqrt{T_t} = 41$ is read corresponding to the airplane flight conditions. The required velocity ratio is

$$\frac{U_{inlet}}{U_{airplane}} = \frac{33}{41} = 0.80 \qquad \text{(1B-70)}$$

(b) Fig. 1B-10 is entered at the flight Mach number of 0.9 and the temperature ratio is found to be

$$\frac{T_t}{T_s} = 1.16 \qquad \text{(1B-71)}$$

The total temperature is therefore

$$T_t = 1.16 \times 400 = 464°R \qquad \text{(1B-72)}$$

From part (a) of this solution,

$$\left.\frac{U}{\sqrt{T_t}}\right]_{M=0.9} = 41$$

Thus

$$U_{airplane} = 41\sqrt{464} = 883 \text{ ft/sec}$$

and since

$$\frac{U_{inlet}}{U_{airplane}} = 0.80$$

from part (a) the inlet throat velocity is

$$U_{inlet} = 0.80 \times 883 = 706 \text{ ft/sec} \quad \text{(1B-73)}$$

(c) In determining the static pressure ratio between inlet throat and free stream, the flow is assumed to be isentropic between these two stations. Fig. 1B-12 is entered at a Mach number of 0.7, corresponding to inlet throat conditions, and the pressure ratio $P_t/P_{s(inlet)} = 1.39$ is obtained. The same figure is entered at the flight Mach number of 0.9 and the pressure ratio $P_t/P_{s(ambient)} = 1.69$ is obtained. The required pressure ratio is

$$\frac{P_{inlet}}{P_{ambient}} = \frac{1.69}{1.39} = 1.22 \quad \text{(1B-74)}$$

Example 2: An airflow of 60 lb/sec is flowing through a duct. At a station in the duct where the cross-sectional area is 1.5 ft^2, the total pressure is 2100 lb/ft^2 and the total temperature is 520°R. What is the Mach number in the duct at this station?

Solution: Using the data given, determine the value of the parameter $w\sqrt{T_t}/P_tA$:

$$\frac{w\sqrt{T_t}}{P_t A} = \frac{60\sqrt{520}}{2100 \times 1.5} = 0.434 \quad \text{(1B-75)}$$

Fig. 1B-14 is entered with this value for $w\sqrt{T_t}/P_tA$ and the required Mach number is found to be 0.57.

Example 3: Air is flowing adiabatically through a duct at a Mach number of 0.5. A screen placed in the duct causes a 10% loss in total pressure. How much must the duct area be enlarged downstream of the screen to maintain a Mach number of 0.5 just after the screen?

Solution: Let the stations immediately upstream and downstream of the screen be 1 and 2, respectively. The requirement that the Mach number M_2 be the same as M_1 stipulates that the continuity parameter $w\sqrt{T_t}/P_tA$ be the same before and after the screen; that is,

$$\left(\frac{w_1\sqrt{T_{t1}}}{P_{t1}A_1}\right) = \left(\frac{w_2\sqrt{T_{t2}}}{P_{t2}A_2}\right) = 0.40 \text{ at } M = 0.5 \quad \text{(1B-76)}$$

(See Fig. 1B-14.) Since, by continuity, $w_1 = w_2$, and $T_{t1} = T_{t2}$ for adiabatic flow, Eq. 1B-76 reduces to

$$\frac{A_2}{A_1} = \frac{P_{t1}}{P_{t2}} \tag{1B-77}$$

noting that, for the 10% loss in total pressure, $P_{t2}/P_{t1} = 0.90$, the duct area downstream of the screen must be enlarged as follows:

$$\frac{A_2}{A_1} = \frac{1}{P_{t2}/P_{t1}} = \frac{1}{0.90} = 1.11 \tag{1B-78}$$

6.9 Forces on Internal Flow Passages

In the analysis of aircraft systems, it is frequently necessary to estimate the forces acting on internal flow passages such as inlet ducts and exhaust nozzles. Accordingly, certain generalized momentum expressions of value in determining such forces are included herein. Consider the flow between stations 1 and 2 in the duct shown in Fig. 1B-15.

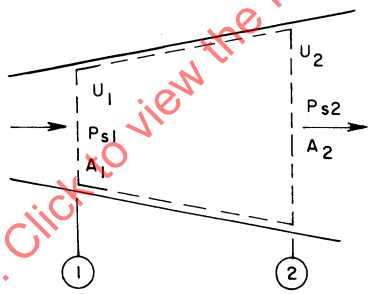

Figure 1B-15 - Flow in a Duct

Applying the momentum theorem to the flow through the control surface yields

$$F' + P_{s1}A_1 - P_{s2}A_2 = \rho_{s2}U_2^2A_2 - \rho_{s1}U_1^2A_1 \tag{1B-79}$$

or

$$F' = \left(\rho_{s2}U_2^2A_2 + P_{s2}A_2\right) - \left(\rho_{s1}U_1^2A_1 + P_{s1}A_1\right) \tag{1B-80}$$

where F' is the absolute force acting on the duct. In practical problems involving forces on aircraft components, the force usually of interest is the differential (gage) force per unit area, denoted herein as F. The differential force is obtained by using differential pressure instead of absolute pressures in the pressure-area terms of the force equation. Replacing the absolute pressures by differential pressures in Eq. 1B-80 yields

$$F = \left[\rho_{s2}U_2^2A_2 + \left(P_{s2} - P_a\right)A_2\right] - \left[\rho_{s1}U_1^2A_1 + \left(P_{s1} - P_a\right)A_1\right] \tag{1B-81}$$

The pressure, P_a, is the atmospheric ambient static pressure that depends on the altitude at which the aircraft is operating, and is readily obtainable from tables of atmospheric properties, such as those of Ref. 5. For a perfect gas $\rho_s U^2 = \gamma P_s M^2$. Thus the differential force acting on the duct between stations 1 and 2 can be expressed in terms of Mach number, static pressure, and duct areas:

$$F = \left[P_{s2}A_2\left(\gamma M_2^2+1\right)-P_aA_2\right] - \left[P_{s1}A_1\left(\gamma M_1^2+1\right)-P_aA_1\right] \qquad \text{(1B-82)}$$

The expression in the brackets, $[P_sA(\gamma M^2+1)-P_aA]$, is usually referred to as the "total momentum" at a station in the flow. Thus the difference in total momentum between two flow stations in a duct represents the duct force between the two stations. The force acting on the duct will be a thrust force (acting in the upstream direction) if the total momentum at station 2 is greater than the total momentum at station 1. Conversely, if the total momentum at station 1 is greater than that at 2, the force on the duct will be in the drag (downstream) direction. Finally, the force on the duct, calculated by taking the change in total momentum between the two stations, includes both forces due to pressure on the duct walls and those due to viscous stresses.

6.10 General Duct Flow

The analysis of air flow through a duct generally involves three principal factors: area change, heat transfer, and duct wall friction. With the aid of the three equations of continuity, energy, and momentum, and the basic concepts developed in Pars. 6.1 through 6.9, the effect of each of these variables on the flow properties may be investigated. The present discussion will be limited to flow in which the properties are assumed to vary continuously, in contrast to discontinuous flow involving shocks.

An overall qualitative picture of duct flow can best be interpreted from

$$\left(M^2-1\right)\frac{du}{U} = \frac{dA}{A} - \frac{\gamma\tau\,df}{\rho a_o^2 A} - \frac{\gamma-1}{\gamma}\frac{dQ}{RT} \qquad \text{(1B-83)}$$

which is easily derived from the general energy equation (in differential form) in combination with the equations of state, continuity, and momentum (Ref. 6, pp. 297 - 298). A simple inspection of this equation, considering one variable at a time, shows that duct convergence, wall friction, and heat addition cause acceleration of a subsonic flow and deceleration of a supersonic flow. It is recalled that the three conservation equations were postulated for one-dimensional flow. Although friction introduces two and three dimensionality in the flow, it has been shown experimentally that for fully developed viscous flow (that is, similar velocity profiles in the streamwise direction), the departure from one-dimensional flow does not seriously affect the theoretical results.

In the subsequent three paragraphs, the effects of heat transfer and friction on flow properties will be discussed first on an individual basis and then in combination. The effect of area change in isentropic flow will be discussed in Par. 6.18.

6.11 Constant Area Duct Flow With Heat Transfer And No Friction

While the process to be considered herein is difficult to duplicate in practice, the gross conclusions that can be derived from the analysis are of much practical significance.

If heat addition or removal from the stream is assumed to take place in a short distance, the effect of friction is obviously small. Furthermore, any property changes due to friction must be negligible compared to changes caused by heat transfer. The derivation of the fundamental relation between the change in duct Mach number and the quantity of heat transfer is outlined below. A more complete analysis may be found in Refs. 7 or 8. For the control volume shown in Fig. 1B-16, the energy equation applied at station 1 or 2 may be written, using the general equation

$$T_t = T_s\left(1 + \frac{\gamma-1}{2}M^2\right)$$

in the following manner:

$$\frac{T_{t2}}{T_{t1}} = \frac{T_{s2}}{T_{s1}}\left(\frac{1+[(\gamma_2-1)/2]\,M_2^2}{1+[(\gamma_1-1)/2]\,M_1^2}\right) \tag{1B-84}$$

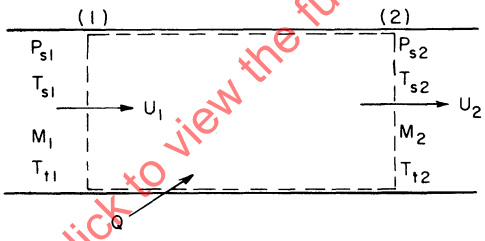

Figure 1B-16 - Control Volume

Similarly, for continuity and momentum,

$$\frac{\rho_2}{\rho_1} = \frac{U_1}{U_2}$$

$$P_{s1}-P_{s2} = \frac{m}{A}\left(U_2-U_1\right) \tag{1B-85}$$

which may be rearranged as

$$\frac{P_{s2}}{P_{s1}} = \frac{1+\gamma_1 M_1^2}{1+\gamma_2 M_2^2} \tag{1B-86}$$

From the perfect gas relation,

$$\frac{P_{s2}}{P_{s1}} = \frac{\rho_2 R_2 T_{s2}}{\rho_1 R_1 T_{s1}} \tag{1B-87}$$

and hence Eqs. 1B-86 and 1B-87 may be combined with the equation of continuity, Eq. 1B-85, to obtain

$$\frac{T_{s2}}{T_{s1}}\frac{R_2}{R_1} = \left(\frac{U_2}{U_1}\right)\frac{1+\gamma_1 M_1^2}{1+\gamma_2 M_2^2} \tag{1B-88}$$

From the definition of Mach number

$$\frac{U_2}{U_1} = \frac{M_2}{M_1}\left[\frac{\gamma_2 R_2 T_{s2}}{\gamma_1 R_1 T_{s1}}\right]^{1/2} \tag{1B-89}$$

and therefore

$$\frac{T_{s2}}{T_{s1}}\frac{R_2}{R_1} = \frac{M_2^2}{M_1^2}\left(\frac{\gamma_2}{\gamma_1}\right)^{1/2}\frac{(1+\gamma_1 M_1^2)^2}{(1+\gamma_2 M_2^2)^2} \tag{1B-90}$$

which when substituted back into Eq. 1B-84 gives

$$M_2\frac{\left[\gamma_2\left[1+\left[(\gamma_2-1)/2\right]M_2^2\right]\right]^{1/2}}{1+\gamma_2 M_2^2} = \left(\frac{T_{t2}}{T_{t1}}\frac{R_2}{R_1}\right)^{1/2} M_1\frac{\left[\gamma_1\left[1+\left[(\gamma_1-1)/2\right]M_1^2\right]\right]^{1/2}}{1+\gamma_1 M_1^2} \tag{1B-91}$$

In the solving of practical problems, it is convenient to utilize a plot of the Mach number function

$$\frac{M\left[\gamma\left[1+\left[(\gamma-1)/2\right]M^2\right]\right]^{1/2}}{1+\gamma M^2}$$

versus Mach number as given in Fig. 1B-17.

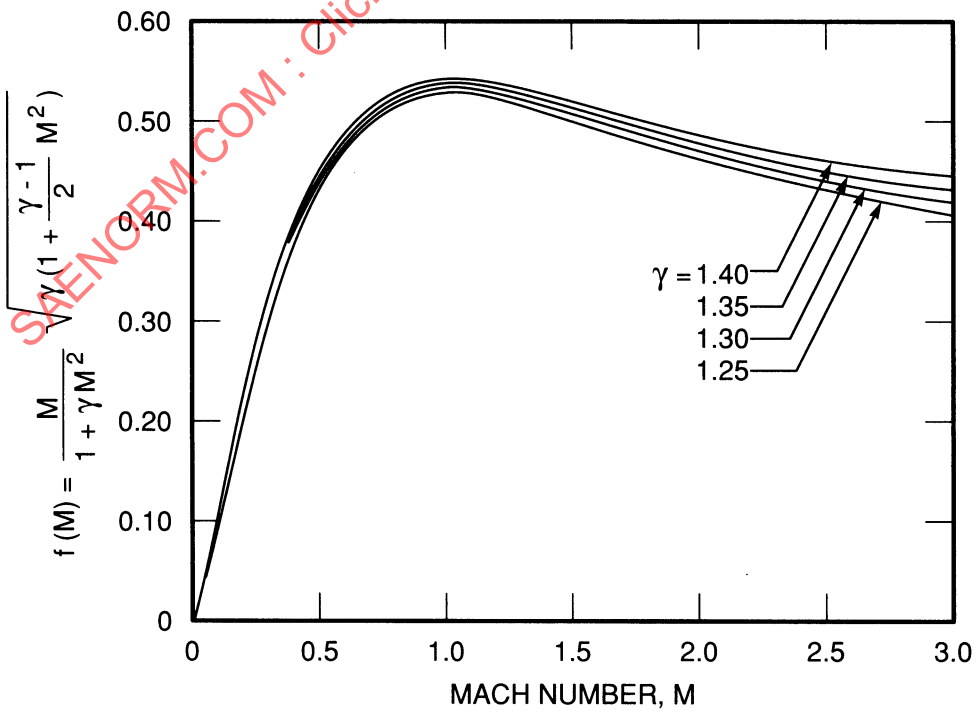

Figure 1B-17 - Mach Number Function in a Constant Area Duct

If a particular problem involves a known quantity of heat transfer, Q, rather than a desired stagnation temperature ratio, the actual total temperature ratio may be calculated from the basic energy equation, noting that, per pound of gas:

$$Q = \left(c_{p2}T_{s2}+\frac{U_2^2}{2}\right) - \left(c_{p1}T_{s1}+\frac{U_1^2}{2}\right) = \left(c_{p2}T_{t2}\right) - \left(c_{p1}T_{t1}\right) \qquad \text{(1B-92)}$$

Thus, with known values of Q and T_{t1}, the stagnation temperature after heat transfer, T_{t2}, may be computed. If the amount of heat transfer is large, some iteration on c_{p2} will be required to obtain an accurate solution for T_{t2}.

The additional properties of static temperature, static pressure, density, and total pressure at a station downstream of heat transfer may be found in several ways. One very simple means involves the use of the continuity parameters developed in Par. 6.7. Employing tautology, the following relation for the total pressure ratio across the point of heat addition is found to be

$$\frac{P_{t2}}{P_{t1}} = \frac{\left(w\sqrt{T_t}/P_tA\right)_1}{\left(w\sqrt{T_t}/P_tA\right)_2}\left(\frac{T_{t2}}{T_{t1}}\right)^{1/2} \qquad \text{(1B-93)}$$

where the parameter $w\sqrt{T_t}/P_tA$ is a function only of local Mach number. The reader should be cautioned that the continuity parameters are usually found plotted for a specific heat ratio of 1.4 and therefore, if the amount of heat transfer is relatively large, the parameter values based on the appropriate γ and R functions should be used. Once the Mach number and the stagnation properties of temperature and pressure are known, the static properties at station 2 can be obtained directly from the isentropic relations developed in Par. 6.6 utilizing the proper value of γ.

Several conclusions of practical significance can be obtained from Fig. 1B-17. It can be seen that a limit exists for heat addition at an initial subsonic or an initial supersonic Mach number. This limit corresponds to accelerating or decelerating the flow to Mach 1.0 or, in other words, "choking the flow." It is of interest at this point to observe that for heat transfer in one direction only (that is, heat addition or subtraction), flow initially subsonic cannot exceed Mach 1.0; similarly, flow initially supersonic cannot become subsonic unless a normal shock is formed.

Theoretically, it is possible to pass through Mach 1.0 without a discontinuity if the direction of heat transfer is reversed at Mach 1.0. For example, an initial subsonic flow could be heated to sonic velocity and then cooled to go supersonic. If too much heat is added to a subsonic stream (that is, if the stagnation temperature rise exceeds the value for choking), the flow will be forced to readjust itself such that the initial to final duct velocity ratio corresponds to the desired temperature rise. A situation of this sort often arises in the design of the combustion chamber for a ram-jet propulsion system.

It is also of interest to note that heat addition always results in a loss in total pressure, whereas cooling always produces increases in total pressure. The latter effect, however, is generally difficult to obtain in practice, since other factors are usually present and tend to offset this single effect.

An example problem is presented to illustrate the general method outlined above. Consider a constant area duct with the following initial flow conditions:

$M_1 = 0.2 \quad T_{t1} = 1000°R \quad P_{t1} = 20$ psia

If sufficient heat is added to raise the stream total temperature (T_{t2}) to 2000°R, calculate the downstream values of M_2, T_{s2}, P_{t2}, and P_{s2}. Also compute the quantity of heat, Q, required to obtain the specified stagnation temperature ratio. Assume that $R_2 = R_1$, and $\gamma_2 = \gamma_1 = 1.4$.

Solution:

$$\left(\frac{T_{t2}}{T_{t1}}\frac{R_2}{R_1}\right)^{1/2} = 1.414 \qquad \text{(1B-94)}$$

Then, from Fig. 1B-17,

$$f(M_1) = 0.225 \text{ at } M_1 = 0.2$$

and from Eq. 1B-91,

$$f(M_2) = (1.414)(0.225) = 0.318$$

and from Fig. 1B-17,

$$M_2 = 0.30$$

From isentropic flow tables,

$$\left(\frac{T_s}{T_t}\right)_{M_2} = 0.9823 \qquad \text{(1B-95)}$$

and therefore $T_{s2} = 1965°R$

From Equation 1B-93,

$$P_{t2} = \frac{\left(w\sqrt{T_t}/P_t A\right)_{M_1}}{\left(w\sqrt{T_t}/P_t A\right)_{M_2}} \left(\frac{T_{t2}}{T_{t1}}\right)^{1/2} P_{t1} = 19.46 \text{ psia} \qquad \text{(1B-96)}$$

Again, from the isentropic flow tables,

$$\left(\frac{P_s}{P_t}\right)_{M_2} = 0.9395$$

and $P_{s2} = 18.27$ psia

Also $Q = c_p(T_{t2} - T_{t1}) = 0.24(2000 - 1000)$ (1B-97)

$= 240$ Btu per lb of air flowing

It is important to realize that if substantial quantities of heat are added to or removed from the stream, the values of R and γ may change significantly between stations 1 and 2, thereby requiring some iteration to improve the accuracy of the answer. An iteration for M_2 is illustrated as:

(a) Assume values of R_2 and γ_2 based on an estimated T_{s2}.

(b) With the first estimate of M_2 compute a new T_{s2} from the relation

$$T_{s2} = T_{s1}\left(\frac{T_{s2}/T_{t2}}{T_{s1}/T_{t1}}\right)\frac{T_{t2}}{T_{t1}} \tag{1B-98}$$

(c) Repeat step (a) for the T_{s2} value obtained in (b).

(d) Calculate a new M_2 based on γ_2 and R_2 estimates of step (c). Normally, not more than one iteration is required to converge on an accurate solution.

6.12 Constant Area Duct Flow with Friction and No Heat Transfer

One-dimensional adiabatic flow with wall friction is a very good approximation to a wide variety of engineering problems involving flow through constant, or nearly constant, area ducts.

As in the case of heat transfer without friction, Par. 6.11, it is necessary to find only the relation between duct Mach number and the independent parameter (in this case, friction) in order to provide a basis for ready computation of all other flow properties. The derivation of this relation will be outlined briefly. A more complete derivation may be found in Refs. 6 and 7.

The control volume for this analysis (see Fig. 1B-18) is shown as follows: The momentum equation is written as

$$-A\,dP_s - \tau_w\,dA_w = \rho A U\,dU \tag{1B-99}$$

where τ_w is the wall shear stress and dA_w is the wetted duct area on which τ_w acts. By definition,

$$f = \frac{\tau_w}{\rho U^2/2} \tag{1B-100}$$

$$D = \frac{4A}{\text{wetted perimeter}} = \frac{4A}{dA_w}\,dx \tag{1B-101}$$

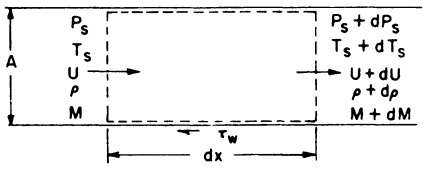

Figure 1B-18 - Control Volume

The continuity equation in logarithmic differential form is

$$\frac{d\rho}{\rho} + \frac{dU^2}{2U^2} = 0 \tag{1B-102}$$

which, in combination with Eqs. 1B-100 and 1B-101, may be substituted into the momentum equation to obtain

$$\frac{dP_s}{P_s} + \frac{\gamma M^2}{2}4f\left(\frac{dx}{D}\right) + \frac{\gamma M^2}{2}\frac{dU^2}{U^2} = 0 \tag{1B-103}$$

In order to eliminate the pressure and velocity terms from Eq. 1B-103, the differential form of the energy equation, equation of state, and the definition of Mach number are employed to yield

$$\frac{dP_s}{P_s} = -\gamma M^2 \frac{[1+(\gamma-1)M^2]}{2(1-M^2)} \bullet 4f\left(\frac{dx}{D}\right) \tag{1B-104}$$

and

$$\frac{dU^2}{U^2} = \frac{dM^2}{M^2}\left[\frac{1}{1+((\gamma-1)/2)M^2}\right] \tag{1B-105}$$

The final differential form of the equation relating Mach number and friction factor, f, is then

$$4f\left(\frac{dx}{D}\right) = \frac{1-M^2}{\gamma M^4[1+((\gamma-1)/2)M^2]}\,dM^2$$

which may be integrated over the limits of 0 to L_{max} for dx, and M^2 to 1.0 for Mach number. In integral form, the result is

$$4\bar{f}\,\frac{L_{max}}{D} = \frac{1-M^2}{\gamma M^2} + \frac{\gamma+1}{2\gamma}\ln\left[\frac{(\gamma+1)M^2}{2(1+((\gamma-1)/2)M^2)}\right] \tag{1B-106}$$

where $\bar{f}$ denotes the average friction coefficient between any duct station, x, and a maximum duct length, L_{max}. It may be noted from the final differential form of the equation that the Mach number always tends toward Mach 1.0 with friction; hence a maximum duct length, L_{max}, exists over which the acceleration or deceleration to Mach 1.0 occurs, assuming no discontinuities in the flow. Since $4\bar{f}\,(L_{max}/D)$ is only a function of Mach number, the length, L, of the duct required to change from one Mach number to another can be found from the expression

$$4\bar{f}\left(\frac{L}{D}\right) = \left(4\bar{f}\,\frac{L_{max}}{D}\right)_{M_1} - \left(4\bar{f}\,\frac{L_{max}}{D}\right)_{M_2} \tag{1B-107}$$

Similarly, the Mach number reached after a given length of run in a duct with known average wall friction and initial Mach number may also be found from Eq. 1B-107. A plot of $4\bar{f}\,(L_{max}/D)$ versus Mach number is given in Fig. 1B-19.

It is usually desired to determine the total pressure losses associated with friction. The differential equation

$$\frac{dP_t}{P_t} = -\frac{\gamma M^2}{2}\,4\bar{f}\left(\frac{dx}{D}\right) \tag{1B-108}$$

indicates that friction always causes stagnation pressure losses in either subsonic or supersonic flow. The actual value of total pressure ratio can be calculated most simply by use of a continuity parameter:

$$\frac{P_{t2}}{P_{t1}} = \frac{w\sqrt{T_t}/P_t A\,]_{M_1}}{w\sqrt{T_t}/P_t A\,]_{M_2}} \tag{1B-109}$$

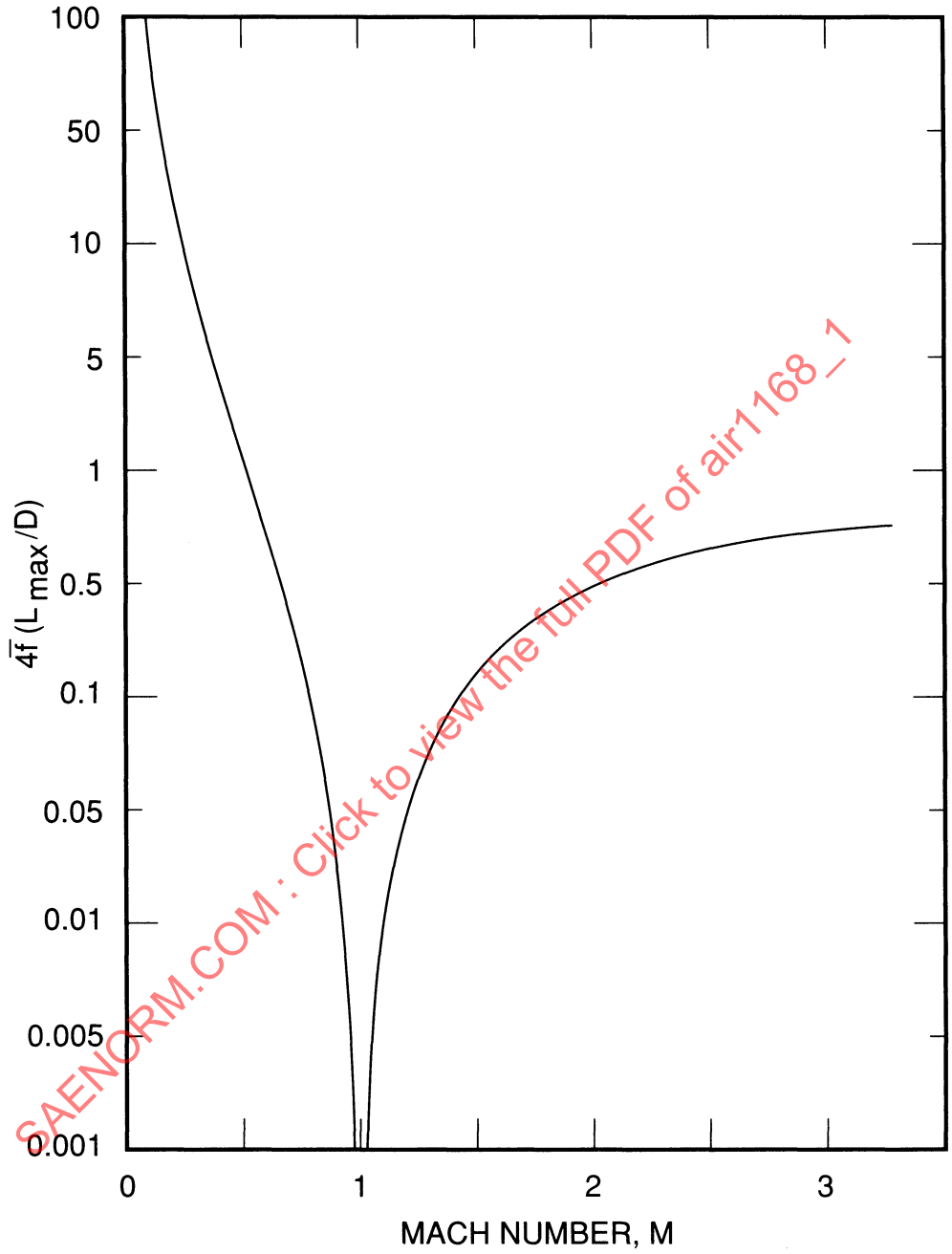

Figure 1B-19 - Friction Factor in Duct Flow

Any additional flow properties at the downstream duct station may be found directly from the isentropic flow relations. It is often convenient, however, for quick order-of-magnitude analyses to have available a chart such as that shown in Fig. 1B-20 (Ref.7). These curves have been obtained by integrating the differential forms of the equation for each flow property between a given Mach number and Mach 1.0, as denoted by the superscript asterisk (*). The direction of change in each property may be seen as a function of changes in $4\overline{f}\ (L_{max}/D)$.

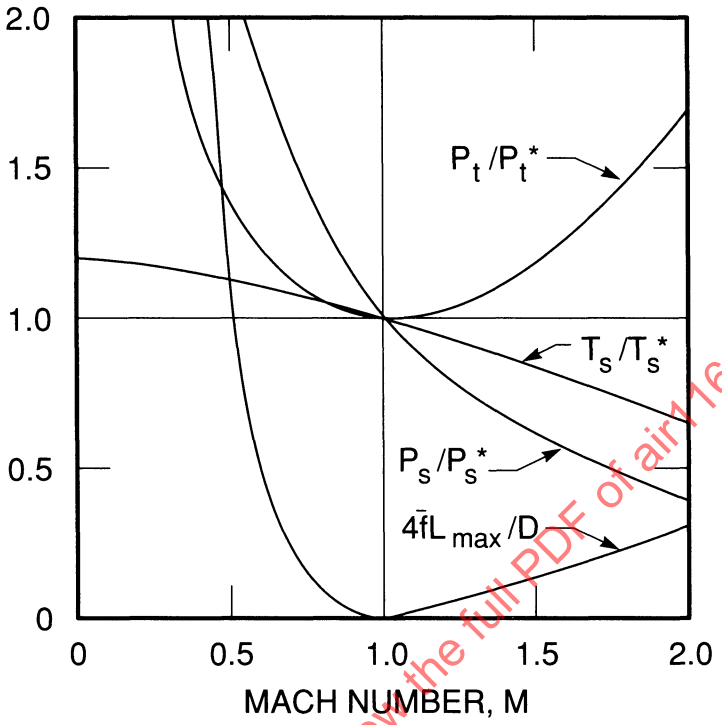

Figure 1B-20 - Effect of Wall Friction on Duct Flow Properties (The asterisk denotes integration of differential forms of flow property equations.)

6.12.1 Effect of Mach Number on Choking

From a practical standpoint, it should be emphasized that choking of the flow, due to friction, becomes quite critical as initial flow Mach number is increased for flow initially subsonic, and as initial Mach number is decreased for flow initially supersonic. The data below illustrate this fact for an assumed friction factor, $f=0.0025$ (Ref. 7).

M =	0.25	0.75	1.0	3.0	∞
L_{max}/D =	850	110	0	52	82

Furthermore, large losses in total pressure occur for supersonic duct speeds. For example, choking from Mach 3.0 would reduce the total head to approximately 24% of its original value.

6.12.2 Friction Coefficients

For fully developed pipe flow at subsonic speeds, the skin friction coefficient, f, is found to be relatively insensitive to Mach number and essentially is only a function of Reynolds number and duct relative roughness. At supersonic speeds, however, f is dependent upon Reynolds number, roughness, Mach number, and initial boundary layer thickness and turbulence. For order-of-magnitude analyses, it is usually sufficient to use an average f of 0.0025 for the Mach number range of 1.0 to 3 and duct Reynolds number from 25,000 to 700,000, based on the experimental results of Ref. 9. In subsonic duct flow, the variation in f is relatively large (0.003 – 0.0065) and therefore it is recommended that friction values based upon the incompressible Karman-Nikuradse equation be used. A plot of this relation may be found in any mechanical engineering handbook.

6.13 Constant Area Duct Flow with Heat Transfer and Friction

The theoretical analyses of Pars. 6.11 through 6.12 may be extended to include the effects of simultaneous changes in heat transfer and wall friction. Since the one-dimensional analysis of duct area change with friction is essentially limited to the case of accelerating flows, the behavior of duct flow with combined heat transfer, wall friction, and area change will not be considered.

For the case of heat transfer and wall friction in a constant area duct, the general equation for one-dimensional, continuous duct flow derived in Ref. 7 may be simplified to the following form:

$$\frac{dM^2}{M^2} = \frac{(1+\gamma M^2)\,[1+((\gamma-1)/2)M^2]}{1-M^2}\,\frac{dT_t}{T_t} + \frac{\gamma M^2\,[1+((\gamma-1)/2)M^2]}{1-M^2}\left(4f\frac{dx}{D}\right) \qquad \text{(1B-110)}$$

For an infinitesimal length of duct, dx, the rate of heat transfer can be expressed as

$$m\,dQ = \frac{\pi}{4}D^2\rho\,U\,c_p\,dT_t \qquad \text{(1B-111)}$$

or

$$m\,dQ = h\pi D\,dx\left(T_{sw}-T_{saw}\right) \qquad \text{(1B-112)}$$

where T_{sw} and T_{saw} denote the duct wall temperature and adiabatic wall temperature, respectively, and h is the coefficient of heat transfer.

If the temperature recovery factor through the wall boundary layer is assumed to be unity, then

$$T_{saw} = T_t$$

and the equations for rate of heat transfer may be combined to give

$$\frac{dT_t}{T_{sw}-T_t} = \frac{4\,h\,dx}{\rho\,U\,c_p\,D} \qquad \text{(1B-113)}$$

Experiments have indicated a so-called Reynolds analogy relating friction and heat transfer as

$$\frac{h}{\rho\,U\,c_p} = \frac{f}{2} \qquad \text{(1B-114)}$$

which may be used to simplify the heat transfer equation to

$$\frac{dT_t}{T_{sw}-T_t} = 2f\left(\frac{dx}{D}\right) \qquad \text{(1B-115)}$$

When this relation is substituted into the original differential equation involving Mach number, stagnation temperature, and wall friction, the result is

$$\frac{dM^2}{M^2} = \left[\frac{(1+\gamma M^2)\,[1+((\gamma-1)/2)M^2]}{1-M^2} + \frac{2T_t}{T_{sw}-T_t}\,\frac{\gamma M^2\,[1+((\gamma-1)/2)M^2]}{1-M^2}\right]\frac{dT_t}{T_t} \qquad \text{(1B-116)}$$

For the case of constant wall temperature, Eq. 1B-115 may be integrated to obtain

$$\frac{1}{2}\left[\frac{4f(x_2-x_1)}{D}\right] = \ln\left(\frac{T_{sw}-T_{t1}}{T_{sw}-T_{t2}}\right) \qquad \text{(1B-117)}$$

where subscripts 1 and 2 denote stations upstream and downstream of the heat transfer, respectively. T_{t2} is thus readily calculated for known upstream values of T_{t1}, f, D, and T_{sw}.

The differential equation of Mach number variation is not amenable to a closed analytic integration and must be integrated either graphically or numerically. A numerical integration method, from Ref. 7, is outlined below.

(a) For known upstream conditions, specify station 2 as the downstream duct location where the stagnation temperature ratio T_{t2}/T_{t1} is close to unity. The location of station 2 in terms of x is found directly from the integrated relation between f, x, T_{sw}, T_{t1}, and T_{t2}.

(b) Using the finite-difference principle, approximate integration yields

$$M_2^2 - M_1^2 = 2\left(\frac{T_{t2}}{T_{t1}} - 1\right) \bullet \left[\frac{\overline{F}_{Tt}}{(T_{t2}/T_{t1} + 1)} + \frac{2\overline{F}_f}{2(T_{sw}/T_{t1}) - (T_{t2}/T_{t1}) - 1}\right] \quad \text{(1B-118)}$$

where $\overline{F}_{Tt}$ and $\overline{F}_f$ represent the average values of

$$\overline{F}_{Tt} = \frac{M^2(1+\gamma M^2)\,[1+((\gamma-1)/2)M^2]}{1-M^2} \quad \text{(1B-119)}$$

$$\overline{F}_f = \frac{\gamma M^4\,[1+((\gamma-1)/2)M^2]}{1-M^2} \quad \text{(1B-120)}$$

(c) Assume a value of M_2 and compute $\overline{F}_{Tt}$ and $\overline{F}_f$ for the average value of M_1 and assumed M_2.

(d) Solve the finite difference equation for M_2 and compare with assumed value of M_2 in step (c).

(e) Repeat steps (c) and (d) until the desired accuracy for M_2 is obtained.

This process may be continued along the duct in small increments until the end of the duct or choked flow is reached. Once the stagnation temperature and Mach number ratios between stations 1 and 2 have been established, the remaining static properties may be obtained from the continuity and isentropic relations developed in Pars. 6.2 through 6.8.

For other approximate and graphical solutions of this problem, refer to Refs. 7 and 10.

6.14 Mach Waves and Prandtl-Meyer Flow

Consider a point disturbance of infinitesimal strength moving with supersonic velocity. Sound waves propagated outward from the disturbance form a wave front or so-called Mach line of either two- or three-dimensional characteristics. Fig. 1B-21 illustrates this phenomenon and shows that all fluid upstream of the Mach line is unaffected by the presence of the point disturbance (Ref. 6). The angle μ between the Mach line and the path of the point motion is a function only of the local Mach number; that is,

$$\mu = \sin^{-1}\left(\frac{1}{M}\right) \tag{1B-121}$$

It does not apply to subsonic flow conditions, since waves are then projected ahead of the disturbance. It is apparent that the flow must undergo an instantaneous change in properties across the Mach line; if, however, the disturbance is of infinitesimal strength, so are the changes in properties. A finite deflection of the flow corresponds to a shock wave, which will be discussed in Par. 6.15.

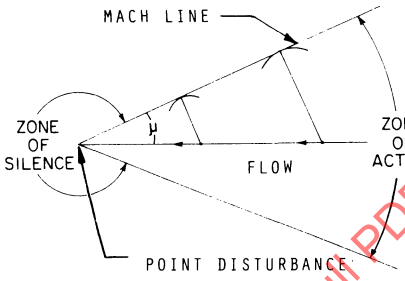

Figure 1B-21 - Mach Wave Formation

The concept of the Mach line is necessary to analyze the isentropic compressive or expansive flow of a supersonic stream or so-called Prandtl-Meyer flow. The case of expansive flow through an infinitesimal deflection is shown in Fig. 1B-22. The flow is assumed to follow the wall and must therefore turn through the angle, $d\theta$, about the sharp point, A. For two-dimensional flow, the amount of turning is constant at any point along the Mach line. It can be shown from considerations of continuity and equilibrium that the tangential velocity component, U_t, of the flow remains constant across the Mach wave, and thus the entire change in velocity is due to the component normal to the wave, as shown in Fig. 1B-22. The rate of change of velocity and pressure can be readily derived as follows:

$$U = \left(U_n^2 + U_t^2\right)^{1/2} \tag{1B-122}$$

Since U_t is constant,

$$dU = \frac{U_n}{U}\, dU_n \tag{1B-123}$$

The angle between the velocity U and the Mach wave is

$$\mu = \tan^{-1}\left(\frac{U_n}{U_t}\right) \tag{1B-124}$$

The angular change of θ in the direction of U is

$$d\theta = \frac{U_t}{U^2}\, dU_n$$

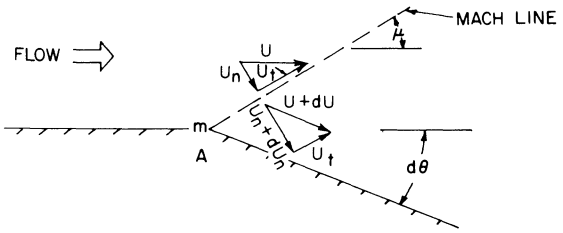

Figure 1B-22 - Infinitesimal Flow Deflection

and therefore

$$\frac{dU}{d\theta} = U\frac{U_n}{U_t} = U\tan\mu$$

If $\sin\mu = 1/M$, then $\tan\mu = 1/\sqrt{M^2-1}$

$$\text{and } \frac{dU}{d\theta} = \frac{U}{\sqrt{M^2-1}} \qquad \text{(1B-125)}$$

which indicates that a clockwise change in flow direction produces a speed increase, whereas a counterclockwise change results in a speed decrease. For steady compressible flow, Bernoulli's equation may be written in differential form as

$$\frac{dU}{U} = \frac{-dP_s}{U^2\rho} \qquad \text{(1B-126)}$$

Employing the basic definition of the speed of sound

$$\frac{dU}{U} = -\frac{1}{\gamma M^2}\frac{dP_s}{P_s}$$

which, when combined with the relation between velocity and flow angle change, gives

$$\frac{dP_s}{d\theta} = -\frac{\gamma M^2}{\sqrt{M^2-1}}P_s \qquad \text{(1B-127)}$$

showing that the static pressure is decreased through an expansion wave and increased through a compression wave.

For finite changes in flow direction, the end properties may be considered as resulting from an infinite number of infinitesimal changes that occur between the initial and final Mach waves of a typical expansion fan shown in Fig. 1B-23.

The total change in stream direction, θ, may be related to the net change in Mach number by integrating the differential equation for an infinitesimal change, Eq. 1B-125. In order to integrate, however, the Mach number function must be expressed in terms of velocity by utilizing the definition of the speed of sound and the energy equation. It is conventional to define $\theta = 0$ as the flow direction for Mach 1.0, and hence the equation for θ is integrated between $U = a_0^*$ and U. The resulting form may then be transposed back in terms of Mach number to give

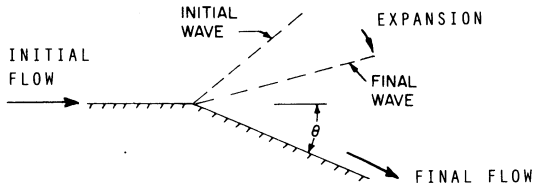

Figure 1B-23 - Expansion Fan

$$\theta = -\frac{1}{2}\left(\frac{\gamma+1}{\gamma-1}\right)^{1/2}\left\{\sin^{-1}\left[\left(\frac{1-\gamma^2}{2}\right)\left(\frac{M^2}{1+((\gamma-1)/2)\,M^2}\right)+\gamma\right]-\frac{\pi}{2}\right\}$$
$$-\frac{1}{2}\left\{\sin^{-1}\left[\gamma-2\left(\frac{1+((\gamma-1)/2)\,M^2}{M^2}\right)\right]+\frac{\pi}{2}\right\} \qquad \text{(1B-128)}$$

which is valid for a deflection of the stream in either direction. When applied to the case of compressive turning, however, the change in surface velocity must occur over a finite distance, in contrast to an expansion flow, which may originate about a point as well as over a finite distance. The variation of θ with local Mach number plotted in Fig. 1B-24 shows the interesting fact that the turning angle approaches 130.5 deg at Mach infinity. This curve, or a tabulation such as that found in Ref. 4, may be used to determine the change in Mach number through any amount of isentropic compression or expansion of a two-dimensional flow from any initial Mach number.

An example, using the tables of Ref. 4, is as follows: For an initial Mach number of 1.5, assume a two-dimensional turning angle of 10 deg in either direction, and determine the final Mach number. The value of θ for Mach 1.5 is read as 11.905 deg. In other words, the flow is required to turn approximately 12 deg in order to expand isentropically fom Mach 1.0 to 1.5. The new net turning angle is therefore $\theta_1 \pm 10° = 21.905°$, or $1.905° = \theta_2$. The final Mach number, based on θ_2, is read from the tables as 1.84 or 1.13, corresponding to expansion and compression, respectively. Since the flow is isentropic, any of the static properties may be found by using the static-to-stagnation ratios developed in Pars. 6.5 and 6.6.

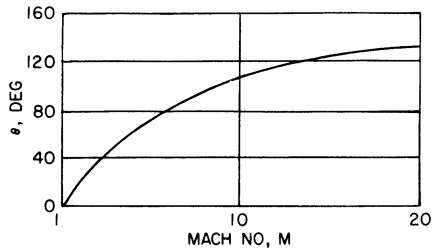

Figure 1B-24 - Prandtl-Meyer Function

6.15 Normal, Oblique, and Conical Shock Waves

6.15.1 Normal Shocks

When compressive turning occurs instantaneously in supersonic flow, a discontinuity (termed a shock) is formed. Turning of the flow, however, is not necessary for the formation of a normal shock, which is most commonly formed in duct or ductlike flows. For certain prescribed relations between final and initial pressures across a diverging channel or duct, it is found that no completely isentropic steady flow solution is satisfactory, and hence the concept of a shock discontinuity normal to the flow is introduced. (The possibility of the existence of a shock was predicted mathematically in 1860 by Riemann. Flow visualization methods such as Schlieren photography have pictured the actual shock wave.) In real flow, a discontinuity of infinitesimal dimensions cannot exist, but both theory and experiment show that the thickness of a shock wave is in the order of the molecular mean free path.

In order to calculate the change in flow properties through a shock, it is necessary only to apply the three equations of conservation across an assumed discontinuity. For two-dimensional flow, either an oblique or a normal shock can occur. It is emphasized that there is basically no difference in the development of the oblique shock theory from that of the normal shock. Because of the simplicity of geometric parameters, however, the theory of the normal shock will be discussed in more detail.

The notation for this analysis is shown in Figure 1B-25.

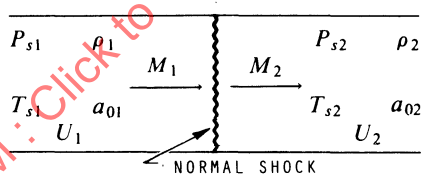

Figure 1B-25 - Notation for Normal Shock Wave Analysis

By continuity:

$$\rho_1 U_1 = \rho_2 U_2 \tag{1B-129}$$

By momentum:

$$P_{s1} + \rho_1 U_1^2 = P_{s2} + \rho_2 U_2^2 \tag{1B-130}$$

$$\text{or} \quad U_1 - U_2 = \frac{P_{s2}}{\rho_2 U_2} - \frac{P_{s1}}{\rho_1 U_1}$$

By energy:

$$\rho_1 U_1 \left(\frac{1}{2} U_1^2 + h_1\right) = \rho_2 U_2 \left(\frac{1}{2} U_2^2 + h_2\right)$$

$$\text{or} \quad \frac{1}{2} U_1^2 + \frac{1}{\gamma - 1} a_{o1}^2 = \frac{1}{2} U_2^2 + \frac{1}{\gamma - 1} a_{o2}^2 \tag{1B-131}$$

from which it is seen that the total enthalpy, and hence total temperature, remains constant across a shock wave. In order to find the very useful relation between the Mach numbers before and

after a normal shock, it is convenient to use the concept of a_0^*, or critical speed of sound. On either side of the shock the energy equation may be written as

$$\frac{1}{2}U^2 + \frac{a_o^2}{\gamma-1} = \frac{a_{ot}^2}{\gamma-1} \tag{1B-132}$$

where a_{ot} represents the speed of sound based on total or stagnation conditions. Since the critical speed of sound, a_0^*, is defined as the flow velocity that exactly equals the local speed of sound, $U = a_o = a_0^*$, which may be combined with the energy equation, Eq. 1B-132, to obtain

$$\frac{1}{2}U^2 + \frac{a_o^2}{\gamma-1} = \frac{1}{2}\left(\frac{\gamma+1}{\gamma-1}\right)a_o^{*2}$$

Since

$$a_o^2 = \gamma\frac{P_s}{\rho}$$

the energy equation may be written as

$$\frac{1}{2}U^2 + \frac{\gamma}{\gamma-1}\frac{P_s}{\rho} = \frac{1}{2}\left(\frac{\gamma+1}{\gamma-1}\right)a_o^{*2}$$

and substituted into the momentum equation to obtain

$$\left(U_1 - U_2\right) = \left(U_1 - U_2\right)\left(\frac{\gamma+1}{2\gamma}\frac{a_o^{*2}}{U_1 U_2} + \frac{\gamma-1}{2\gamma}\right) \tag{1B-133}$$

which has two obvious solutions:

$$U_1 = U_2 \quad \text{and} \quad U_1 U_2 = a_o^{*2} \tag{1B-134}$$

From a consideration of entropy change across a shock, it is concluded that the flow upstream of a shock must be supersonic; that is, $U_1 > a_0^*$. If $U_1 > a_0^*$ then $U_2 < a_0^*$, and thus the flow downstream of a normal shock is always subsonic. The energy equation written in terms of a_0^* is

$$\left(\frac{U}{a_0^*}\right)^2 = \frac{\gamma+1}{(\gamma-1) + (2/M^2)}$$

and may be substituted into the relation $U_1\, U_2 = a_o^{*2}$ to obtain the relation between M_1 and M_2:

$$M_2^2 = \frac{1+((\gamma-1)/2)\, M_1^2}{\gamma M_1^2 - ((\gamma-1)/2)} \tag{1B-135}$$

Returning to the equations of continuity and momentum, the relations for static pressure and density across the shock are

$$\frac{P_{s2}}{P_{s1}} = \frac{2\gamma M_1^2 - (\gamma-1)}{\gamma+1} \tag{1B-136}$$

and

$$\frac{\rho_2}{\rho_1} = \frac{(\gamma+1)\,M_1^2}{(\gamma-1)\,M_1^2+2} \qquad \text{(1B-137)}$$

From Eqs. 1B-135, 1B-136, and 1B-137 and the isentropic relations for local flow conditions, all possible combinations of static and total pressure properties across a normal shock can be derived in terms of the upstream Mach number. The numerical values of these parameters can be found in tabular form (Ref. 4) or in curve form (Ref. 8).

Changes in flow properties through a normal shock can be qualitatively summarized as follows:

(a) Stagnation temperature ratio remains constant.

(b) Total pressure ratio decreases, approaching zero as upstream Mach number approaches infinity.

(c) Density, static pressure, static temperature, and entropy ratios increase with increasing upstream Mach number.

6.15.2 Oblique Shocks

The flow parameters across an oblique shock, that is, one for which the shock wave angle is less than 90 deg relative to the upstream flow, can be found directly from the normal shock and certain geometric relations. In accordance with Fig. 1B-26, where U_N is the velocity in the normal direction and U_t the velocity in the tangential direction, the momentum equations written in the normal and tangential directions are

$$P_{s1} + \rho_1 U_{N1}^2 = P_{s2} + \rho_2 U_{N2}^2$$

and

$$\rho_1 U_{N1} U_{t1} = \rho_2 U_{N2} U_{t2}$$

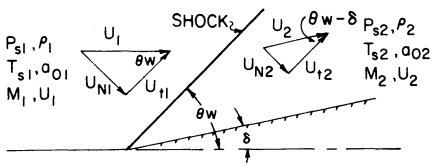

Figure 1B-26 - Oblique Shock Diagram

From continuity,

$$\rho_1 U_{N1} = \rho_2 U_{N2}$$

and therefore

$$U_{t1} = U_{t2} \qquad \text{(1B-138)}$$

It should be apparent that the three equations of conservation involve only the normal velocity component, U_N, and are identical to those derived for the normal shock case. If the M_1 and M_2 terms of the normal shock case are replaced by $M_1 \sin\theta_w$ and $M_2 \sin(\theta_w - \delta)$, respectively, the static and stagnation property ratios across an oblique shock are obtained immediately in terms of

M_1 and θ_w, θ_w and δ, or M_1 and δ. Furthermore, the changes remain qualitatively the same as for the normal shock case. Oblique shock functions are most conveniently presented in curve form, such as in Ref. 8.

From the geometry depicted in Fig. 1B-26, it is possible to obtain the relation between the flow deflection angle and the shock wave angle relative to the original stream direction:

$$\tan\delta = \frac{M_1^2 \sin^2\theta_w - \frac{\gamma-1}{\gamma+1} M_1^2 \sin\theta_w - \frac{2}{\gamma+1}}{\frac{\gamma-1}{\gamma+1} M_1^2 \frac{\sin^2\theta_w}{\cos\theta_w} + \frac{2}{\gamma+1}\frac{\sin\theta_w}{\cos\theta_w} + M_1^2 \sin\theta_w \cos\theta_w} \qquad \text{(1B-139)}$$

Since the relation for θ is of quadratic form, two solutions are mathematically possible and have been termed the "weak" and the "strong" solutions. It has been observed experimentally that the "weak" solution (shock angle closest to Mach wave angle) always occurs in cases of flow deflection past a straight boundary at Mach numbers above that for detachment. On the other hand, for the case of detached curved shock (as formed in front of a blunt body or at Mach numbers below that for detachment), all possible strengths of waves from strong to weak occur along the shock structure (Ref. 8).

6.15.3 Conical Shocks

The analysis of conical flow is quite involved mathematically; however, Taylor and Maccoll (Ref. 11) were able to reduce the equations of motion to ordinary differential form by assuming that all flow properties were constant along conical surfaces originating at the cone vertex. This assumption has been experimentally substantiated.

The most useful presentation of conical flow parameters is given in Ref. 8, which includes the cone surface properties as a function of freestream Mach number and cone angle as well as static pressure and flow deflection functions for points located anywhere in the conical field.

The flow conditions immediately behind a conical shock may be obtained directly from oblique shock tables using parameters of freestream Mach number and an equivalent two-dimensional wedge angle that would produce the actual conical shock angle. For quick order-of-magnitude calculations, flow properties between the cone surface and the conical shock wave may be linearly interpolated as a function of local ray angle. The characteristics of conical shock flow may be summarized as follows:

(a) Flow properties are constant along rays (conical surfaces) emanating at the cone vertex.

(b) Static and stagnation property ratios across the shock vary qualitatively in the same manner as for normal or oblique shocks.

(c) Local flow deflection reduces from a maximum at the boundary of the cone to a minimum behind the shock.

(d) Isentropic compression occurs between the shock boundary and the cone surface.

(e) For equal freestream Mach numbers and surface flow deflection angles, all properties change less through a conical shock than through an oblique shock.

(f) For a given freestream Mach number, the cone deflection angle for shock detachment is larger than the deflection angle for a two-dimensional surface.

6.16 Subsonic Diffusers

The field of subsonic diffuser research and design covers an enormous amount of work. It is beyond the scope of this AIR to present a complete coverage of the subject. Accordingly, only a brief review of salient principles is presented.

A large amount of experimental work has been accomplished on subsonic diffusers, the history of which is given in Ref. 12. Studies on subsonic diffusers have, of necessity, been largely experimental in nature because turbulent boundary layer theory as yet has not reached a state of refinement that permits the theoretical design of optimum subsonic diffusers for modern aircraft.

The losses in subsonic diffusers, having turbulent boundary layers, can be viewed in a somewhat simplified fashion as being composed of two major components: wall frictional losses and losses due to boundary layer profile distortion or separation. In general, in subsonic diffusers, an examination of the turbulent boundary layer flow at a given station reveals that if the local wall friction is high, then the boundary layer distortion or separation loss is low. Conversely, if the local wall friction loss is low, the local distortion or separation loss is high. In an actual diffuser, the losses caused by boundary layer distortion or separation, characteristically large for a short diffuser, must be balanced against the increased wall friction losses of a long diffuser. It is the inability of existing turbulent boundary layer theory to account accurately for the balance between these subsonic diffuser loss components in compressible flow that requires the application of experimental techniques and data for determining appropriate subsonic diffuser geometry in modern aircraft systems.

Although the existing turbulent boundary layer theory has not reached a sufficient state of refinement to be used for subsonic diffuser design purposes, several investigators (Refs. 13 and 14) have used the theory to obtain significant clues regarding optimum diffuser design. Systematic methods for subsonic diffuser design, based on correlation of empirical boundary layer and diffuser data, are presented in Ref. 14. From the results reported in Ref. 14 and others, certain general rules can be formulated for the design of subsonic diffusers for application to modern aircraft induction systems. In the following discussion of these rules, the parameter used to describe subsonic diffuser performance is the total pressure recovery, which is the ratio of the total pressure at the diffuser exit to the total pressure at the diffuser inlet.

The following general rules apply to design of subsonic diffusers operating with throat Mach numbers near unity (Ref. 14):

(a) The total pressure recoveries of subsonic diffusers are as sensitive to initial boundary layer conditions as to diffuser shapes, for a substantial range of duct shapes. For thin initial boundary layers, the flow can be diffused relatively rapidly. Conversely, with thick initial boundary layers, the flow can be diffused gradually.

(b) When the flow at the subsonic entrance is highly nonuniform or separated, as is often the case in supersonic inlets following shock wave boundary layer interactions, slightly diverging (approximately 0.5 – 1.0 deg) mixing sections should be used ahead of the subsonic diffuser to enable the boundary layer to reattach and provide a high-energy profile prior to entering the subsonic diffuser. The use of a mixing section of this nature will provide higher pressure recovery and more uniform flow at the subsonic diffuser exit if the entry flow is highly distorted.

(c) The initial wall slope at the entrance of subsonic diffusers operating at near-sonic throat conditions should be zero, to provide a low initial adverse pressure gradient on the boundary layer.

(d) The rate of turning of subsonic diffusers away from the direction of the initial inlet flow should be held to an absolute minimum. The larger the rate of turning from the initial flow direction, the larger are the resulting losses. Data on subsonic diffuser turning are presented in Ref. 14.

The performance of subsonic diffusers is frequently specified in terms of a total pressure loss coefficent, $(P_{t1}-P_{t2})/q_1$. Although this parameter varies with subsonic diffuser Mach number, as indicated in Ref. 14, it is in many cases nearly constant for a sizable range of diffuser entrance Mach numbers. The value of the pressure loss coefficient is a function of both subsonic diffuser entrance boundary layer conditions and subsonic diffuser geometry, as shown in Ref. 14, for example. A typical range of values for well designed diffusers is from 0.05 for a thin diffuser entrance boundary layer to 0.20 for a thick diffuser entrance boundary layer.

The geometric properties of a number of subsonic diffusers reported in Ref. 14 are shown in Fig. 1B-27. The effects on total pressure loss coefficient resulting from these geometric variations and diffuser entrance boundary layer conditions are shown in Fig. 1B-28. The effects of throat length, wall divergence, and entrance boundary layer on diffuser performance are consistent with the general rules stated above. Additional subsonic diffuser data may be obtained from Refs. 15 through 18.

An example of how the total pressure loss coefficient is applied to estimate subsonic diffuser performance is as follows:

Problem: A subsonic diffuser has a total pressure loss coefficient

$$\frac{P_{t1}-P_{t2}}{q_1} = 0.10$$

The subsonic diffuser entrance Mach number is 0.7. What is the total pressure recovery, P_{t2}/P_{t1}, of the diffuser under these conditions?

Solution: The total pressure recovery can be written as

$$\frac{P_{t2}}{P_{t1}} = 1 - \left(\frac{P_{t1}-P_{t2}}{q_1}\right)\left(\frac{q_1}{P_{t1}}\right) \qquad \text{(1B-140)}$$

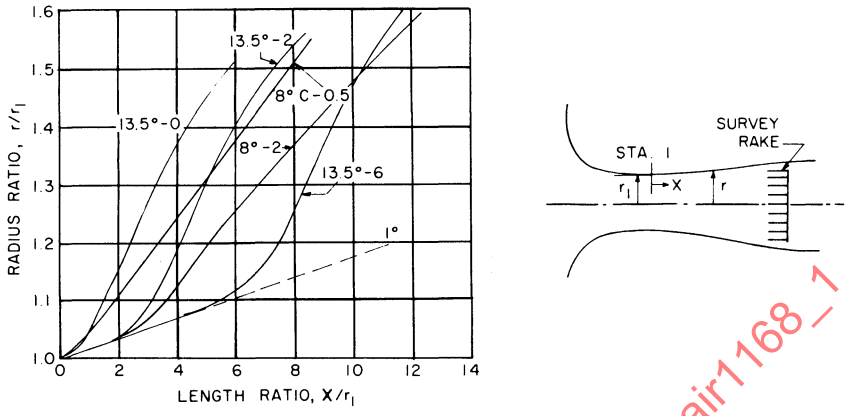

Figure 1B-27 - Geometric Properties of Diffusers Reported in Ref. 14 ($A_1/A_2 = 0.510$ rake station; $r_1 = 1.50$ in. Diffuser identification system: (1) first number refers to maximum total divergence angle, (2) second number refers to throat extension in terms of inlet throat radii, (3) letter C refers to conical diffuser).

Note that q_1/P_{t1} is a function of Mach number; thus $q_1/P_{t1} = 0.247$ for the diffuser entrance Mach number of 0.7 from the tables of Ref. 4. Thus

$$\frac{P_{t2}}{P_{t1}} = 1 - 0.1(0.247) = 0.975 \qquad \text{(1B-141)}$$

6.17 Auxiliary Inlets and Diffusers

6.17.1 Introduction

Auxiliary inlets are required to supply air for a variety of auxiliary systems in modern aircraft. Typical among these are air conditioning, electronic cooling, and oil cooling systems. The purpose of this section is to introduce some of the types and locations of auxiliary inlets normally considered for aircraft applications, to describe their general operating characteristics, and to present methods for estimating their performance in the subsonic and supersonic flight regimes.

6.17.2 Types of Auxiliary Inlets

Two principal types of auxiliary inlets are considered: ram scoop and flush inlet. The ram scoop may be located in a region of substantial boundary layer or at the leading edge of a wing or fuselage where the boundary layer is almost negligible. Frequently, the flush auxiliary inlet is located in a boundary layer. Fig. 1B-29 illustrates the ram type of scoop operating both in a boundary layer, such as that encountered well aft on a wing or fuselage, and at the leading edge of a wing or fuselage. The flush scoop is shown operating in a region of appreciable boundary layer.

6.17.3 Characteristics of Auxiliary Inlets

Much of the definitive experimental information of auxiliary inlet performance characteristics was classified when this material was originally written, particularly that covering the high subsonic, transonic, and supersonic flight regimes. Some unclassified data existed for particular auxiliary inlet configurations in each of these regimes. Since unclassified data were not available

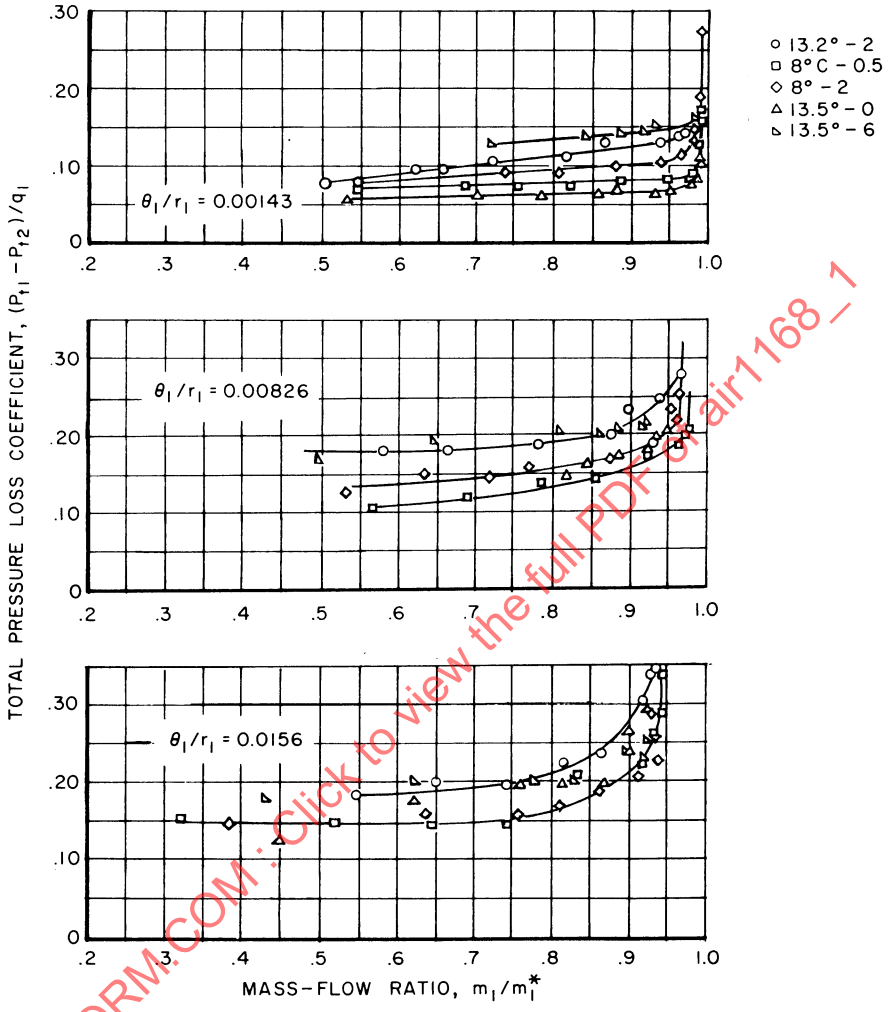

Figure 1B-28 - Effects of Diffuser Geometry Variations and Boundary Layer Thickness on Performance (m_1 = mass flow ($\rho_1 v_1 A_1$); m_1^* = maximum mass flow based on sonic isentropic entrance conditions; Momentum thickness: $\theta = \int_0^\delta [\rho_u/\rho_0 U_0^2] (U_0 - u)\, dy$)

for a wide range of configurations in each of the speed regimes, it was necessary to limit the following discussion to general characteristics of auxiliary inlets and to indicate principles that may be useful in designing and understanding the operation of auxiliary inlets. Pertinent unclassified experimental data are referred to where possible, in an attempt to aid in the understanding of such systems.

Auxiliary inlets are sometimes deliberately located in regions of substantial boundary layer, and permitted to ingest the low-energy boundary layer flow generated by a fuselage or wing in order to minimize drag penalty due to the inlet and, in some cases, to minimize the icing problem. The

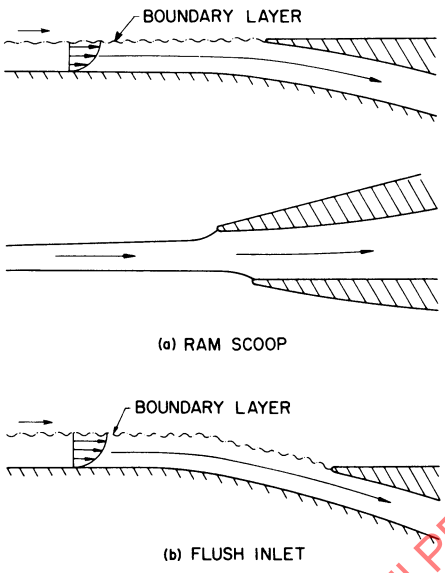

Figure 1B-29 - Types and Locations of Auxiliary Inlets: (a) Ram Scoop; (b) Flush Inlet

ingestion of low-energy boundary layer air is also possible in many auxiliary inlet applications, since the attainment of high total pressure relative to freestream total pressure often is not necessary for auxiliary systems. It is important, however, that auxiliary inlets recover a high percentage of the total pressure that is available in the boundary layer in order to minimize the drag penalty imposed by taking air aboard the aircraft and discharging it. In supplying air for auxiliary sytems in which a high total pressure relative to free stream is required, this requirement can be met by locating the inlet either at a wing leading edge or fuselage nose or outside the boundary layer on a fuselage or wing.

Consider the general characteristics of auxiliary inlets operating at subsonic flight speeds in a boundary layer of considerable thickness, such as that generated by a wing or a fuselage. The internal flow characteristics usually are described in terms of ram recovery ratio as a function of inlet mass flow ratio. Ram recovery ratio is defined as the ratio of the dynamic pressure $(P_t - P_{so})$ at the scoop throat (or subsonic diffuser exit) to the dynamic pressure $(P_{ta} - P_{so})$ in the free stream. The inlet mass-flow ratio is defined as the mass flow entering the inlet divided by the mass of air in the free stream flowing through an area equal to the inlet throat area at freestream conditions. The ram pressure recovery-mass ratio characteristics of a flush auxiliary inlet operating at subsonic flight speeds are shown qualitatively in Fig. 1B-30 and are compared with those of an auxiliary inlet located at the nose of a fuselage or wing leading edge. The latter inlet will hereafter be referred to as a nose inlet. The flush inlet attains a lower ram pressure recovery than the nose inlet at all mass flow ratios. This results primarily from the fact that less pressure recovery is available to the flush inlet, since it ingests boundary layer air that has a lower average total pressure because of the nonuniform boundary layer velocity profile. The flush inlet likewise attains a lower maximum mass flow ratio than the nose inlet as a result of the nonuniform velocity in the boundary layer air it ingests. The magnitude of the total pressure and mass flow